JOURNAL OF APPLIED PHYSICS

JOURNAL
OF
APPLIED PHYSICS

SEPTEMBER, 1942 Vol. 13, No. 9

In This Issue

Page

Mass Spectrometer as an Industrial Tool 525

Short History of Isotopes and the Measurement of Their Abundance E. B. JORDAN AND LOUIS B. YOUNG 526

Measurement of Relative Abundance with the Mass Spectrometer E. B. JORDAN AND N. D. COGGESHALL 539

Gas Analysis with the Mass Spectrometer JOHN A. HIPPLE 551

Some Applications of Mass Spectrometric Analysis to Chemistry D. RITTENBERG 561

Contributed Original Research

Diffraction Adapter for the Electron Microscope J. HILLIER, R. F. BAKER AND V. K. ZWORYKIN 571

Reflection of Electromagnetic Waves from a Parabolic Friction-Free Ionized Layer OLOF E. H. RYDBECK 577

Variation of Axial Aberrations of Electron Lenses with Lens Strength E. G. RAMBERG 582

In Every Issue

Here and There 570

Calendar of Meetings 594

Index to Advertisers x

BOARD OF EDITORS

ELMER HUTCHISSON, *Editor*

Associate Editors

FRANCIS BITTER
W. F. BUSSE
S. H. CALDWELL
ROBLEY D. EVANS
MORRIS MUSKAT
FREDERICK SEITZ
B. E. WARREN
J. B. WHITEHEAD

Publication of the
American Institute of Physics

ADMINISTRATIVE STAFF

HENRY A. BARTON, *Director*

MADELINE M. MITCHELL, *Publications Manager*

JOHN T. TATE, *Adviser on Publications*

GOVERNING BOARD

PAUL E. KLOPSTEG, *Chairman*
GEORGE B. PEGRAM, *Secretary*
R. B. DOW
L. A. DUBRIDGE
FLOYD A. FIRESTONE
HARVEY FLETCHER
R. C. GIBBS
K. S. GIBSON
ARTHUR C. HARDY
GEORGE R. HARRISON
HERMANN MARK
A. G. WORTHING
JOHN T. TATE
N. W. TAYLOR
WALLACE WATERFALL

The JOURNAL OF APPLIED PHYSICS, published monthly at Prince and Lemon Sts., Lancaster, Pa., is devoted to physics in its role as the science basic to other natural sciences and to the arts and industries. Previous to 1937 this publication was known as PHYSICS. It aims to be of service not only in physical laboratories, but also in the laboratories of industrial, chemical, geological, geophysical, meteorological, radio, and similar concerns. The JOURNAL OF APPLIED PHYSICS publishes editorials, news of physicists and reviews, as well as technical papers of applied physics.

Manuscripts should be submitted to Elmer Hutchisson, Editor, American Institute of Physics, 175 Fifth Avenue, New York, New York.

Subscriptions and orders for back numbers should be addressed to Prince and Lemon Streets, Lancaster, Pa. or to the American Institute of Physics, 175 Fifth Avenue, New York, N. Y.

SUBSCRIPTION PRICE

	U. S. AND CANADA	ELSEWHERE
To members of scientific societies	$5.00	$5.70
To all others	7.00	7.70

Single copies are $.70 each.

Changes of address and proofs should be addressed to the Publications Manager.

Advertising rates supplied on request. Orders, advertising copy and cuts should be sent to the American Institute of Physics.

Entered as second class matter at the Post Office at Lancaster, Pennsylvania, under the Act of March 3, 1897. Accepted for mailing at the special rate of postage provided for in the Act of February 28, 1925, authorized May 2, 1932.

Copyright 1942, by the American Institute of Physics.

Journal of APPLIED PHYSICS

Volume 13 September, 1942 Number 9

Mass Spectrometer as an Industrial Tool

ONE of the principal purposes of the *Journal of Applied Physics* is to bring to the attention of those in industry the new tools which are continually being developed in the pure physics laboratory. This issue concerns the mass spectrometer; an instrument which gives directly information about the relative abundance of different kinds of atomic and molecular ion fragments formed in a given chemical process or when molecules of a particular kind are struck by electrons of known energy.

There may be some who will ask not what a mass spectrometer is but how it does its work. This question may be briefly answered by quoting from a recent industrial bulletin in which the mass spectrometer is described as "essentially a high vacuum tube in which the gas to be studied is admitted to a pressure of the order 10^{-4} mm Hg. The molecules of the gas are ionized by electrons of controlled energy from a thermionic filament and accelerating grids. Ions of many different types are formed even in a pure gas corresponding to various modes of breaking down the molecule accompanied by ionization. The ions so formed are then drawn out of the ionizing chamber by an applied electric field and are caused to move through a combination of electric and magnetic fields designed so as to sort out the ions according to their m/e or mass-to-charge ratio."

One application of mass spectrometry described in this issue is in the field of gas analysis. There are undoubtedly many other industrial applications. If any suggest themselves to the reader, this issue will have served its purpose well.

The Editor wishes to express his appreciation to Dr. John A. Hipple, who has taken a leading part in the organization of this issue, and to the other contributors. He wishes also to thank Professors A. J. Dempster and A. O. Nier for supplying photographs to illustrate this issue.

A Short History of Isotopes and the Measurement of Their Abundances

By E. B. Jordan and Louis B. Young
University of Illinois, Urbana, Illinois

OUR modern ideas concerning the constitution of matter are inevitably linked with the past through the contributions of such great scientists as Dalton, Prout, Faraday, Maxwell, Becquerel, P. and M. Curie, Rutherford, Soddy, J. J. Thomson, Aston, Einstein, and Bohr.

A study of the discoveries associated with many of these names will reveal the importance of one common subject of investigation in the early evolution of our ideas. It is not surprising that the study of atomic weights has led to so many great discoveries.

Dalton was the first one to realize the importance of atomic weight measurements and published his first table in 1803.[1] A few of these values, together with values published in a later paper, are listed in Table I. In 1808, in a paper on chemical synthesis,[2] Dalton made the following statement:

> In all chemical investigations it has justly been considered an important object to ascertain the relative weights of the simples which constitute the compound. But unfortunately enquiry has terminated here. . . . Now it is one great object of this work to show the importance and advantage of ascertaining the relative weights of the ultimate particles, both of simple and compound bodies, the number of simple elementary particles which constitute one compound particle, and the number of less compound particles which enter into the formation of one more compound particle.

Of all the great postulates laid down by Dalton, one only needs to be modified to this day. In 1808, in his new system of chemical philosophy, he made the following statement:

> The ultimate particles of all homogeneous bodies are perfectly alike in weight, figure, etc. In other words, every particle of water is like every other particle of water, every particle of hydrogen is like every other particle of hydrogen.

It was not until a century later that differences between the particles of any one substance were detected.

The very accurate atomic weight measurements made by Berzelius from 1810 to 1830, and the influence of Prout's hypothesis* enunciated in 1815, are well known. By this time the atomic weights of a number of elements had been measured with greater precision, and nearly all the values were found to be whole numbers. Because of its simplicity and plausibility, it is not surprising that Prout's hypothesis concerning the unity of matter attracted considerable attention and created the incentive for further work on atomic weights. As to why the atomic weights of most of the elements were found to be multiples by whole numbers of that of hydrogen, is explained in part by the accuracy obtainable at that time. In 1816, Meinecke,[3] a contemporary of Prout's wrote:

> These comparative calculations led us to adopt particular round numbers, not so much for the simplification of calculation as because we are satisfied from the divergences in the analyses made by the most accurate chemists, as well as from our own experience, that for the present nothing more could be given than approximations in round numbers.

Some of the chemical atomic weights adopted by Prout are also shown in Table I. These values were, for the most part, deduced from the specific gravity measurements of Davy, Biot, Arrago, and others.

By 1833 extended investigations revealed a number of exceptions to Prout's rule and doubts arose concerning its validity, although it was not until the turn of the century that the discrepancies were fully understood. For comparison, some of the atomic weight measurements made considerably later by Richards[4] are also shown in Table I. They clearly demonstrate the deviations, in certain cases, from the whole number rule.

* In a paper published in the Annals of Philosophy **7**, 111–113 (1816), and reprinted in the Alembic Club series No. 20, Prout made the following statement:
"If the views we have ventured to advance be correct, we may almost consider the *primordial substance of the ancients* to be realized in hydrogen; an opinion by the by, not altogether new."

An explanation of these fractional atomic weights, now definitely known to be characteristic of certain elements and not due to experimental errors, came about in a diverse and unexpected manner.

RADIOACTIVITY AND THE DISCOVERY OF ISOTOPES

In 1896, the radioactivity of uranium was discovered by H. Becquerel,[5] and shortly thereafter (1898) other radioactive substances, notably thorium, polonium, and radium were isolated by P. and M. S. Curie.[6] The method of separation depended, in each case, upon the similarity of the chemical properties of the unknown radioactive substance and those of a known element.

As a possible explanation of the radioactivities observed, Mme. Curie, in 1900, said:

> If anything changes, it must be the atom, since it is the atom to which is attached the radioactivity.

Experimentation in this field was rapid, and within the next few years a wealth of data was accumulated. In 1903, Ramsey and Soddy[7] produced, for the first time, definite chemical evidence of a real transmutation when they established the relation between thorium and the inert gas thoron. In the same year, E. Rutherford and F. Soddy[7] set forth their theory of radioactive transformations in which it was proposed that there was a continuous reproduction of new kinds of radioactive matter by the radioactive elements. This law predicted many new genetic relationships, and the stimulus afforded by it soon led to the discovery of a large number of new radioactive elements. Most disturbing of all, a new type of complexity appeared.

Since 1906, the chemists[8–11] had observed that certain pairs of radioactive elements, notably ionium and thorium, mesothorium and radium, could not be separated chemically even with extremely sensitive methods. Also disturbing was the number of additional pairs isolated as new radioactive elements were discovered. By 1910 Soddy, as well as others, was fully aware of the importance of understanding these anomalies. In his report[12] on radioactivity for that year, Soddy made the following statement:

> These regularities may prove to be the beginning of some embracing generalization, which will throw light, not only on radioactive processes, but on elements in general and the periodic law.

Two years later Russell and Rossi[13] showed that ionium and thorium were spectroscopically

TABLE I. A table of atomic weights.

Element	Dalton's relative weights of ultimate particles of gaseous and other bodies 1803 values	1808 values	Values adopted by Prout 1815–1816	Later measurements by T. W. Richards 1870–1910	International values 1939	Mass nos. of Isotopes	Abundance %	Masses	Atomic weights
Hydrogen	1*	1*	1	1.008	1.0081	1 2	99.985 0.015	1.008127 2.01473	1.0080
Carbon	4.3	5	12	12.00	12.010	12 13	98.92 1.08	12.00381 13.00741	12.0113
Nitrogen	4.2	5	14	14.01	14.008	14 15	99.63 0.37	14.00750 15.00489	14.0073
Oxygen	5.5	7	16	16.00*	16.00*	16 17 18	99.762 0.041 0.204	16.000000 17.0045 18.0049	16.00000*
Chlorine	—	—	36	35.46	35.457	35 37	75.43 24.57	34.9805 36.9786	35.462
Copper	—	—	—	63.57	63.57	63 65	68 32	62.956 64.955	63.59
Silver	—	100	—	107.88	107.880	107 109	52.5 47.5	106.948 108.947	107.897

* Standard.

identical, and the next year, (1913) Rutherford and Andrade[14] established the identity of the x-ray spectra in radium B and lead. The existence of such pairs was now definitely accepted, and Soddy, in 1913, suggested as a name for them, the word isotopes (meaning same place in the periodic table).

Perhaps the best idea concerning the state of knowledge of isotopes at this time is contained in Soddy's report[15] to the British Association for the Advancement of Science in 1913. In this he states:

> The chemical analysis of matter is thus not an ultimate one. It has appeared ultimate hitherto, on account of the impossibility of distinguishing between elements which are chemically identical and non-separable unless these are in the process of change the one into the other. But in that part of the periodic table, in which the evolution of the elements is still proceeding, each place is seen to be occupied not by one element, but on the average, for the places occupied at all, by no less than four, the atomic weights of which vary over as much as eight units. It is impossible to believe that the same may not be true for the rest of the table, and that each known element may be a group of non-separable elements occupying the same place, the atomic weight not being a real constant, but a mean value of much less fundamental interest than has been hitherto supposed. Although these advances show that matter is even more complex than chemical analysis alone has been able to reveal, they indicate at the same time that the problem of atomic constitution may be more simple than has been supposed from the lack of simple numerical relations between the atomic weights.

A chart of the radioactive elements published by Soddy in 1913 is shown in Fig. 1.

Assisted by a knowledge of radioactive transformations, the radioactive displacement law for *alpha*-particles first suggested by Soddy in 1911, and information obtained by studying the scattering of alpha-particles by matter, Rutherford had already in 1911 put forward his theory of atomic structure.† This theory, which is accepted

† Rutherford assumed that the atom consisted of a heavy central charged nucleus surrounded by a sphere of electrification containing an equal and opposite charge. The outer charge distribution was assumed to be uniform [Phil. Mag. **237** [6], 669 (1911)].

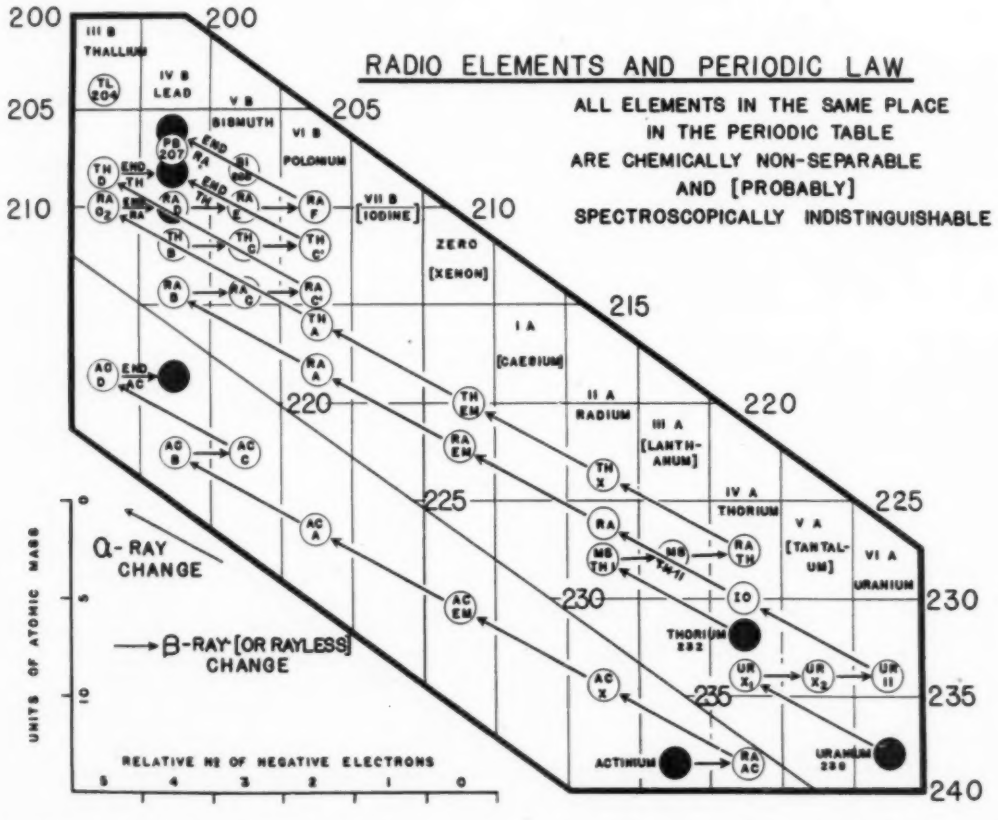

FIG. 1. Chart of the radioactive elements published by Soddy in 1913. [Copied from one of Soddy's papers published in the *Report of the British Association for the Advancement of Science* (Birmingham, 1913), p. 446.]

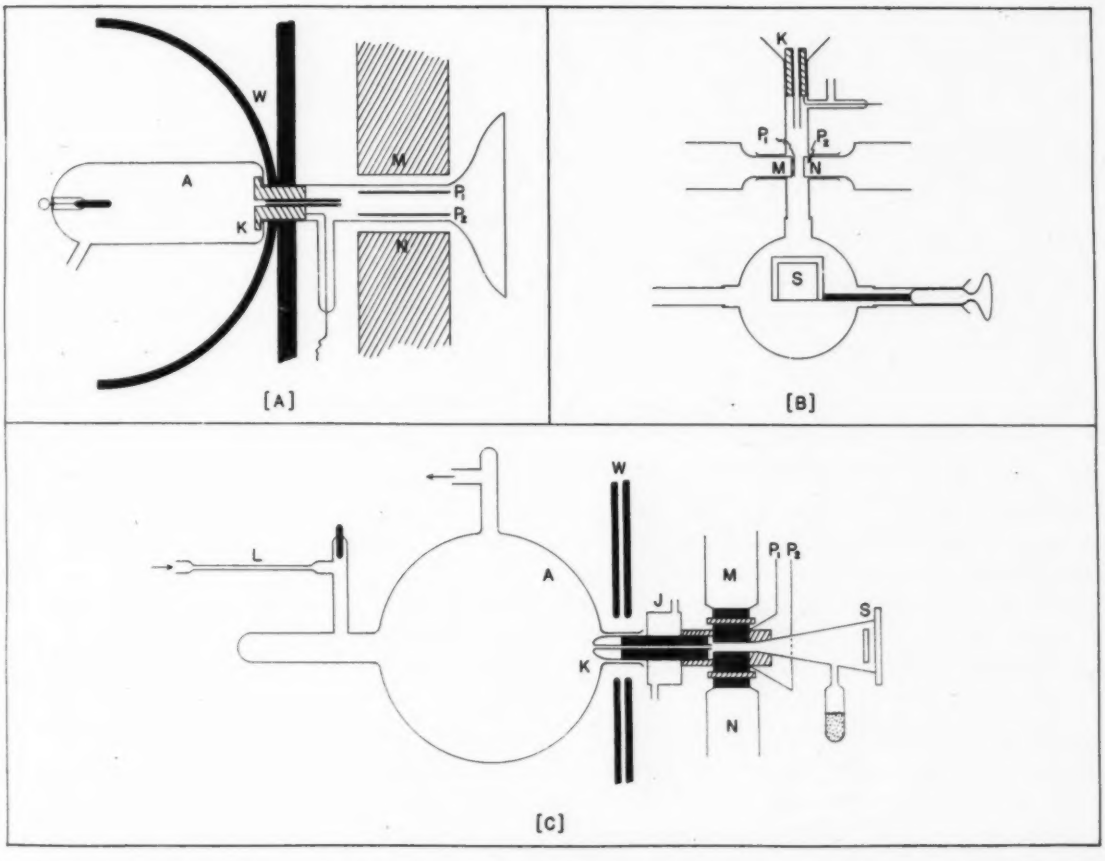

FIG. 2. Thomson's parabola spectrometers. Ions from a discharge tube *A* passed through a small defining hole in the cathode *K* into a region *MN* in which superimposed electric and magnetic fields existed. The parabolic images produced on the photographic plate *S* were functions of the mass to charge ratios of the deflected ions. (Copies of diagrams in original papers published in *The Philosophical Magazine* in 1909, 1911, and 1912.)

to this day, greatly clarified the whole subject; and when the existence of isotopes was definitely established, it was possible to understand how two atoms could have different masses but practically indistinguishable chemical properties.

Although contrary to Dalton's hypothesis that the ultimate particles of all homogeneous bodies are perfectly alike in weight, the possibility of isotopes among the stable elements was immediately seized upon as an explanation of the fractional atomic weights previously observed. Surprisingly enough, it was at the same time that Soddy gave the report quoted above, that Sir J. J. Thomson obtained direct evidence from positive ray analysis that neon consisted of two isotopes.

In an address to the Royal Institution in 1913, he reported this work in the following words:

> I now turn to a photograph of the lighter elements; here we find the lines of helium, of neon (very strong), of argon, and in addition, there is a line corresponding to an atomic weight twenty-two, which cannot be identified with the line due to any known gas.

Different types of positive ray parabola instruments used by Thomson are shown in Fig. 2—a, b, c.

Additional support for the complexity of neon was obtained by Aston[16] in the same year by making density measurements on atmospheric neon which had been subjected to fractional diffusion. It was not until after the war in 1919, however, that definite proof of the existence of an isotope of neon of mass twenty-two was obtained. This Aston[17] did using a new type of positive ray apparatus which he named a mass spectrograph. A schematic diagram of this instrument is shown in Fig. 3.

In a very short time, by means of this mass spectrograph and later improved instruments,

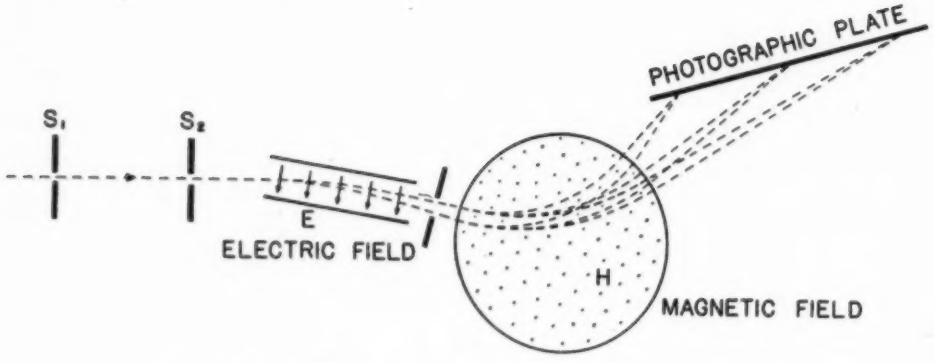

FIG. 3. Schematic diagram of Aston's first mass spectrograph.

Aston[18] was able to show that most of the elements were complex, having in some cases as many as ten isotopes, and in addition, he was able to obtain fairly accurate measurements of their abundances. Calculations of atomic weights using these measurements gave excellent agreement for those cases which are characterized by fractional values.

As an example, the stable isotopes, their abundances and masses as now known, are listed in columns seven, eight and nine, Table I. The corresponding values of the atomic weights calculated by means of these values are listed in the last column. The close agreement between the two sets of values, i.e., those obtained by physical methods (column ten) and those obtained by chemical methods (column six) leaves little to be desired.

MASS SPECTROMETERS

At this stage, the casual observer might have been inclined to think that little of interest remained to be done, but the study of isotopes has, up to the present, ever been an exciting, profitable, and expanding field for research.

The measurement of isotopic masses is important not only as a means of determining the atomic weight of an element, but also because of the Einstein relation that mass is equivalent to energy. In transmutation investigations, to men-

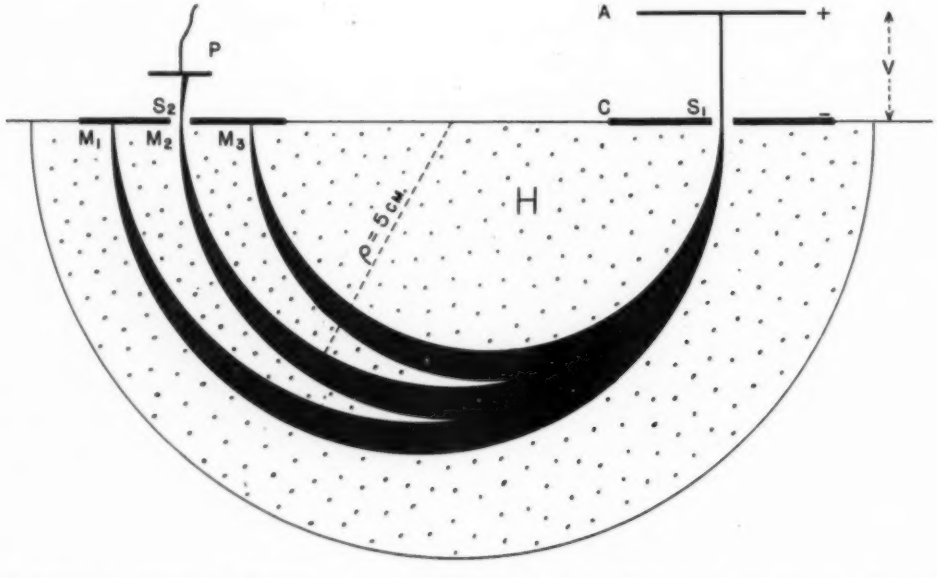

FIG. 4. Schematic diagram of Dempster's mass spectrometer. Dimensions are those given by Dempster in a paper published in Phys. Rev. 11, 316 (1918).

tion but one example, an accurate knowledge of masses enables one to predict those reactions which are permitted from energy considerations, and the energy that would be released in a specific reaction. Most important of all, isotopic mass is one of the few measurable quantities essential to a complete understanding of the nucleus of the atom. Accuracy in these measurements is ever to be strived for.

Spectrographs designed especially for making mass measurements have been constructed by Aston,[19] Bainbridge,[20] Dempster,[21] Bainbridge and Jordan,[22] Mattauch,[23] and Jordan.[24]

The main purpose of this paper, however, is not to trace the side of the story of isotopes dealing with mass measurements, i.e., mass spectroscopy, but rather to consider that other branch, commonly called mass spectrometry, which has to do with abundance measurements and allied work. This we will limit mainly to a discussion of the instruments.

Although relative abundance measurements can be made quite easily using a mass spectrograph in which the rays are recorded photographically (and with little alteration, may also be recorded electrically), it is not necessary to use such a complicated instrument for this type of problem, and from the point of view of operation, intensity considerations, etc., it is even better to use a more compact, simple apparatus.

The different types of instruments which have been designed especially for this purpose are discussed in the following pages.

π RADIAN SPECTROMETERS

Shortly after the development of the mass spectrograph by Aston, Dempster[25] constructed an instrument which was fundamentally simpler, and which was well-suited for making abundance determinations, although it could not be used for making accurate mass measurements. The method employed was essentially the same as that previ-

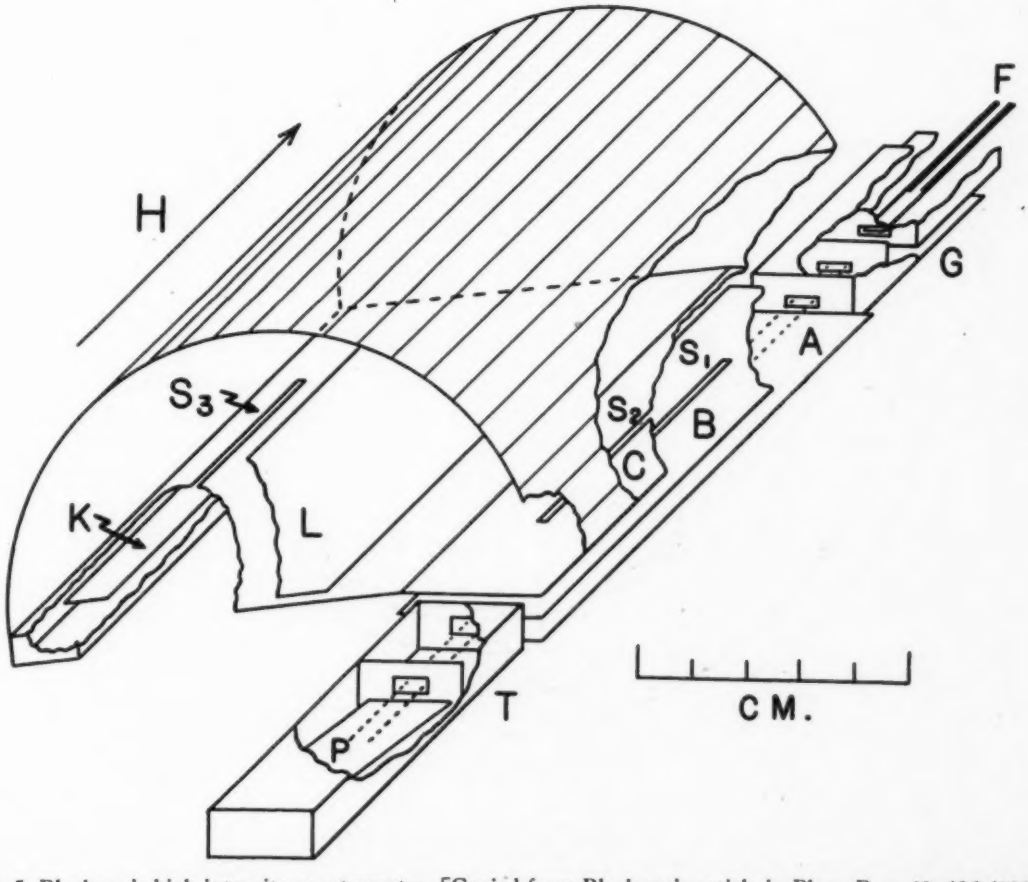

FIG. 5. Bleakney's high intensity spectrometer. [Copied from Bleakney's article in Phys. Rev. **40**, 496 (1932).]

ously used by Classen[26] in determining the ratio of charge to mass for electrons.

A schematic diagram of Dempster's spectrometer is shown in Fig. 4.

Ions of the elements investigated were formed either by heating a salt of the element or by electron bombardment. Upon emerging from the source A (Fig. 4), these ions were accelerated through a definite potential difference V by an electrical field maintained in the region between A and C. A slit S_1 in plate C, allowed a narrow bundle of them to pass on into the region of the magnetic field H.

Since in a uniform magnetic field arranged as in this case ions are bent in semi-circles with radii of curvature proportional to their respective momenta, and since upon emerging from the slit S_1 they all had the same energy, the incident beam was dispersed into a number of bundles (see Fig. 4), each one of which was characterized by a given mass value. By varying the potential difference V, the different bundles were, in turn, made to pass through a second slit S_2 to a collector plate P. The currents to this plate were then measured by means of an electrometer.

The elements hydrogen, lithium, magnesium, potassium, oxygen, calcium, zinc, and sodium were all investigated by Dempster[27] at this time.

In the ensuing years this type of spectrometer came into wide use not only as a means for measuring isotopic abundances, but also for studying the products of ionization and dissociation produced by electrons in gases and vapors.[28–35]

The first important change in instrument design came in 1932 when Bleakney[36] described a spectrometer which, although utilizing the π radian focusing property of a uniform magnetic field, was radically different in detail from the instrument previously used by Dempster. A cavalier drawing of this apparatus, copied from Bleakney's article, is shown in Fig. 5.

The design was an outgrowth from an earlier instrument[37] used primarily to study the forma-

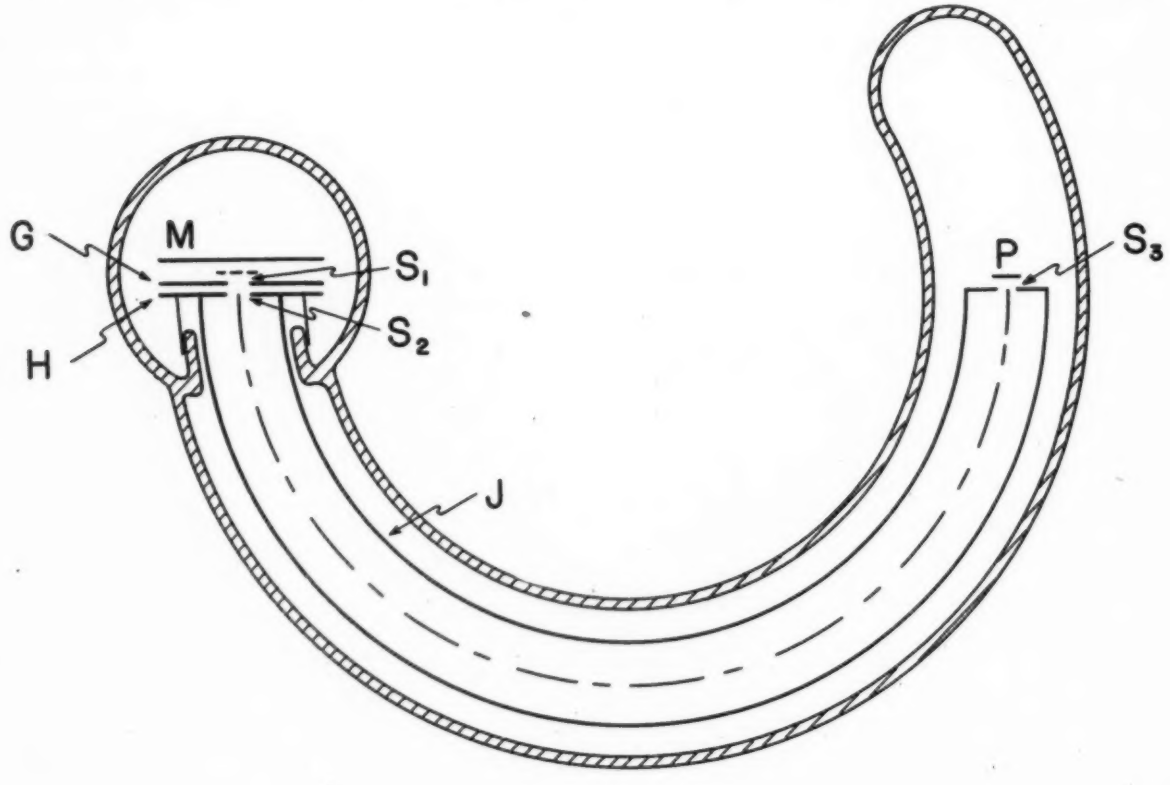

FIG. 6a. Spectrometer used by Tate, Smith, and Nier. [Copied from Nier's paper, Phys. Rev. 50, 1041 (1936).]

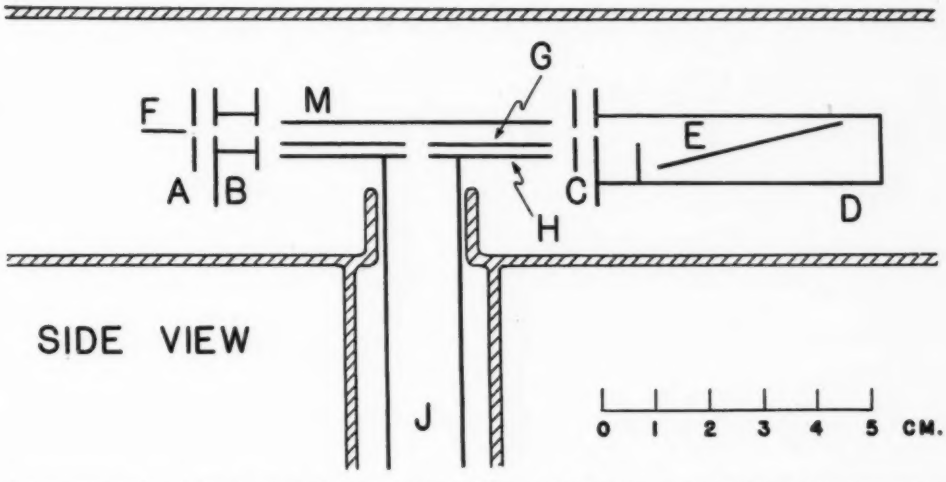

FIG. 6b. Spectrometer used by Tate, Smith, and Nier. [Copied from Nier's paper, Phys. Rev. **50**, 1041 (1936).]

tion and efficiency of production of multiply charged particles in gases and vapors. In order to gain intensity the ions were collected from a relatively long region (5.5 cm), use being made of the uniform magnetic field produced by a solenoid (field strength ~1500 Gauss). Also, contrary to previous practice, the magnetic field in the source region was not shielded out, but instead played an essential role.

Ions of the vapor or gas to be studied were created by means of an electron beam (indicated by dotted lines in Fig. 5) which, moving parallel to the magnetic field, was kept accurately aligned with the rest of the apparatus by this field, even in the presence of an electric field. A weak electric field, maintained between the plates A and B, served to accelerate the ions so formed toward the slit S_1 and those which passed through this slit were again accelerated by a stronger field (20–40 volts/cm) between the plates B and C. The emerging ion beam, now collimated by slits S_1 and S_2, was dispersed by the magnetic field as previously described, the component mass bundles being separated out and brought to a focus after traversing an angular path of approximately π radians (effective radius ≃3.5 cm). Here again the total accelerating potential V was varied in order to collect the ions at the plate K. The entire assembly was mounted within an evacuated glass bulb and could be baked out thoroughly before a run was made.

This type of apparatus has served as a model for many of the instruments constructed and used in the last ten years. Tate, Smith, and Vaughan[38] used a very similar instrument (effective radius ≃3.5 cm) to measure the ionization potential of nitrogen and to study the products of ionization and dissociation in various gases. Some abundance measurements were also made at the same time. Later, automatic recording was added as an additional feature by P. T. Smith, Lozier, L. G. Smith, and Bleakney.[39] Urey has also made use of this type of spectrometer as an aid in isotopic concentration work, and recently it has been used by Rittenberg, Keston, Rosebury, and Schoenheimer[40] in biological tracer studies.

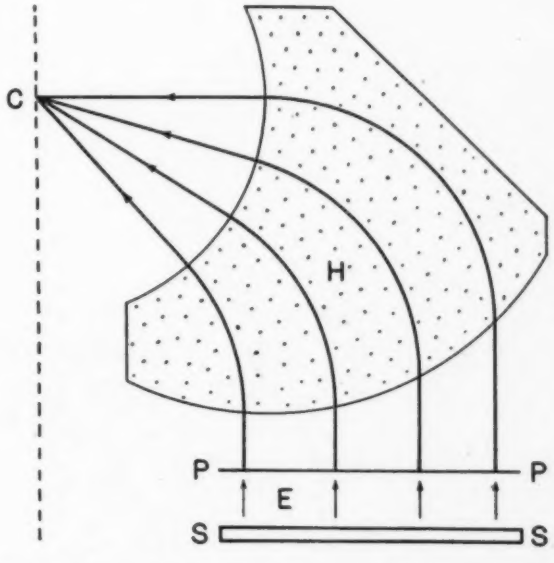

FIG. 7. Schematic diagram of magnetic lens spectrometer designed for collecting small quantities of isotopes.

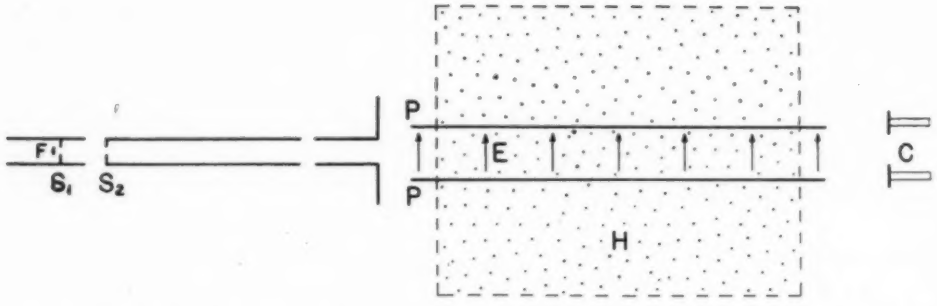

FIG. 8. Schematic diagram of the crossed field spectrometer used by Oliphant, Shire, and Crowther. [See diagram in Proc. Roy. Soc. **A146**, 922 (1934).]

One variation which has proven to be very effective is that used by Tate and P. T. Smith[41] and later by Nier[42] to study the heavier elements. Differing principally in size, this type is in effect only a short section of Bleakney's high intensity spectrometer. The construction was greatly simplified by this change, however, and at the same time magnetic fields of greater intensity, produced by electromagnets and other special arrangements such as the spherical coil constructed by Hipple,[43] could be used. A sketch of this type is shown in Fig. 6 a, b.

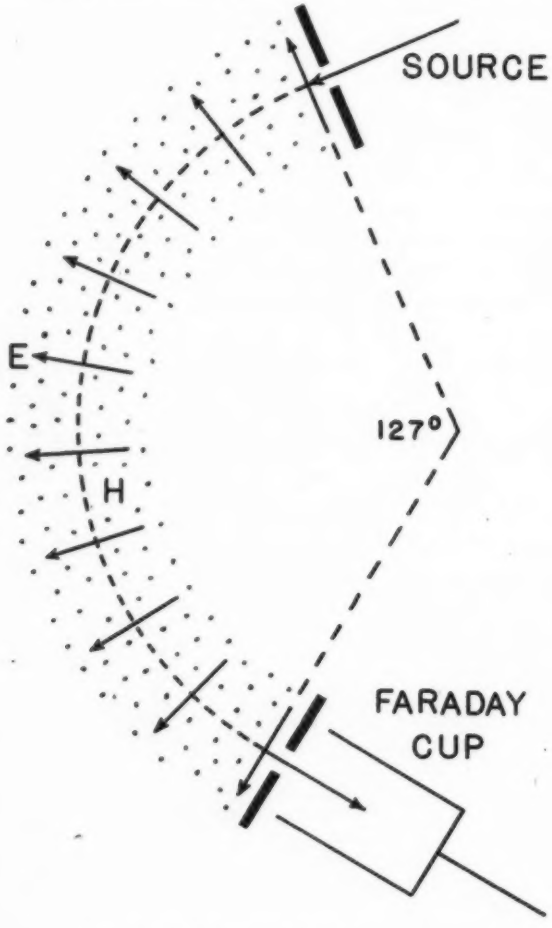

FIG. 9. Radial crossed field spectrometer.

MAGNETIC LENS SPECTROMETER

While the methods previously described are very good for determining abundance ratios and for studying associated problems, they are not, in general, satisfactory for collecting large quantities of a particular isotope. On the other hand, the only known method of preparing a pure isotopic sample when three or more isotopes are present is that of mass spectrometry. The first spectrometer designed primarily for separation purposes was reported by Smythe, Rumbaugh, and West[44] in 1934.

Radically different, and much more complicated than the π radian type of spectrometer, this instrument was designed to concentrate ions from an extended source 30 sq. cm in area, and at the same time to separate them out according to mass. Figure 7 is a schematic diagram of the arrangement used.

Ions from the source *SS* were first accelerated in an electrical field (between the plates *P* and *S*) to form a beam homogeneous in direction and energy. They were then sent through a uniform magnetic field lens, whose boundaries were shaped so that all particles of a certain mass would be focused on a slit beyond the field (see Fig. 7). Isotopic currents of the order of magnitude of 0.1 milliampere were obtained, and samples weighing a milligram could be collected in seven hours. This instrument was later used by Smythe and Hemmendinger[45] to collect sam-

ples of the potassium isotopes, and Rumbaugh,[46] using a similar instrument, collected the lithium isotopes in sufficient quantity (200 micrograms of Li^7, 18 micrograms of Li^6) for disintegration purposes.

CROSSED FIELD SPECTROMETERS

In the last few years, a number of spectrometers employing the combined action of crossed electric and magnetic fields have been constructed. Included in this class are instruments reported by M. L. Oliphant, E. S. Shire, and B. M. Crowther;[47] H. Bondy, G. Johannsen, and K. Popper;[48] and by W. Bleakney and J. A. Hipple, Jr.[49]

Oliphant, Shire, and Crowther used a straight tube arrangement in which ions of a given energy were directed through a slit system into crossed fields as shown in the schematic diagram, Fig. 8. When the slit openings lie on a straight line as they do in this case, the combined fields act as a velocity filter since the two forces, i.e., electric and magnetic, are in opposite directions, and since one of these forces, the magnetic, depends upon the velocity of the charged particles. Consequently, a constant energy ion beam entering such a device is broken up into its component parts, and those component mass beams which do not have the critical velocity are deflected to one side. This instrument was designed and used primarily for collecting small quantities (5×10^{-8} g) of the lithium isotopes for disintegration purposes.

The idea of using crossed fields as a velocity filter for ions, however, was well known long before this, and indeed was used quite effectively in several earlier instruments. Bleakney used it in an instrument, already referred to,[37] for studying the efficiency of production of multiply charged ions. Later the idea was employed in a mass spectrograph constructed by Bainbridge.[20] Although some abundance measurements were made with this latter instrument, it was used mainly for accurate mass determinations.

To go into the details of the precision mass spectrographs such as this one and others already referred to[19–24] is quite beyond the scope of this paper. Although as previously mentioned, these instruments can, with very little alteration, be used for making accurate abundance determinations, they are more valuable as instruments when used to determine that very important quantity "isotopic mass."

The crossed field spectrometer constructed by H. Bondy, G. Johannsen, and K. Popper[48] was designed to obtain both velocity and direction focusing. Instead of a uniform electric field as used in the velocity selector, a radial electric field, maintained between the plates of a cylindrical condenser and directed away from the center of curvature, was employed (see Fig. 9). The uniform magnetic field, which field gave rise to the predominant force on the ions, was perpendicular to the electrical field and oriented so that the force due to it was, for the central ion beam, oppositely directed. The isotopes of a given substance were investigated by keeping the initial

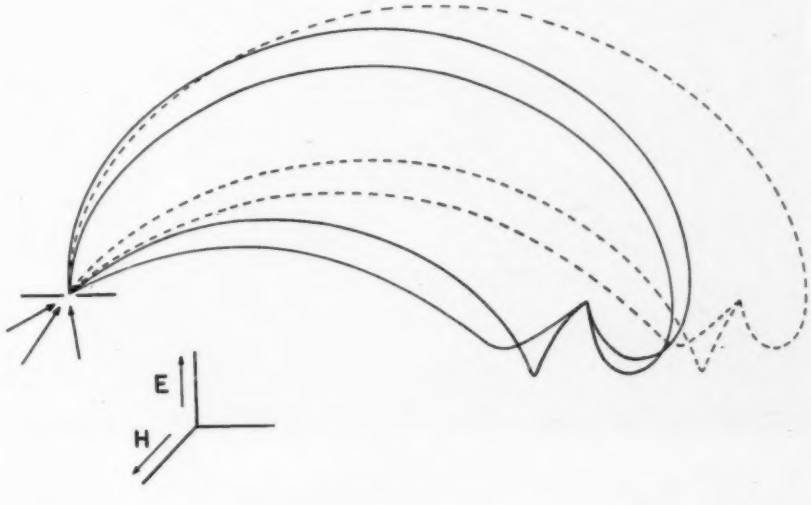

FIG. 10. Ion paths in crossed field spectrometer used by Bleakney and Hipple. [See W. Bleakney and J. A. Hipple, Jr., Phys. Rev. 53, 521 (1938).]

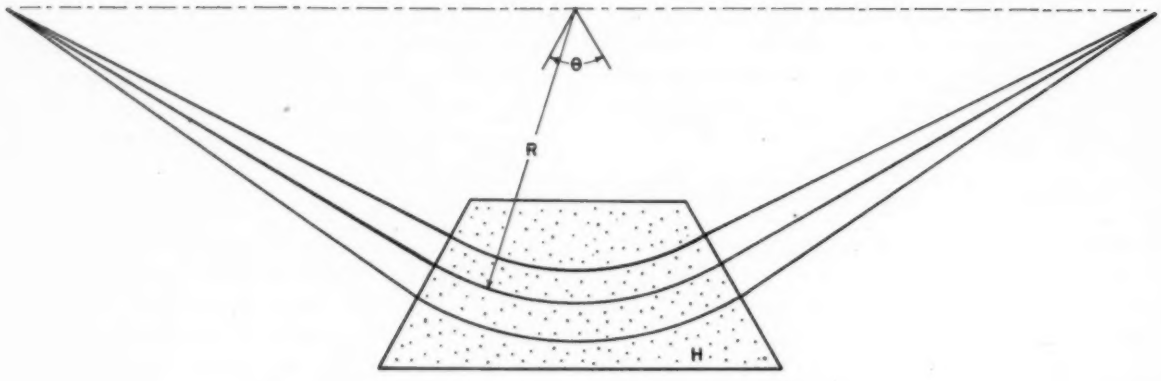

FIG. 11. Refocusing produced by truncated sector shaped field.

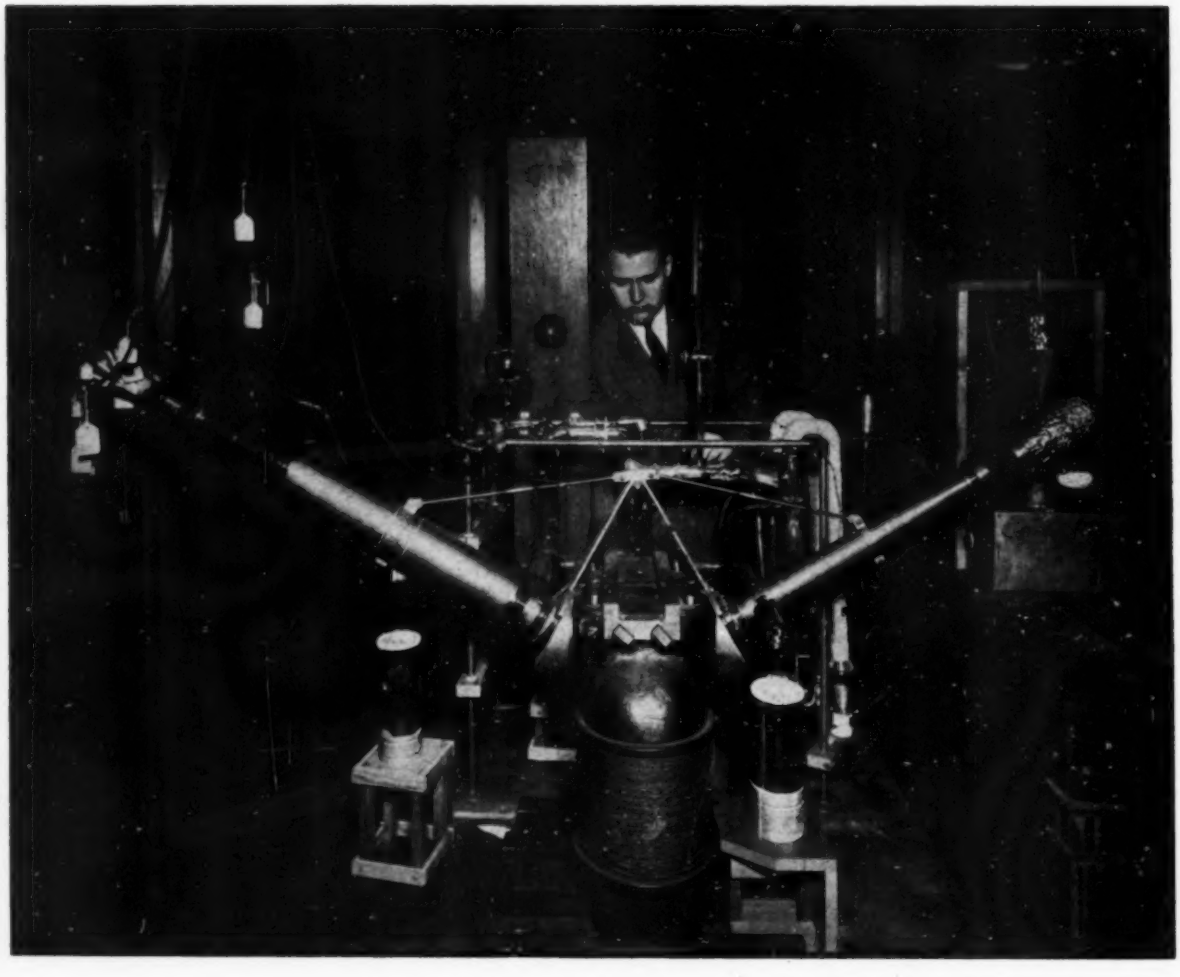

FIG. 12. University of Illinois spectrometer.

ion accelerating potential V constant, the radial electrical field E constant, and by varying the magnetic field H. The theoretical details for this arrangement may be found in an earlier paper published by Bartky and Dempster.[50]

Another crossed field instrument recently reported by Bleakney and Hipple[49] was designed to give double focusing over a wide range of initial velocities and directions. Although both fields are uniform, the incident ion beam direction and consequently the ion paths are quite different from those in any of the cases previously mentioned. In Fig. 10, two sets of paths, representing ions having two different m/e values, and incident directions varying over a wide angle are shown. This instrument has been used primarily to study the dissociation of various gases by electron impact.

SECTOR SPECTROMETERS

In 1933, Barber[51] pointed out that if the central beam of a diverging bundle of ions enters and leaves a uniform magnetic field normal to the pole edges, the ions are brought to a focus on a line extended from the source through the center of curvature of the central beam. (See Fig. 11.) A particular case is the 180° refocusing already discussed.

In view of this general property, the possibilities for sector shaped fields are practically unlimited, and to date they have been used in many different investigations. To mention just a few, W. E. Stephens,[52] in 1934, used a 90° sector refocusing field as an electron lens to verify the theory; Later in 1936, a 60° sector field was used by Bainbridge and Jordan as part of a double focusing mass spectrograph.

The first use of the sector field in mass spectrometry, however, was reported in 1940 by Nier.[53] Using the now common electron beam type of source, Nier was able to obtain fairly high resolution with an inexpensive magnet. The construction of the spectrometer tube proper was also greatly simplified by using metal to glass seals.

Although very satisfactory for the purposes intended, i.e., to measure differences in the relative abundance of isotopes in samples obtained from various sources, the author cautions[54] us

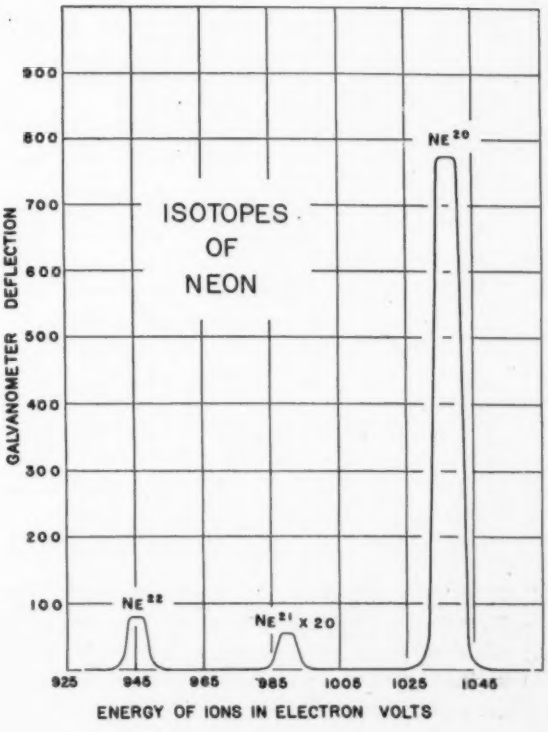

FIG. 13. Neon peaks (preliminary run).

that it is not satisfactory for determining absolute abundance ratios owing to possible discriminations in the spectrometer. Any constant error in the absolute values, however, is believed to be small, e.g., less than 2 percent in the C^{12} to C^{13} ratio.

Recently, in an instrument designed to be free from possible discriminations, N. D. Coggeshall[55] has also utilized a 60° sector focusing field. Using a new source arrangement, it was possible to eliminate the auxiliary magnetic field usually maintained in the source region to keep the electron beam in alignment. The entire construction is of metal, and the source as a separate unit, can readily be removed from the rest of the apparatus. A picture of the spectrometer is shown in Fig. 12 and a plot of the neon peaks obtained with it in Fig. 13.

While no attempt has been made to cover every spectrometer which has been reported to date, we have endeavored to include those types which have proven to be most useful.

To Professor Goldhaber, who has carefully read the manuscript, we wish to express our appreciation.

BIBLIOGRAPHY

(1) Dalton, *Foundations of the Atomic Theory*, Alembic Club Reprint No. 2.

(2) Dalton, *New System of Chemical Philosophy* (Manchester 1808), pp. 211–220. Reprinted in the Alembic Club series reprint No. 2.

(3) Meinecke, J. d. Pharmacie (Trommsdorff) **25** (1816) Sec., Part. 72, pp. 200–202. Reprinted in the Alembic Club series No. 20, p. 8.

(4) T. W. Richards, *Determination of Atomic Weights* (Carnegie Institution of Washington, 1910).

(5) H. Becquerel, Comptes rendus **122**, 420 (1896).

(6) P. and M. S. Curie, Comptes rendus **127**, 175, 1215 (1898).

(7) See, for example, the book *The Interpretation of the Atom* by F. Soddy.

(8) Boltwood, Am. J. Sci. **22**, 537 (1906); **24**, 370 (1907).

(9) Keetman, Jahr Radioactivitag **6**, 269 (1909).

(10) Marckwald, Ber. d. chem. Ges. **40**, 3420 (1910).

(11) F. Soddy, Chem. Soc. Ann. Rep., 285 (1910).

(12) F. Soddy, Chem. Soc. Ann. Rep., 285 (1910).

(13) Russell and Rossi, Proc. Roy. Soc. **A77**, 478 (1912).

(14) Rutherford and Andrade, Phil. Mag. **27**, 854 (1914).

(15) F. Soddy, "The radio elements and the periodic law," *Report of the British Association for the Advancement of Science* (1913), p. 445.

(16) F. W. Aston, *Report of the British Association for the Advancement of Science* (1913), p. 403.

(17) F. W. Aston, Phil. Mag. **38**, 709 (1919).

(18) F. W. Aston, *Mass Spectra and Isotopes* (first edition).

(19) F. W. Aston, Proc. Roy. Soc. **163**, 391 (1937).

(20) K. T. Bainbridge, Phys. Rev. **40**, 130 (1932).

(21) A. J. Dempster, Proc. Am. Phil. Soc. **75**, 755 (1935).

(22) K. T. Bainbridge and E. B. Jordan, Phys. Rev. **50**, 282 (1936).

(23) J. Mattauch, Phys. Rev. **50**, 617 (1936).

(24) E. B. Jordan, Phys. Rev. **57**, 1072 (1940).

(25) A. J. Dempster, Phys. Rev. **11**, 316 (1918).

(26) Classen, Jahrb. d. Hamburg Wiss. Anst. (Buheft, 1907).

(27) A. J. Dempster, Phys. Rev. **18**, 415 (1921); **20**, 631 (1922).

(28) H. A. Barton, Phys. Rev. **30**, 614 (1927).

(29) H. D. Smythe, Phys. Rev. **25**, 452 (1925).

(30) T. R. Hogness and R. W. Harkness, Phys. Rev. **32**, 936 (1928); **32**, 784 (1928); **32**, 942 (1928).

(31) H. A. Barton and J. H. Bartlett, Jr., Phys. Rev. **31**, 822 (1928).

(32) K. T. Bainbridge, Phys. Rev. **34**, 752 (1928).

(33) A. K. Brewer and P. D. Kueck, Phys. Rev. **46**, 894 (1934).

(34) M. B. Sampson and W. Bleakney, Phys. Rev. **50**, 456 (1936).

(35) H. Brown, J. J. Mitchell, and R. D. Fowler, Rev. Sci. Inst. **12**, 435 (1941).

(36) W. Bleakney, Phys. Rev. **40**, 496 (1932).

(37) W. Bleakney, Phys. Rev. **34**, 157 (1929); **35**, 139 (1930).

(38) J. T. Tate, P. T. Smith, and A. L. Vaughan, Phys. Rev. **48**, 525 (1935).

(39) P. T. Smith, W. W. Lozier, L. G. Smith, and W. Bleakney, Rev. Sci. Inst. **8**, 51 (1937).

(40) D. Rittenberg, A. S. Keston, F. Rosebury, and R. Schoenheimer, J. Biol. Chem. **127**, 291 (1939).

(41) J. T. Tate and P. T. Smith, Phys. Rev. **46**, 773 (1934).

(42) A. O. Nier, Phys. Rev. **50**, 1041 (1936); **52**, 933 (1937).

(43) J. A. Hipple, Jr., Phys. Rev. **55**, 597 (1939).

(44) W. R. Smythe, L. H. Rumbaugh, and S. S. West, Phys. Rev. **45**, 724 (1934).

(45) W. R. Smythe and A. Hemmendinger, Phys. Rev. **51**, 178 (1937).

(46) L. H. Rumbaugh, Phys. Rev. **49**, 882 (1936).

(47) M. L. Oliphant, E. S. Shire, and B. M. Crowther, Proc. Roy. Soc. **A146**, 922 (1934).

(48) H. Bondy, G. Johannsen, and K. Popper, Zeits. f. Physik **95**, 46 (1935).

(49) W. Bleakney and J. A. Hipple, Jr., Phys. Rev. **53**, 521 (1938).

(50) W. Bartky and A. J. Dempster, Phys. Rev. **33**, 1019 (1929).

(51) N. F. Barber, Proc. Leeds Phil. Soc. **2**, 427 (1933).

(52) W. E. Stephens, Phys. Rev. **45**, 513 (1934).

(53) A. O. Nier, Rev. Sci. Inst. **11**, 212 (1940).

(54) B. F. Murphey and A. O. Nier, Phys. Rev. **59**, 771 (1941).

(55) N. D. Coggeshall, Bull. Am. Phys. Soc., Baltimore meeting, 1942, A37; N. D. Coggeshall and E. B. Jordan, to be published soon.

Measurement of Relative Abundance with the Mass Spectrometer

BY E. B. JORDAN AND N. D. COGGESHALL
University of Illinois, Urbana, Illinois

This paper covers the general methods employed in mass spectrometry, machine design, and possible sources of error in relative-abundance measurements which are inherently associated with instrument design. Also included are graphs for determining the critical constants of the usual types of instruments.

INTRODUCTION

THE variety of problems which have recently been studied with the aid of a "relative-abundance" spectrometer makes apparent the growing importance of this instrument in a modern physics laboratory. Not only as an instrument for measuring the natural abundances[1,2] of the isotopes of an element and for studying the products of ionization and dissociation by electron impact[3] may it be used, but also to study the fine variations[4] in isotopic abundances as related to the origin of the element, to search for faint missing isotopes, and to separate isotopes[5] in quantities sufficient for disintegration experiments. It is also an indispensable instrument in the study of methods of separating isotopes[6] and in problems involving the use of separated isotopes as tracers.[7]

As is well known, the mass spectrograph as well as the mass spectrometer can be used for making abundance measurements, and indeed the majority of isotopes as now known were first discovered and their abundances measured by Dr. Aston using a mass spectrograph. Since the problems have now become more specialized, it is more satisfactory to use a spectrometer for abundance measurements and to design a mass spectrograph* primarily for mass measurements, the latter instrument being of inestimable value for this purpose alone. On the other hand, the abundance spectrometer, although it cannot in any way be used for mass measurements, is designed primarily for the types of problems listed above and is a much simpler instrument to construct, easier to use, and much less expensive.

When used for abundance measurements, a mass spectrograph is inconvenient since a photographic plate is employed to record the different isotopic ions and the procedure of determining abundances from the plate traces is both more tedious and less reliable than the direct measurements made with a mass spectrometer. This is the case since the density of the image produced on the plate is an unknown function of the intensity of the corresponding ion beam, and it is necessary to make a number of tests, none of which is conclusive separately, before a correct interpretation may be reached. In addition, the ions follow entirely different paths and consequently corrections have to be made for the line breadths.

The abundance spectrometer method of making these measurements, however, is both comparatively easy and quite reliable once the apparatus is set up and working. In this method the isotopic ions are made to follow approximately the same paths and the isotopes are recorded electrically by means of an electrometer tube, the relative heights of the peaks indicating the relative numbers of the isotopes present. With this instrument, it is also possible to measure the ionization potential and the shape of the ionization probability curve for any particular ion, information which is important as evidence for or against the existence of a particular species.

* Recently, when money was granted by the Graduate School Research Board of Illinois for building up a research laboratory in mass spectroscopy, it thus appeared more desirable, in view of these considerations, to build a separate machine for making relative abundance measurements and to use the new mass spectrograph (see reference 8) exclusively for mass measurements. A description of this new spectrometer will be published shortly.

Since the peaks are plotted one at a time and several minutes are required to record the complete spectrum of an element, it does, however, require a steady source of ions.

ION SOURCES

A survey of existing spectrometers[9–13] revealed the interesting fact that in every case the ions are drawn from a region in which there is a crossed electric and magnetic field. In most cases the source region is in the same uniform magnetic field that is used to resolve the ions after they leave the source. In those instruments[12] in which this is not the case, an auxiliary magnetic field is supplied by means of a small horseshoe magnet. Even when it does not occur naturally, the presence of a magnetic field in this region is essential to the particular arrangements used. On the other hand, its presence leads to a number of inconveniences, especially in the case of the sector type magnetic field instruments, as well as to a number of small systematic errors, which combined probably amount to no more than one or two percent, depending of course upon the magnitude of the isotopic abundance ratio and the mass difference. For comparison, a brief description of the different arrangements in common use is included.

The most general arrangement is that shown in Fig. 1. The ions are created by means of an electron beam BB which is moving in a direction perpendicular to the plane of the figure and parallel to the magnetic field. A gas pressure of approximately 10^{-4} mm Hg is usually maintained within this region. The longer sides of the slits S_1, S_2 are also parallel to the magnetic field and thus to the direction in which the electrons are moving. Ions which are formed in the region BB are accelerated towards the slit S_1, by means of a weak electric field E_1 (20 to 30 volts/cm). A second acceleration then takes place between the plates P_1 and P_2 in which region they acquire from 300 to 1000 electron-volts energy. After passing through S_2, the ions may either be bent in a circle by the same uniform magnetic field H, coming to a focus at different positions along the plane S_2F a distance away equal to twice the radius of curvature, or else they may be directed through a neutral region into a V-shaped magnetic field, the focusing properties of which have been discussed by Barber,[14] and Stephens and Hughes.[15]

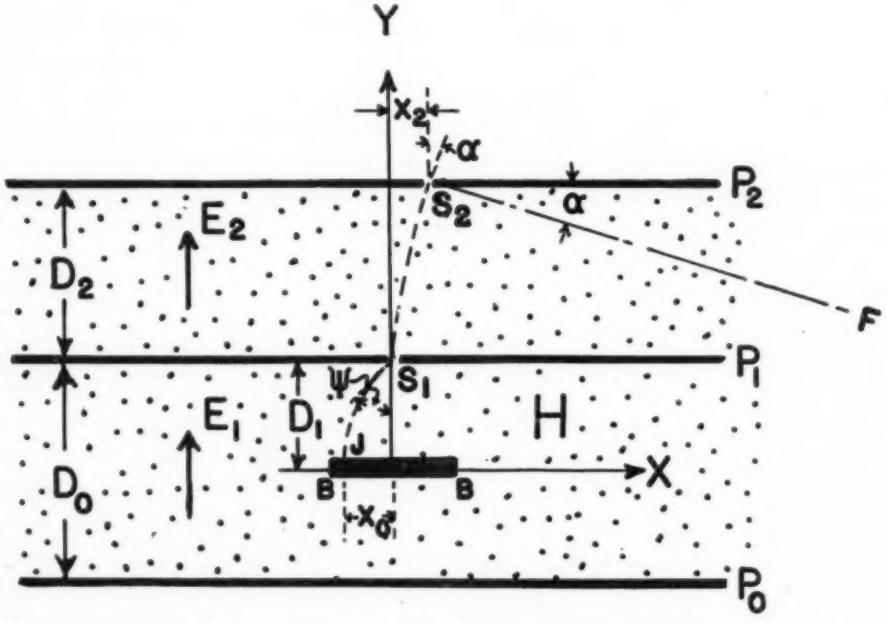

FIG. 1. Schematic cross-section diagram of a crossed field spectrometer source: BB represents the cross section of the electron beam which is used to create the ions; D_1 represents the perpendicular distance from the plane of the beam to the plane of the slit S_1; P_0, P_1, and P_2 are the plates across which the accelerating potentials are placed; JS_1S_2 is an exaggerated representation of the path of an ion starting from rest in the plane of the electron beam. The magnetic field H is assumed to be pointing out of the paper.

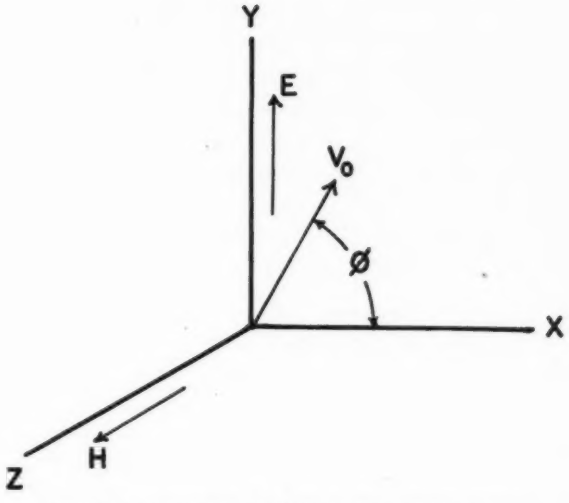

FIG. 2. Arrangement of fields in the source region.

A. Electron Beam

The first problem which is of interest is to find the shape of the electron beam BB which is used to create the ions. It is important to know the shape of this beam and whether or not it is influenced appreciably by the electric and magnetic fields since it determines the origin and the conditions under which the ions originate.

Figure 2 is a diagram showing the particular arrangement of fields in the source region. V_0 represents the component of the initial velocity of a charged particle in the xy plane, and ϕ the angle that V_0 makes with the x axis. The path of a charged particle in such a combination of fields has been discussed by a number of authors.[16,17] As is well known, its projection on the xy plane is a cycloid, the particular type of cycloid being determined by the initial conditions. The parametric solutions of the differential equations representing this motion are:

$$x=-\frac{V_0}{\gamma}\sin(\phi-\gamma t)+\frac{1}{\gamma}\left(V_0\sin\phi-\frac{Ec}{H}\sin\gamma t\right)+\frac{Ec}{H}t+x_0, \quad (1)$$

$$y=\frac{V_0}{\gamma}\cos(\phi-\gamma t)-\frac{1}{\gamma}\left(V_0\cos\phi+\frac{Ec}{H}\cos\gamma t-\frac{Ec}{H}\right)+y_0. \quad (2)$$

E represents the electric field strength in e.s.u., H the magnetic field strength in e.m.u., t the time in seconds, and γ is defined by the relation

$$\gamma=eH/Mc, \quad (3)$$

where e, M, and c represent the charge in e.s.u., M the mass of the charged particle in grams, and c the velocity of light in cm/sec.

For convenience, let us assume that the incident electron beam is not diverging and that it is moving parallel to the magnetic field H. As no force is exerted in the direction of the magnetic lines of force and since there is no component of the electric field in this direction, the motion of the electrons parallel to the Z axis is one of constant velocity. By letting $V_0=0$ in Eqs. (1) and (2), which is the case for a non-diverging beam, we see that the projected path of the

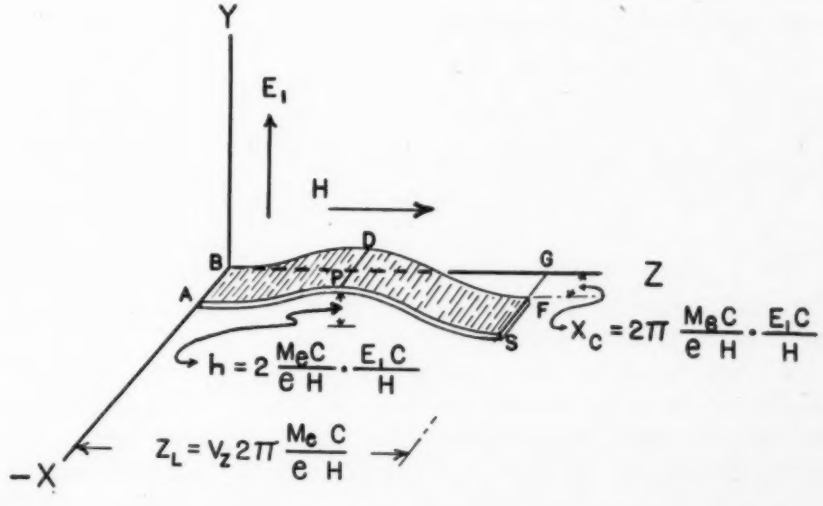

FIG. 3. Diagrammatic sketch of one loop of electron beam. The maximum height "h" of the beam as shown is greatly exaggerated in comparison to other dimensions.

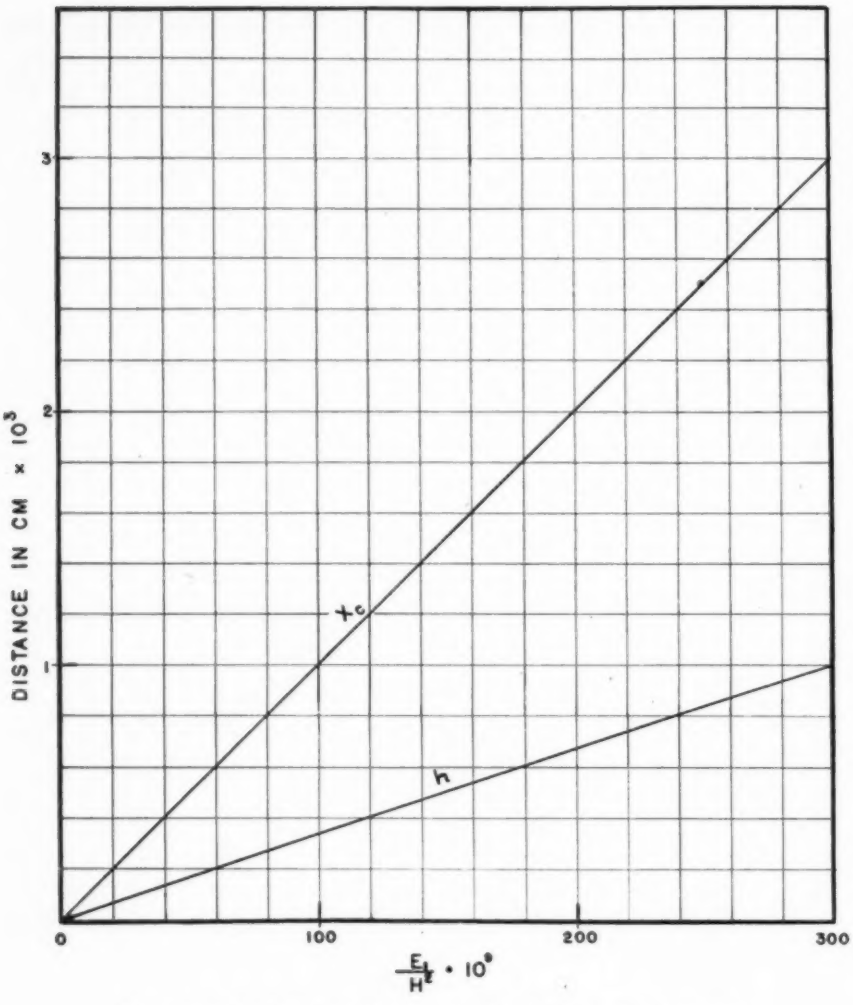

FIG. 4. Plot showing variation in x_e and h as a function of E_1/H^2.

beam on the xy plane is that of a common cycloid with cusps in the xz plane. The distance between the cusps of the projected paths is

$$x_c = 2\pi \cdot \frac{M_e c}{eH} \cdot \frac{E_1 c}{H} \text{cm} \tag{4}$$

and its maximum deviation from the xz plane is

$$h = 2 \cdot \frac{M_e c}{eH} \cdot \frac{E_1 c}{H} \text{cm}. \tag{5}$$

Here M_e represents the mass of the electron and other symbols have their usual significance.

A rough sketch of one loop of a very narrow portion of this beam is shown in Fig. 3. We thus see that the beam not only shifts in position, i.e., x_e changes when either H or E (Fig. 3) is altered, but also that h and Z_L change. These variations are quite small, however, as can be seen by referring to Fig. 4 in which the magnitudes of "x_e" and "h" are plotted as a function of the field strengths. E.g., if E_1/H^2 is altered by a factor of 300, the changes in "x_e" and "h" are 0.003 cm and 0.001 cm, respectively. In practice, the variation in this factor is no more than a few percent. Variations in the beam position of this order of magnitude introduce small errors in a relative abundance measurement which, for the most part, are negligible.

The distance "BG" (Fig. 3) can be determined from the expression "BG" $= Z_L = V_Z 2\pi M_e c/eH$, where V_Z is the component of the initial velocity along the Z axis. For 100-volt electrons and a field strength $H = 2000$ gauss, "Z_L" $= 1$ mm. Thus there are several of these loops in a distance equal to the length of slit S_1 (Fig. 1), which as mentioned previously is parallel to the beam direction.

In reality, the electron beam is not uniform in thickness as shown in Fig. 3, but varies from point to point since the incident beam is diverging ($V_0 \neq 0$). Assuming that V_0 is finite, small, and has a component in the y direction only, and that the beam is diverging from a line source AB in the xz plane, then under these conditions, it diverges and comes to a focus twice, once along the line PD (Fig. 3) and the second time along the line SF.

B. Ion Paths

The main characteristics of this type of source depend primarily upon the paths of the positive ions which originate within the electron beam and

which, under the influence of the field E_1 (Fig. 1), move toward the plate P_1. If second-order errors are present due to selective effects, they depend upon these paths as well as space charge conditions, and thus it is necessary to know if, for a given set of operating conditions, ions having different M/e values originate at the same point, and travel along identical paths.

If, for example, the magnetic field H or the electric field E_1 is changed in order to collect different ions, and if as a consequence the ions do not travel the same paths throughout, the effective solid angles for collection subtended by the defining slit S_1 (Fig. 1) will be different and the abundance ratio will be in error.

Furthermore, when ions of different M/e values originate at different points, then in addition to the above effect, space charge conditions, if present, will also be different.

As has been pointed out by Bainbridge,[18] when space charge conditions exist, a number of selective factors enter in, even if all the ions come from the same point.

The position x_0 (Fig. 1) of the point from which an ion of mass M will start from rest and pass through the center of slit S_1 for a given value of E_1 and H, can also be determined by means of Eqs. (1) and (2), since these equations hold for ions as well as for slow electrons if the proper value of M is used.

To find x_0 the following conditions must be satisfied; i.e., $y_0=0$ at $t=0$, $V_0=0$; and after a time t_1, $x=0$ and $y=D_1$. Putting $U_1=\gamma t_1$ in Eqs. (1) and (2), the resulting expressions are:

$$x_0/(Mc/eH)\cdot(E_1c/H)=\sin U_1-U_1, \quad (6)$$

$$\cos U_1=1-D_1/(Mc/eH)\cdot(E_1c/H). \quad (7)$$

Plots of $-x_0/(Mc/eH)\cdot(E_1c/H)$ and U_1 as functions of $D_1/(Mc/eH)\cdot(E_1c/H)$ are shown in Figs. 5 and 6. A plot of x_0 as a function of M for several sets of values of D_1, E_1, and H is shown in Fig. 7.

Thus, if E_1 and H both remain fixed, the

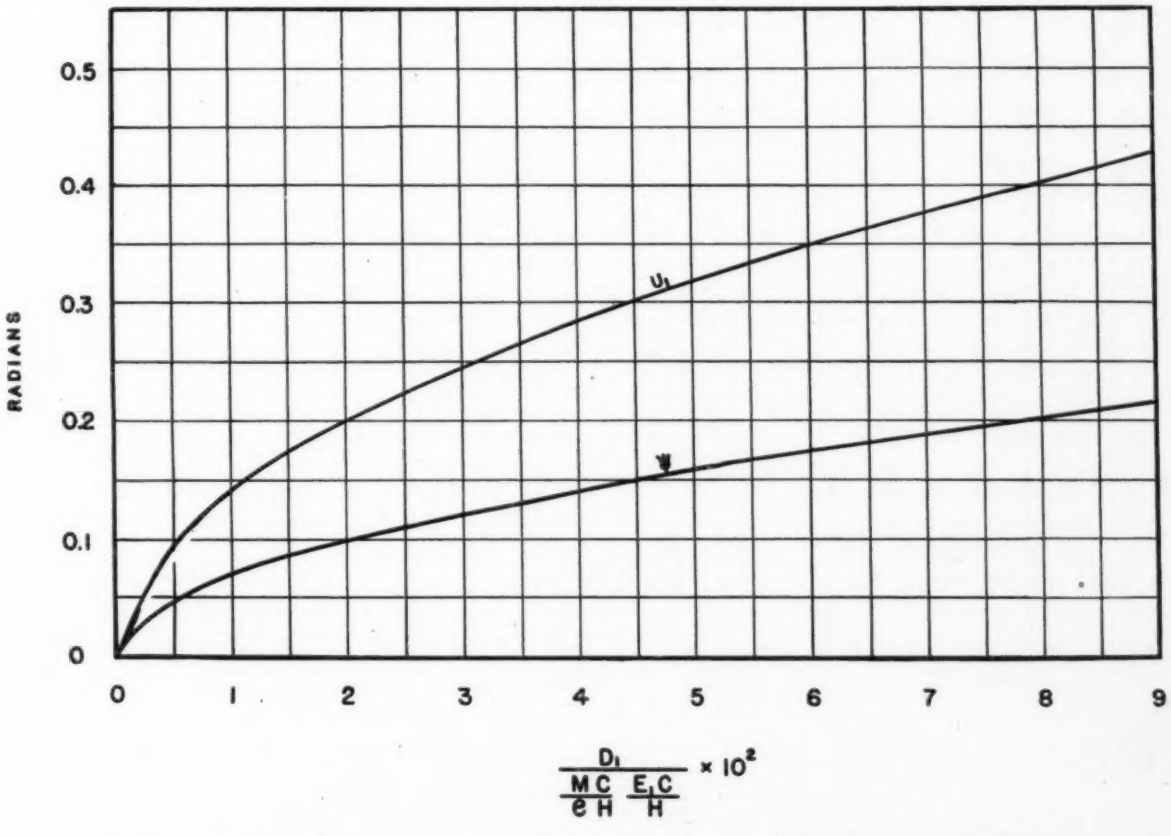

FIG. 5. Plot showing U_1 and ψ as a function of $D_1/(Mc/eH)\cdot(E_1c/H)$.

different isotopic ions which pass through slit S_1 originate at different positions x_0 depending upon their mass M. In one sense this feature may be considered a disadvantage of this type of instrument since if the method[19] of comparing two isotopic peaks at the same time is used it is subject to criticism, the positions at which the different ions originate being slightly different.

For isotopic ions, however, ΔM is seldom greater than four or five units, and thus the difference in position of ion origin is seldom more than a thousandth of a cm. The corresponding error introduced into an abundance measurement is difficult to calculate if varying space charge conditions are present. However, considering selective effects alone, it is only a small fraction of one percent.

In this connection, it is worth noting that when the method of simultaneous comparison of two isotopic beams is used, extreme caution must be exercised that there are no limiting slits between the last source slit and the collector slits, since the paths of the ions are quite different after they leave the source.

When the ion beams are studied one at a time, however, it is possible to make the starting points x_0 the same for ions having different values of M/e by varying H or E_1 in a given manner. If, for example, the magnetic method of collection is used and different isotopic beams are brought to the collector by varying the magnetic field H, E_1, and D_1 having fixed values, and H is varied in such a way that H^2/M remains constant, then $(Mc/eH)\cdot(E_1c/H)$ (Eqs. (6) and (7)) also remains a constant and consequently the ions which are collected, although they have different masses, originate at the same position x_0. In those instruments in which the entire apparatus (i.e., source region and analyzer) is in the same uniform magnetic field, the condition that H^2/M be a constant is automatically satisfied since the final energy of the ions is always the same. All of the earlier instruments used by Tate, Bleakney, and Nier were of this type.

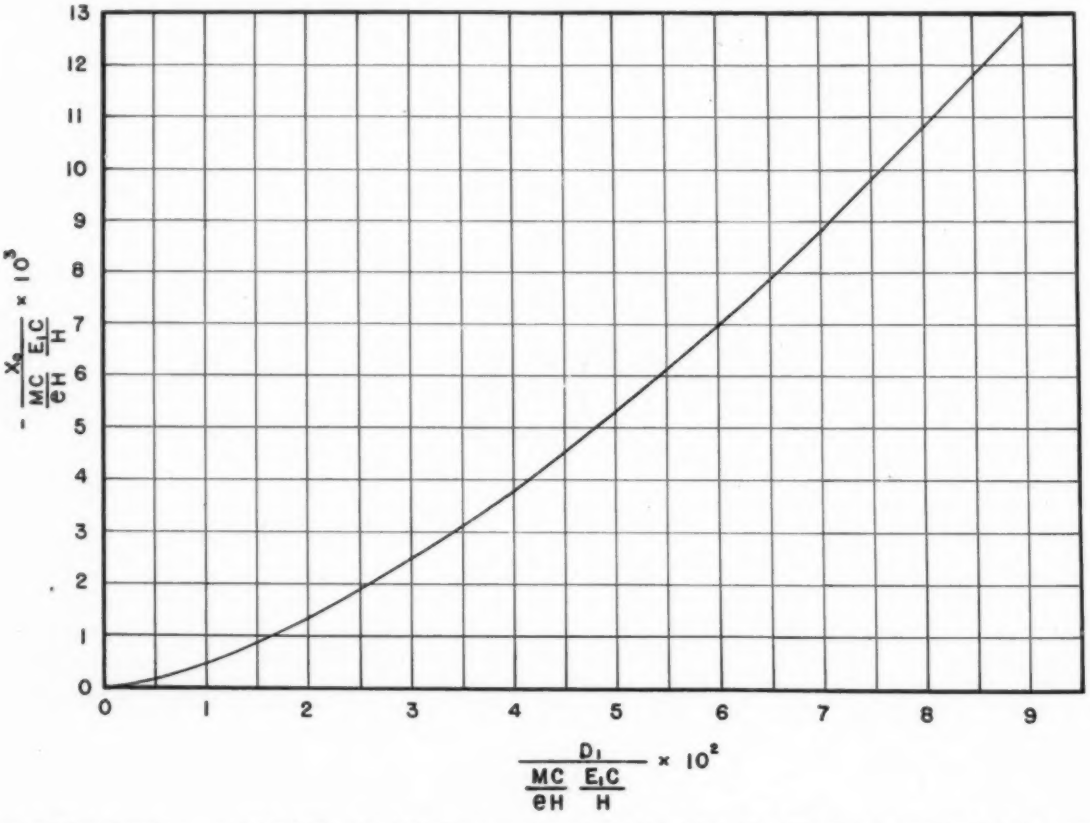

FIG. 6. Plot showing $-x_0/(Mc/eH)\cdot(E_1c/H)$ as a function of $D_1/(Mc/eH)\cdot(E_1c/H)$. x_0 is in cm, if E_1 is in e.s.u., H in e.m.u., M in grams, and D_1 in cm.

In practice the isotopes of a given element are seldom studied using this procedure, since it is difficult to vary the magnetic field in uniform steps (except in the case of a solenoid) and thus to plot the peak shapes. Usually the magnetic field is set at a given value depending on the element to be studied and the different isotopes are brought to the collector by varying the electric fields E_1 and E_2.

In this latter method, it is also possible to insure that ions of different M/e values follow identical paths, by keeping the factor E_1M a constant. If this condition is satisfied, then assuming that D_1, the perpendicular distance from the point where the ions originate to the plane of the slit S_1, remains fixed, the factor $D_1/(Mc/eH)\cdot(E_1c/H)$ (Fig. 6) also remains invariant, H being fixed, and consequently x_0 is the same for different isotopes. While this method satisfies the requirements for identical paths, it does involve the variation of the electrical field strength E_1 in the source region and possible attendant variations in space charge conditions. In addition, if the space charge conditions are altered, then D_1 is changed slightly and the paths of different ions will not be identical.

Although it is impossible to calculate such effects, they can at the most, introduce very small systematic errors only, since in practice the abundance ratio of two isotopes is always checked as a function of the electron beam current density and gas pressure within the source chamber. Also as shown previously, the effect of any reasonable change in E_1 on the shape and position of the electron beam is quite small.

Another factor which is important in this type of source is the angle ψ, (Fig. 1) between the direction of the ion motion at S_1 and the y axis. This angle not only determines the effective aperture of the slit S_1, but also is an important factor in the expression for the position of slit S_2 and for the final angle α at slit S_2, which determines the orientation of the focal plane of the instrument.

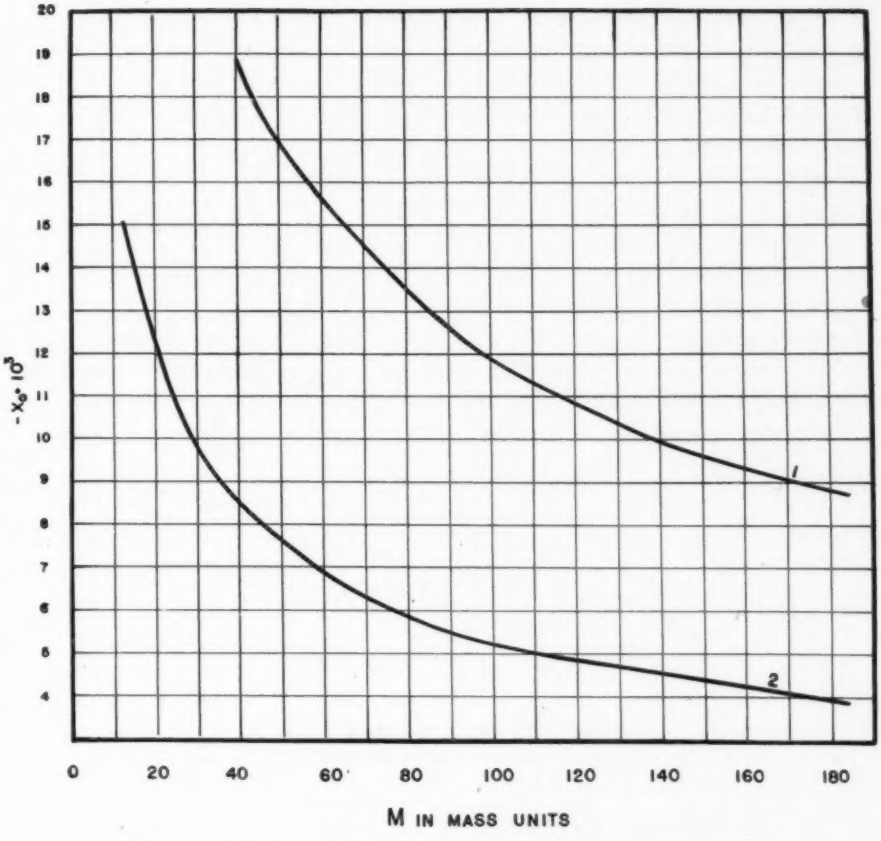

FIG. 7. Plot showing x_0 as a function of M for two sets of values of D_1, E_1, and H. For curve one, the values of these quantities are: $E_1=25$ volts/cm; $D_1=0.1$ cm; and $H=4000$ gauss. For curve two: $E_1=30$ volts/cm; $D_1=0.1$ cm; and $H=2000$ gauss.

Differentiating the equations of motion (1), (2), and substituting the proper initial conditions, the expression for ψ is found to be

$$\psi=\tfrac{1}{2}U_1, \tag{8}$$

where U_1 is the parameter corresponding to the coordinates of slit S_1 and may be determined from Eq. (7). Values of ψ as a function of $D_1/(Mc/eH)\cdot(E_1c/H)$ can be obtained from the lower curve in Fig. 5. The limiting conditions that the ions just reach the slit ($\psi=90°$, and effective aperture equal to zero) is $D_1=2(Mc/eH)(E_1c/H)$.

The fields are always chosen so that ψ is as small as possible and yet so that E_1 is not great enough to influence the electron beam appreciably. For $D_1=0.1$ cm, $E_1=25$ volts/cm, $H=4000$ gauss, and $M=100$ mass units, ψ is equal to $10°\,6'$, and the effective aperture $S_1\cos\psi$ is 98.5 percent of its maximum value.

As has been pointed out in a very simple way by Bleakney,[20] the paths of the ions between plates P_1 and P_2 introduce no additional errors providing certain conditions are satisfied. Substituting the expression found for ψ and putting $\phi=90-\psi$, $x_0=0$, $y_0=D_1$ in Eqs. (1) and (2), the parametric expressions for the ion paths become:

$$\frac{x}{\frac{Mc}{eH}\cdot\frac{E_2c}{H}}-\frac{E_1}{E_2}\sin 2\psi=\left(-\frac{E_1}{E_2}\sin 2\psi\right)\cos U+\left[\frac{D_1}{\frac{Mc}{eH}\cdot\frac{E_2c}{H}}-1\right]\sin U+U, \quad (9)$$

$$+\left[\frac{E_1}{E_2}\sin 2\psi\right]\sin U=\frac{y}{\frac{Mc}{eH}\cdot\frac{E_2c}{H}}-1. \quad (10)$$

From these equations, we see that the paths between plates P_1 and P_2 of ions having different M/e values are identical if the two factors $(Mc/eH)\cdot(E_2c/H)$ and (E_1/E_2) are held constant when either the electric or magnetic field is varied in order to collect different ions. This is the case since $(Mc/eH)\cdot(E_1c/H)$ and thus ψ (Eqs. (7) and (8)) also remain fixed under these conditions.

Both sets of conditions, i.e., for the paths between P_0 and P_1 as well as between P_1 and P_2, are automatically satisfied when the magnetic

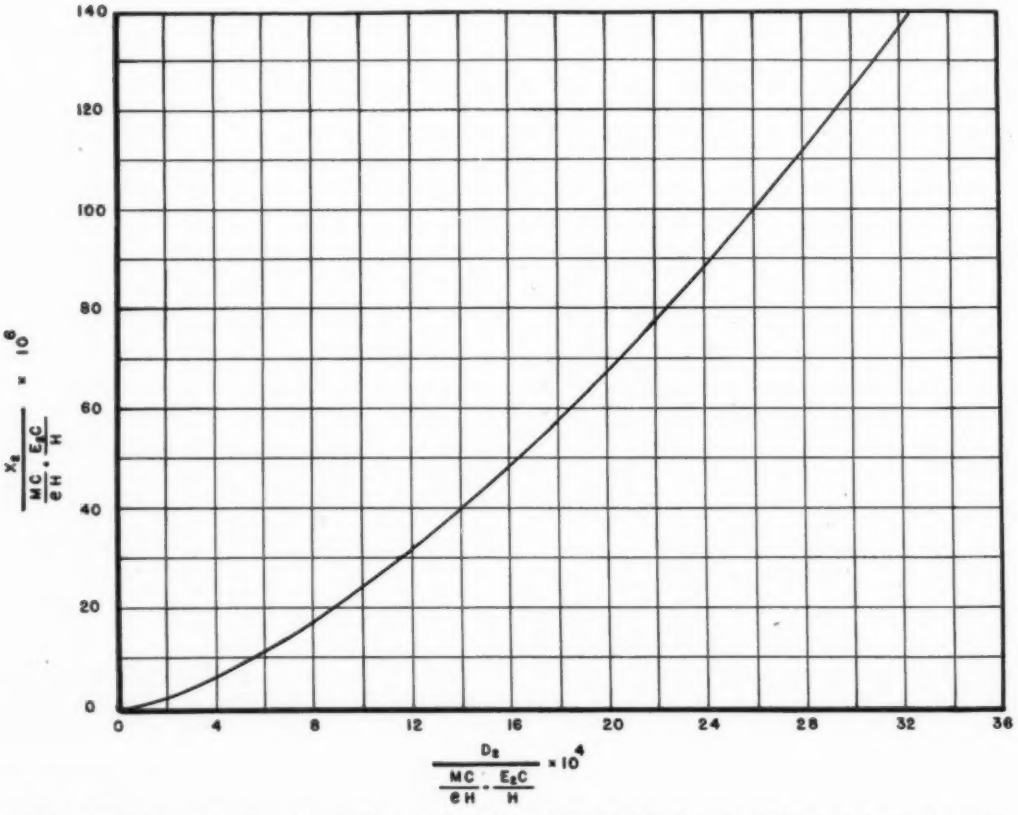

FIG. 8. Plot showing $x_2/(Mc/eH)\cdot(E_2c/H)$ as a function of $D_2/(Mc/eH)\cdot(E_2c/H)$. For the special case $D_2=2D_1$. X_2 is in cm if E_2 and e are in e.s.u., H in e.m.u., M in grams, c in cm/sec., and D_2 in cm. The curve is valid for values of E_2/E_1 from 50 to 300, within the limits of error of the plot.

method of collection previously discussed is used, since H is varied in such a way that H^2/M is a constant and none of the other factors is varied. When the electrical method of collection is used, however, H being fixed, both sets of conditions are satisfied only if E_1 and E_2 are varied in such a way that E_1M and E_2M remain constant. This is equivalent to keeping E_2/E_1 a constant, which condition is easily satisfied experimentally by using a divided potential arrangement.

Another factor which is essential for a description of this type of spectrometer is the displacement x_2. It can be determined from Eqs. (9) and (10) by substituting the values $x=x_2$, $y=D_1+D_2$. In Fig. 8, $x_2/(Mc/eH)\cdot(E_2c/H)$ is plotted as a function of $D_2/(Mc/eH)\cdot(E_2c/H)$ for the special case $D_2=2D_1$. This curve is valid for values of E_2/E_1 from 50 to 300 within the limits of error of the plot.

A corresponding plot for the parameter U_2 (value of U corresponding to $x=x_2$) for the special case $D_2=2D_1$ and for different values of E_2/E_1 is shown in Fig. 9.

"α" the angle which determines the position of the focal plane of the analyzer can be determined in the same way that ψ was determined. The expression for $\tan\alpha$ is

$$\tan\alpha=\frac{1}{\dfrac{Mc}{eH}\cdot\dfrac{E_2c}{H}}\cdot\frac{D_1+D_2}{U_2+\dfrac{E_1}{E_2}\sin 2\psi-\dfrac{x_2}{\dfrac{Mc}{eH}\cdot\dfrac{E_2c}{H}}}. \quad (11)$$

In general, U_2 and $x_2/(Mc/eH)\cdot(E_2c/H)$ can be determined by means of Eqs. (9) and (10) in the same way that they were calculated for the case $D_2=2D_1$ previously discussed. $\psi=U_1/2$ can be obtained from Eq. (7) since $(Mc/eH)\cdot(E_1c/H)$ is fixed by the values chosen for E_2/E_1 and $(Mc/eH)\cdot(E_2c/H)$. For the special case $D_2=2D_1$, U_2 and $x_2/(Mc/eH)\cdot(E_2c/H)$ may be obtained

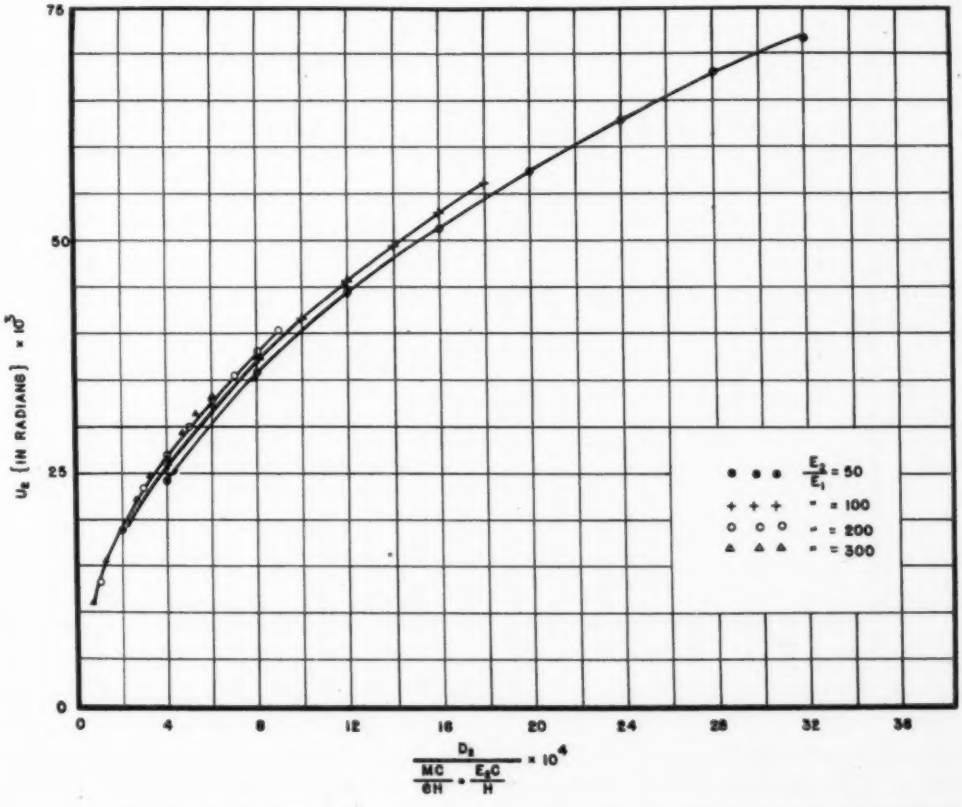

FIG. 9. Plot showing U_2 as a function of $D_2/(Mc/eH)\cdot(E_2c/H)$ for different values of E_2/E_1 and for $D_2=2D_1$.

from the plots shown in Figs. 8 and 9, and for this case "α" is plotted as a function of $D_2/(Mc/eH)\cdot(E_2c/H)$ for different values of E_2/E_1 in Fig. 10.

Although the value of "α" is in most cases quite small, it is important to take it into consideration in the over-all design of an instrument, if the maximum resolving power is to be attained.

The values of these various constants are listed below for an instrument which is designed to handle 1002.5-volt ions of mass number 100, $H=5000$ gauss, $D_2=2D_1=0.2$ cm, and $E_2/E_1=200$. For this case $(Mc/eH)(E_2c/H)=324.0$, $(Mc/eH)(E_1c/H)=1.62$.** Making use of these values and the graphs, the following constants are obtained:

$$x_0=-0.012 \text{ cm}, \quad \psi=10^\circ\,6',$$
$$x_2=0.0035 \text{ cm}, \quad \text{and} \quad \alpha=1^\circ\,30'.$$

The values of H, E_1, and E_2 which would be used in this case to study ions of another mass number could then be found from the conditions for identical paths, i.e., $E_1'/E_1=E_2'/E_2$ and $M'E_2'/(H')^2=ME_2/H^2$, which conditions must be satisfied at all times if the abundance measurements are to be free from error.

INSTRUMENT DESIGN

The over-all design of a spectrometer will depend upon many different factors such as size of magnet available, power, dispersion desired, and the particular use for which the instrument is intended. There are two general types in use at the present time which for convenience may

** E_1 can always be found from the energy relation $e(E_1D_1+E_2D_2)=$ion energy, and the value for E_2/E_1.

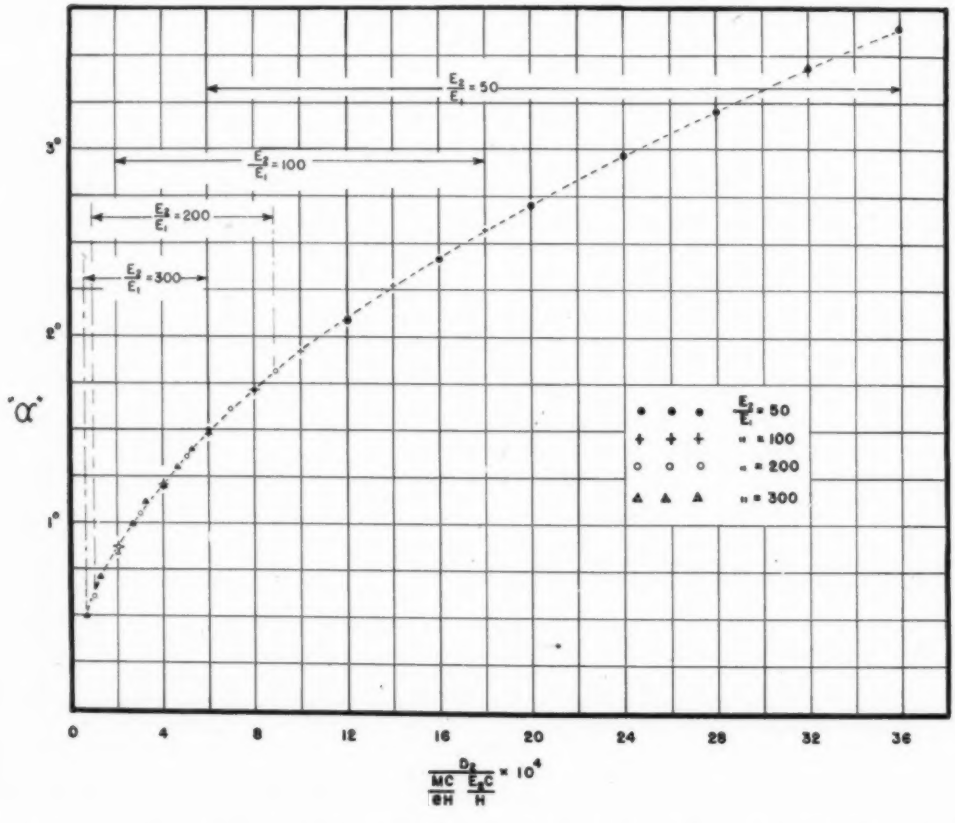

FIG. 10. Plot showing "α" as a function of $D_2/(Mc/eH)\cdot(E_2c/H)$ for the special case $D_2=2D_1$. The region of the curve which is valid for a given value of E_2/E_1 is indicated by the corresponding arrowed line in the upper left-hand corner. It is very possible that the overlapping values are identical for even greater ranges than shown. However, calculations were made only within the limits indicated.

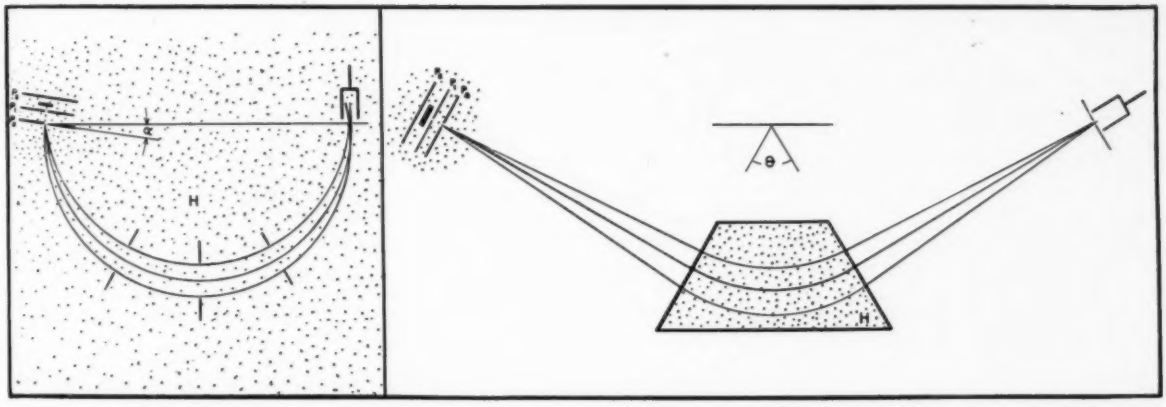

FIG. 11. General types of mass spectrometers: (A) π radian design; (B) sector type magnetic field design.

be classified as the π radian design shown schematically in Fig. 11A and the sector type magnetic field design shown in Fig. 11B.

In both cases, the type of ion source most generally used is that described in the preceding section. In the previous discussion, however, it was assumed that the magnetic field was uniform between the plates P_0, P_1, and P_2, Figs. 1 and 11. This is true only in the case of the π radian type of instrument in which the mass analyzer and source are both in the same uniform magnetic field, and only in this case are the values obtained for "α" (Figs. 10 and 11), and for x_2 (Fig. 8) valid. Other advantages of the π radian instrument include ease of alignment (the conditions within the source being known), maximum effective use of the slit widths and a uniform electron beam shape. It is doubtful if measurements made with this type of instrument under the conditions requisite for identical ion trajectories are in error by more than one or two percent.

Since the same type of source is used in the sector magnetic field type of instrument and since the source region is outside and some distance from the analyzer magnetic field, an auxiliary field, supplied by a bar magnet in most cases, is necessary. In this arrangement, the equations previously obtained no longer apply since the magnetic field is not uniform throughout the source region, and is in fact distorted in those instruments in which magnetic materials are used to fabricate the source.

This also applies to the π radian type of instrument when semicircular pole faces are used and the source is just outside the pole edges in a stray field region. In these cases, it is difficult to calculate the critical constants necessary for the proper orientation of the source relative to the magnetic field and alignment must be made experimentally by trial and error. In addition, if the magnetic field is distorted appreciably in the region traversed by the electron beam near slit S_1 (Fig. 1), one can also expect a loss of resolving power.

It is important to note, however, that although these factors may decrease the intensity and reduce the resolving power insofar as the source is concerned, they do not in any way invalidate the results obtained providing that E_1M and E_2M are always kept constant while making relative abundance measurements. These conditions are the same as those for the uniform magnetic field case, and can be shown to be the requisite conditions for identical ion paths in the source region in the case of a non-uniform magnetic field by the method of Bleakney.[20]

Under these conditions, measurements made with a sector instrument are just as accurate as those obtained with the π radian type of instrument discussed above and the results, in point of view of accumulative errors inherently associated with machine design, are probably accurate to one or two percent.

We wish to express our appreciation to Professors Serber and Morrison for reading the manuscript.

BIBLIOGRAPHY

(1) A. O. Nier, Phys. Rev. **52**, 933 (1937); **54**, 275 (1938).
(2) M. B. Sampson and W. Bleakney, Phys. Rev. **50**, 732 (1936).
(3) See, for example, H. D. Hagstrum and J. T. Tate, Phys. Rev. **59**, 354 (1941).
(4) A. O. Nier, J. Am. Chem. Soc. **60**, 1571 (1938).
(5) A. O. Nier, E. T. Booth, J. R. Dunning, and A. V. Grosse, Phys. Rev. **57**, 546 (1940).
(6) H. C. Urey, J. R. Huffman, H. G. Thode, and M. Fox, J. Chem. Phys. **5**, 856 (1937).
(7) D. Rittenberg, A. S. Keston, F. Rosebury, and R. Schoenheimer, J. Biol. Chem. **127**, 291 (1931).
(8) E. B. Jordan, Phys. Rev. **57**, 1072A (1940).
(9) W. Bleakney, Phys. Rev. **34**, 157 (1929); **40**, 496 (1932).
(10) A. O. Nier, Phys. Rev. **50**, 1041 (1936).
(11) J. T. Tate, P. T. Smith, and A. L. Vaughan, Phys. Rev. **48**, 525 (1935).
(12) A. O. Nier, Rev. Sci. Inst. **11**, 212 (1940).
(13) H. Brown, J. J. Mitchell, and R. D. Fowler, Rev. Sci. Inst. **12**, 435 (1941).
(14) N. F. Barber, Proc. Leeds Phil. Soc. **2**, 247 (1933).
(15) W. E. Stephens, A. L. Hughes, Phys. Rev. **45**, 123A (1934); W. E. Stephens, Phys. Rev. **45**, 513 (1934).
(16) W. Bleakney and J. A. Hipple, Jr., Phys. Rev. **53**, 521 (1938).
(17) Hannes Alfuén, Arkiv f. Mathematik, Astronomi och Fysik **A27**, No. 22, 1 (1940).
(18) K. T. Bainbridge, J. Frank. Inst. **212**, 317 (1931).
(19) H. A. Straus, Phys. Rev. **59**, 102 (1941).
(20) W. Bleakney, Am. Phys. T. **4**, 12 (1936).

Samples of Mass Spectrometer Traces

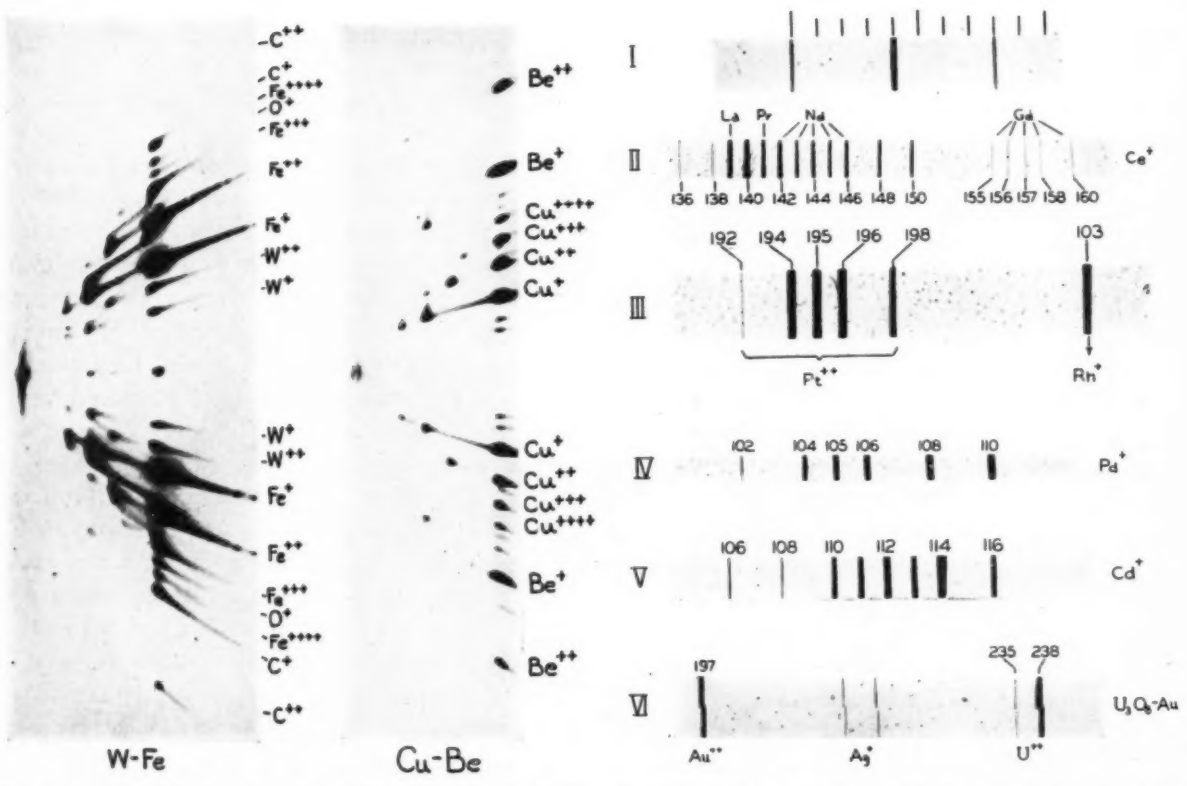

From a paper by A. J. Dempster on "New Methods of Mass Spectroscopy," Proc. Am. Phil. Soc. **75**, 755–766 (1935).

Gas Analysis with the Mass Spectrometer

BY JOHN A. HIPPLE

Westinghouse Research Laboratories, East Pittsburgh, Pennsylvania

VERY early in the development of instruments for mass analysis of ions there occurred a natural diversion of the work into two channels. Those physicists interested in the accurate measurement of the masses of the elements developed instruments with very narrow slits and photographic recording in order to attain the highest resolution possible. Although instruments of high resolution were obtained by this approach, the intensity of the ion current was reduced by the small slits, and the accuracy and convenience of measuring the amount of this current were severely hampered by the necessity of correlating the amount of the blackening of the photographic traces with the number of ions striking the film. Therefore, those physicists more interested in the accurate measurement of the relative amounts of the ions of different masses present worked with instruments with fairly wide slits and measured the ion current electrically. The development of the field of mass spectrometry is described more fully in the first paper in this series.[1] The present paper deals with the use of the mass spectrometer as a tool in gas analysis and for this reason is concerned with the type of work done with instruments of the second class mentioned above. The study of the relative abundance of the isotopes and their use as tracers would come under this classification, but this is such a large and important field that it has been reserved for a special article following this one.[2] With this limitation this discussion will be concerned with the analysis of gases containing a mixture of several molecular species, e.g., the amount of O_2 in a sample of N_2. In recent years there has come an increasing awareness of the possibilities of the mass spectrometer in this field. In discussing this application of the mass spectrometer, there are three main sub-topics:

In the first place, the person interested in this type of gas analysis must be thoroughly familiar with the nature of the data obtained to be able to estimate intelligently whether it is feasible and desirable to apply the mass spectrometer to a specific problem. For this reason it will be necessary to mention as briefly as possible some of the work done with the mass spectrometer on the ionization and dissociation of various molecules by electron impact. This is necessary since the gas to be studied in the instrument is first ionized by an electron beam of controlled energy.

In the second place, with the type of data obtained in mind, the possible applications will be discussed. Applications that have already been made will be mentioned.

Thirdly, it is necessary to say something about the type of instrument desirable for this work. If none is available, the entire discussion is of little importance. Certainly one reason that so little has been done is the lack of available equipment. An instrument that has been developed to fill this need will be described.

I. STUDY OF THE IONIZATION AND DISSOCIATION OF MOLECULES BY ELECTRON IMPACT WITH THE MASS SPECTROMETER

The 180° magnetic deflection spectrometer (π radian instrument in the nomenclature of the previous article) developed by Dempster for the study of isotopes[3] was very soon adapted to the investigation of the processes of ionization of molecules by electron impact. Since then many workers have studied this field—to mention a few, Smyth, Hogness, Kallmann, Bleakney, Tate, and their associates. Smyth's review article[4] covers this field very well up to 1931.

Before discussing some of the results, it is important to have a clear idea of the manner in which the data are obtained and the order of magnitude of the quantities involved. In Fig. 1 a schematic drawing is shown of a mass spectrometer tube of the $\pi/2$ radian type. This type is used here for illustration because it is the one used in the apparatus described more fully later. Almost all of the work of this kind has been

done with the π radian instrument. Recently, Nier[5] successfully adapted the magnetic analyzer part ($\pi/3$ radian) of the Bainbridge and Jordan precision instrument[6] for high sensitivity work. The focusing property of this field arrangement has been described by Barber and Stephens and Hughes.[7] The reasons for using the $\pi/2$ radian type will be mentioned later. In the figure, the sample of gas to be analyzed is admitted to the vacuum tube in the region above S_1 by means of a capillary leak and flows through the tube and out the pumping lead—the tube being pumped continuously by means of mercury or oil diffusion pumps, the pressure being of the order of 10^{-4} mm of Hg or lower. The electron beam shown by the dotted line from the filament to the electron trap 7 ionizes some of the molecules of the gas sample in the region just above S_1. The electron current is of the order of a few microamperes and the electron accelerating voltage usually variable from 0 to 100 volts. The ions are drawn through the slit S_1 and accelerated to S_2 by a difference of potential between these two slits of about 500 to 1000 volts. The beam of ions determined by the slits S_1 and S_2 passes through S_2 and travels in a straight path shown by the dotted line until it reaches the shaded region where there is a magnetic field perpendicular to the plane of the figure. The magnetic field bends the ions into a circular path and, by an appropriate adjustment of the ion accelerating voltage and the magnetic field strength, ions of a particular mass (actually of a particular mass divided by charge) are caused to follow the curve of the vacuum chamber, emerging from the magnetic field region after a deflection of 90° and continuing on to the exit slit S_3. Passing through S_3 the ions strike the Faraday cage and the current corresponding to this particular mass is measured. Suppose, for example, it is desired to analyze a sample containing a mixture of nitrogen (mass 28) and oxygen (mass 32). With

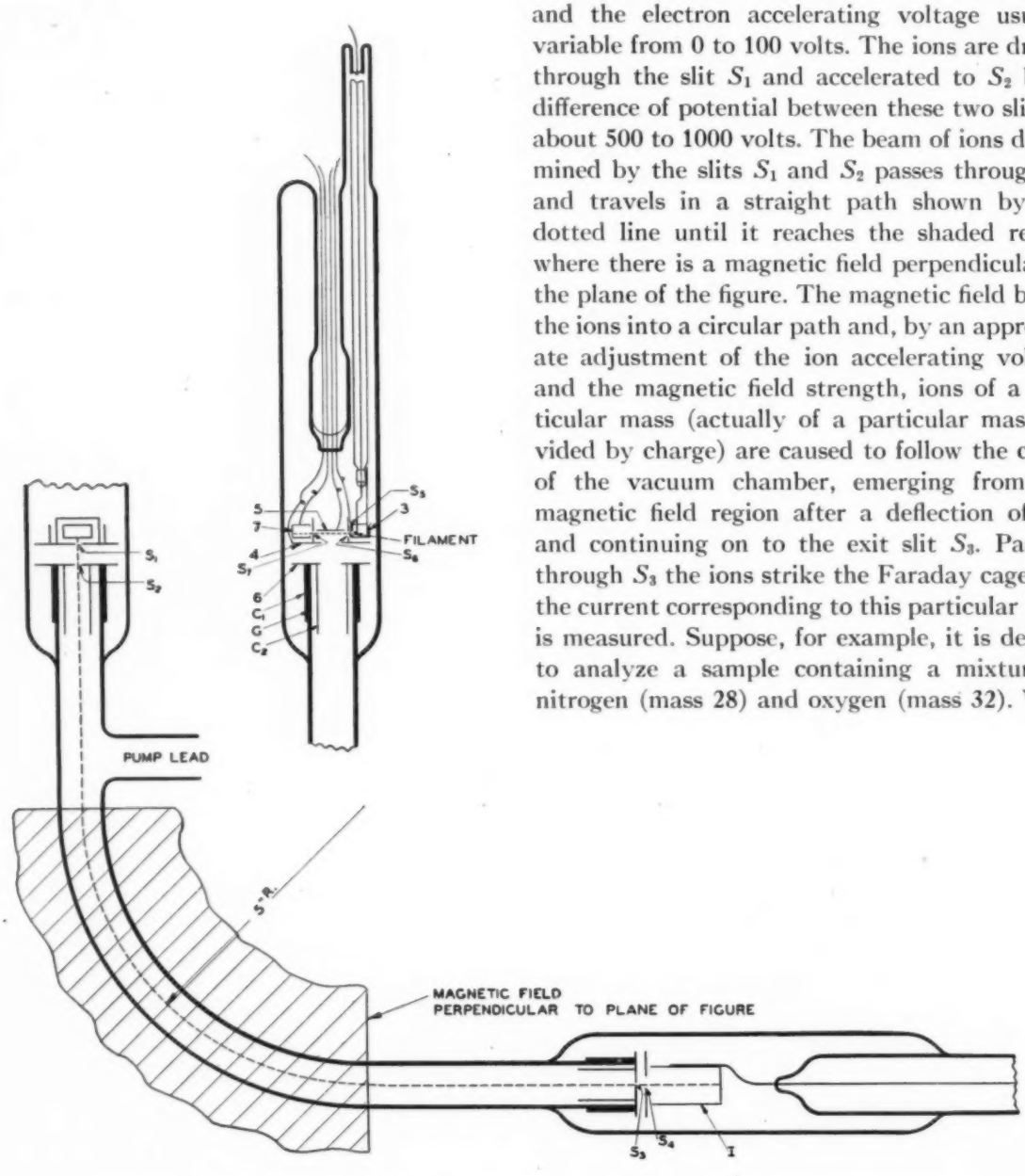

FIG. 1. Mass spectrometer tube.

TABLE I. The most recent references to the molecules that have been studied with the mass spectrometer. As this is not a review article, most of the references have been omitted, the purpose here being to provide a list of the substances that have been studied with the mass spectrometer, together with a recent reference so that the earlier work can be traced.

He—Bleakney, Phys. Rev. **36**, 1303 (1930).
Ne—Bleakney, Phys. Rev. **36**, 1303 (1930).
A—Bleakney, Phys. Rev. **36**, 1303 (1930).
Hg—Bleakney, Phys. Rev. **35**, 139 (1930).
H_2—Hagstrum and Tate, Phys. Rev. **59**, 354 (1941); Bleakney, Phys. Rev. **40**, 496 (1932).
O_2—Hagstrum and Tate, Phys. Rev. **59**, 354 (1941).
CO—Hagstrum and Tate, Phys. Rev. **59**, 354 (1941).
Br_2—Blewett, Phys. Rev. **49**, 900 (1936).
I_2—Hogness and Harkness, Phys. Rev. **32**, 784 (1928).
N_2—Tate, Smith, and Vaughn, Phys. Rev. **48**, 525 (1935).
NO_2—Smyth and Stueckelberg, Phys. Rev. **36**, 478 (1930).
N_2O—Smyth and Stueckelberg, Phys. Rev. **36**, 478 (1930).
NO—Tate, Smith, and Vaughn, Phys. Rev. **48**, 525 (1935).
H_2O—Mann, Hustrulid, and Tate, Phys. Rev. **58**, 340 (1940).
CO_2—Smyth and Steuckelberg, Phys. Rev. **36**, 472 (1930); Kallmann and Rosen, Zeits. f. Physik **61**, 61 (1930); Friedlander, Kallmann, and Rosen, Naturwiss. **19**, 510 (1931).
HCN—Kusch, Hustrulid, and Tate, Phys. Rev. **52**, 843 (1937).
HCl—Nier and Hanson, Phys. Rev. **50**, 722 (1936).
$(CN)_2$—Kusch, Hustrulid, and Tate, Phys. Rev. **52**, 843 (1937).
CS_2—Linder, Phys. Rev. **41**, 149 (1932); Smyth and Blewett, Phys. Rev. **46**, 276 (1934).
SO_2—Smyth and Mueller, Phys. Rev. **43**, 121 (1933).
NH_3—Mann, Hustrulid, and Tate, Phys. Rev. **58**, 340 (1940).
CH_4—L. G. Smith, Phys. Rev. **51**, 263 (1937).
C_2H_6—Hipple, Phys. Rev. **53**, 530 (1938); Stevenson and Hipple, J. Am. Chem. Soc. (May, 1942).
C_3H_8—Delfosse and Bleakney, Phys. Rev. **56**, 256 (1939).
C_4H_{10} (normal)—Stevenson and Hipple, J. Am. Chem. Soc. (To be published).
C_4H_{10} (iso)—Stevenson and Hipple, J. Am. Chem. Soc. (To be published).
C_2H_4—Kusch, Hustrulid, and Tate, Phys. Rev. **52**, 843 (1937).
C_3H_6—Delfosse and Bleakney, Phys. Rev. **56**, 256 (1939).
C_2H_2—Tate, Smith, and Vaughn, Phys. Rev. **48**, 525 (1935); Kusch, Hustrulid, and Tate, Phys. Rev. **52**, 843 (1937).
C_3H_4 (allene)—Delfosse and Bleakney, Phys. Rev. **56**, 256 (1939).
CH_3Cl—Bauer and Hogness, J. Chem. Phys. **3**, 687 (1935).
CH_3OH—Cummings and Bleakney, Phys. Rev. **58**, 787 (1940).
C_2H_5OH—Cummings and Bleakney, Phys. Rev. **58**, 787 (1940).
B_2H_6—Hipple, Phys. Rev. **57**, 350A (1940).
C_6H_6—Hustrulid, Kusch, and Tate, Phys. Rev. **54**, 1037 (1938).
C_6H_{12}—Hustrulid, Kusch, and Tate, Phys. Rev. **54**, 1037 (1938).
C_5H_5N—Hustrulid, Kusch, and Tate, Phys. Rev. **54**, 1037 (1938).
N_2H_4—Taylor, Phys. Rev. **47**, 666 (1935).
$CHBrF_2$—Baker and Tate, Phys. Rev. **55**, 236A (1939).
CCl_2F_2—Baker and Tate, Phys. Rev. **53**, 683A (1938).
CCl_4—Baker and Tate, Phys. Rev. **53**, 683A (1938).

the fields adjusted for mass 28 to pass through the tube, mass 32, being bent less by the magnetic field, will hit the ground inside of the tube and be lost. Having measured the current corresponding to mass 28, the voltage between S_1 and S_2 is decreased until mass 32 passes through all the slits and then this current is measured. These two readings are then a measure of the relative number of molecules of N_2 and O_2 in the original sample. In an instrument of general utility, the slits S_1, S_2, and S_3 are of the order of half a millimeter and the radius of curvature in the magnetic field 10 to 15 cm. The ion current passing through the tube may be 10^{-10} to 10^{-15} ampere. For more details about a tube of this type reference should be made to the article by Nier.[5]

In a short article it is impossible to cover the large amount of work done in this field, since the publication of the review article by Smyth.

TABLE II. Analysis of a 5-component mixture of hydrocarbons as reported by Hoover and Washburn (reference 11).

	Manometer Percent	Mass spectrometer Percent	Difference
Methane	19.1	19.5	0.4
Ethane	37.7	38.0	0.3
Propane	39.6	39.0	0.6
Iso-Butane	2.1	2.0	0.1
N-Butane	1.5	1.5	0
Methane	19.4	20.1	0.7
Ethane	38.0	38.1	0.1
Propane	38.4	37.4	1.0
Iso-Butane	2.4	2.6	0.2
N-Butane	1.8	1.8	0
Methane	39.2	40.1	0.9
Ethane	52.3	51.7	0.6
Propane	3.7	3.2	0.5
Iso-Butane	3.1	3.2	0.1
N-Butane	1.7	1.6	0.1
Methane	42.7	43.5	0.8
Ethane	0	0.4	0.4
Propane	52.6	51.3	1.3
Iso-Butane	3.0	3.0	0
N-Butane	1.7	1.8	0.1

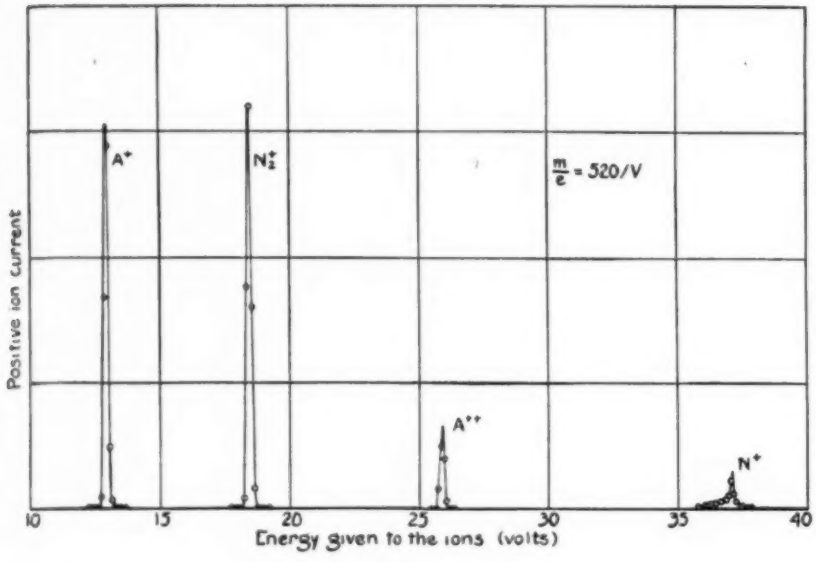

FIG. 2. Spectrum of argon and nitrogen, reprinted from the paper of Tate, Smith, and Vaughan (reference 8) as an example of a simple gas mixture.

Indeed, such a review would not be in order in an article written from the viewpoint of the present one. However, it is important that the person interested in applying the mass spectrometer to the analysis of particular substances have ready access to the past work, if any, that has been done on those substances. For this reason a bibliography has been prepared (Table I) giving the most recent reference or references to the work done on each molecule with the mass spectrometer. Through these references the earlier work can of course be readily traced.

TABLE III. Analysis of a mixture of butane and iso-butane as reported by Hoover and Washburn (reference 11).

	Iso-Butane Percent	*N*-Butane Percent	Difference
Manometer	0.9	99.1	
Mass spectrometer	1.1	98.9	0.2
	1.3	98.7	0.4
	1.1	98.9	0.2
	0.8	99.2	0.1
	1.2	98.8	0.3
	1.2	98.8	0.3
	Iso-Butane Percent	*N*-Butane Percent	Difference
Manometer	97.7	2.3	
Mass spectrometer	97.6	2.4	0.1
	97.6	2.4	0.1
	97.6	2.4	0.1
	97.5	2.5	0.2
	97.5	2.5	0.2

As an example of the type of data obtained, a mass spectrum of a mixture of argon and nitrogen taken from the paper of Tate, Smith, and Vaughan[8] is shown in Fig. 2. The ion accelerating voltage (in this case quite low) is plotted as abscissa and the ion current passing through the analyzer to the Faraday cage is plotted as the ordinate; i.e., with the magnetic field fixed, the ion accelerating voltage is varied and the ions due to the various components are successively made to pass through the exit slit of the instrument. The mass spectrum shown in Fig. 2 has been chosen because it is an example of a mixture of two simple components. The relative heights of the A^+ and N_2^+ peaks would provide a measure of the amount of argon and nitrogen in the original sample. It should, of course, be recognized that equal heights of these peaks does not indicate equal amounts of the two components. For one thing, the ionization efficiencies of different substances vary greatly; i.e., at the same pressure and electron current, a different number of ions is formed in nitrogen than in argon.[9] Also, the rate at which substances pass through the capillary leak used to admit the sample to the ionization region will differ because of the difference in mass. For some substances for which the data are available, a correction can be made which is sufficiently good for a rough analysis. However, if it is desired to make the analysis to an accuracy of about 1 percent,

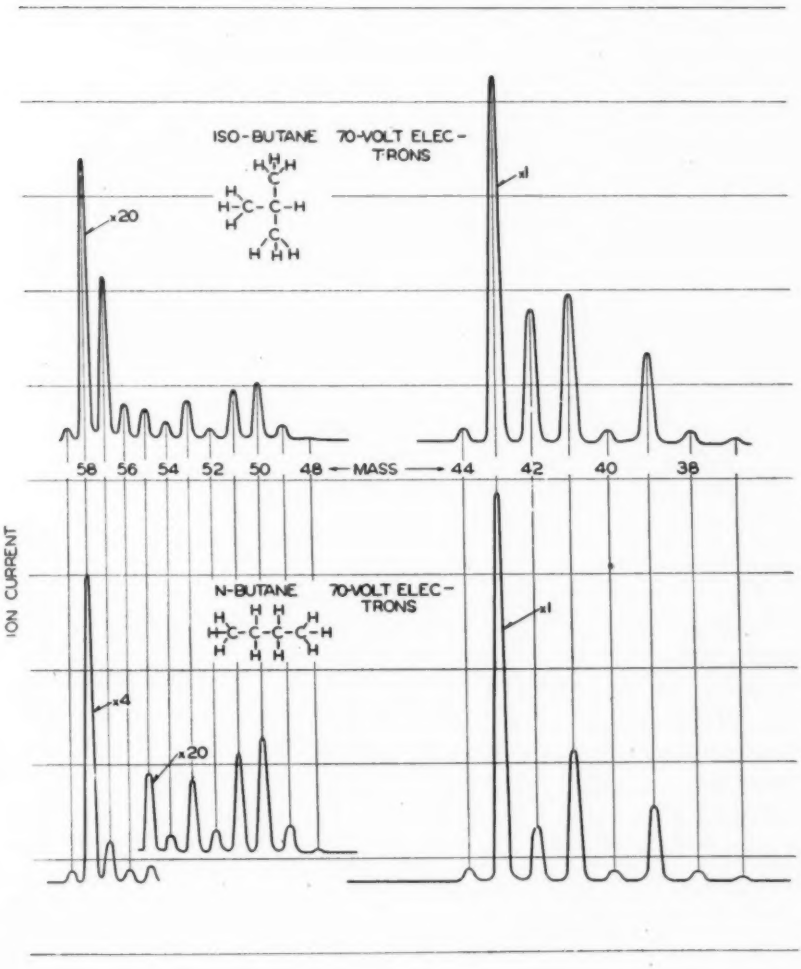

FIG. 3. Portions of the mass spectrums of iso-butane (upper) and normal butane (lower).

a known mixture of the two components should be used for calibration. The height of the peak corresponding to a particular ion is, of course, a function of the electron voltage—below 15.5 volts there will be no ions formed in either argon or nitrogen. It will be noted that the mass spectrum shown was taken with electrons accelerated by a difference of potential of 100 volts. It is customary to compare the relative intensities of different ions using electrons of 75 to 100 volts since the ionization efficiency curves are usually quite flat in this region.

In the figure it will be noted that there is a peak corresponding to doubly charged argon (A^{++}) and one corresponding to N^{+}. The electron energy at which the various fragments first appear has been the subject of a great deal of research that cannot be completely discussed here. Unfortunately, these fragments cause complications when an attempt is made to make an analysis of mixtures of more complicated molecules. This is evident by a glance at Fig. 3, which shows part of the mass spectra obtained for iso-butane and *n*-butane. Consider the upper part of the figure which is the spectrum from mass 37 to mass 59 in iso-butane—there are, of course, other fragments at lower mass numbers.[10] Since so many of the available mass numbers are occupied by the fragments due to iso-butane, in a mixture of similarly complicated molecules there will be an overlapping and perhaps for some of the components there will be no unique mass to measure. In case the several components are of comparable abundance, an analysis can

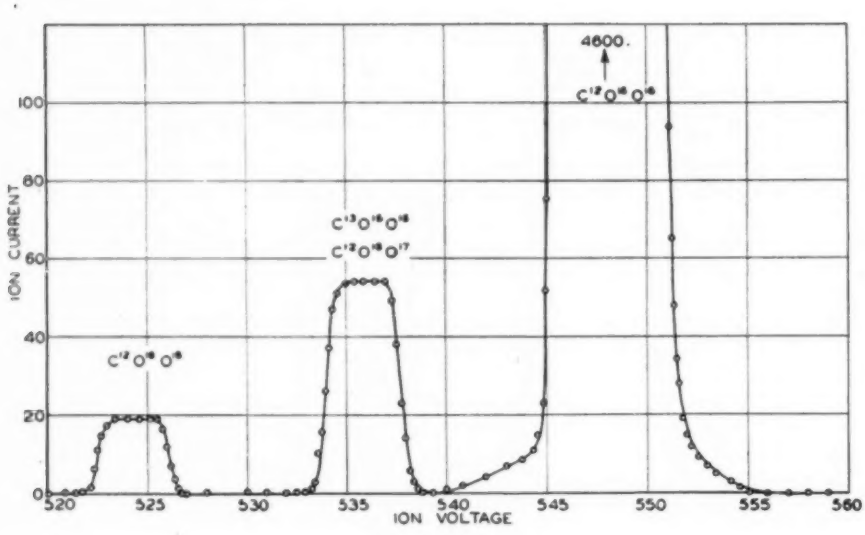

FIG. 4. Mass spectrum of CO_2 showing the carbon and oxygen isotopes and reproduced here to illustrate the performance of the $\pi/2$ radian instrument.

still be made in many cases by subtracting the background due to the known components as the mass spectra are quite reproducible. It will be clear that in general it will be easier to detect a small amount of a heavy component in the presence of a more abundant light component than vice versa, since the fragments are always lighter than the parent ion. In the butanes, the ion at mass 59 is due to the heavy carbon isotope. The differences in the patterns of iso-butane and *n*-butane do permit an analysis to be made, although not as simply as is the case when there are unique ions appearing.

In working with hydrocarbons especially, it is important to avoid thermally dissociating the molecule by the heat from the filament; to get a reproducible mass spectrum, all the dissociation must be due to electron impact. For this reason an oxide-coated filament is used in this work, although a tungsten filament could probably be used if sufficient precautions would be taken. The design is made in such a way that the gas is admitted to the ionization region and then pumped out past the filament.

II. APPLICATIONS

The application of the mass spectrometer to gas analysis is not new. For years, universities having an instrument available have used it from time to time to get a rapid check on the impurities in gas samples. A typical example is the determination of the purity of samples of H_2 and D_2 to be used in ion sources in experiments in the field of nuclear physics. Nevertheless, it is only very recently that any mass spectrometers have been built with the primary object of gas analysis. So many analyses were being made on a large mass spectrometer built for fundamental research at the Westinghouse Research Laboratories that it was decided to build a smaller and more easily operated unit for this work. One application has been the testing of the purity of N_2 used in annealing furnaces—primarily for traces of O_2 of the order of 0.001 percent. In another case, the interest was in traces of carbon compounds. To mention one more example, an analysis was made of the rare gas atmosphere in sealed-off electronic devices. Various problems of this type occur from time to time.

Rather complicated mixtures of hydrocarbons have been successfully analyzed with the mass-spectrometer by Hoover and Washburn.[11] The results of the analysis with the mass spectrometer checked exceedingly well the known composition of the mixture. In this work, mixtures of as many as five components were analyzed. In one case the mixture was methane, ethane, propane, iso-butane, and *n*-butane; in another, the components were iso-butane, 1-butene, 2-butenes (lumped together), iso-butane, and *n*-butane. Results obtained by Hoover and Washburn, as reported in their paper are reproduced in Tables II and III.

It might be well to summarize some problems in which the use of the mass spectrometer would be indicated:

(1) Of course, in all tracer work where stable isotopes are used, this is almost the only method available.

(2) For analysis of small traces of gas in a mixture such as the case of O_2 in N_2 mentioned above.

(3) In many cases analysis of a mixture will be much more rapid than ordinary methods and more information can be obtained. It has been used to measure the helium content in nitrogen and to analyze mixtures of *n*-butane and isobutane.

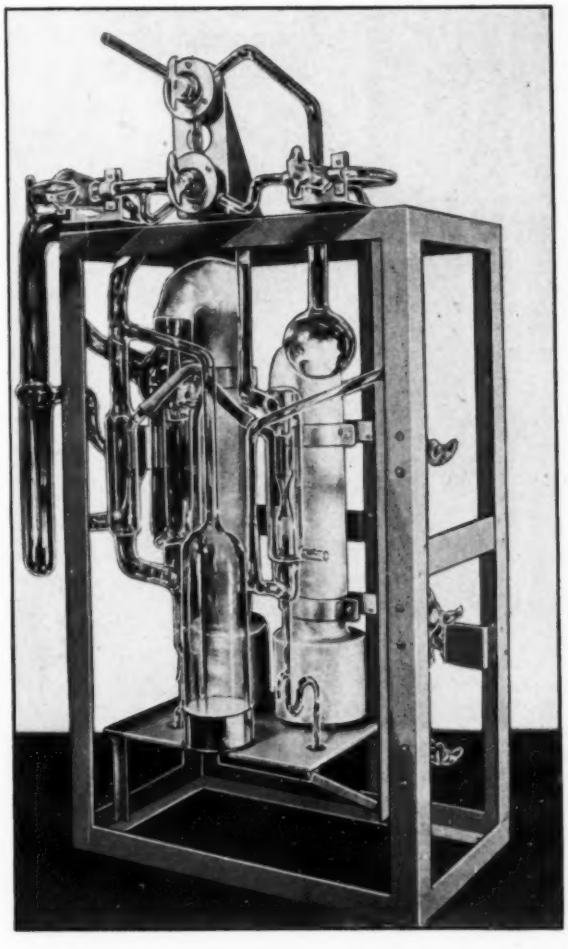

FIG. 5. All the component parts shown in position in Fig. 7 can be readily removed from the main assembly. As an example, the complete pumping and gas-handling system, shown above, has been lifted from the main assembly.

(4) In case there is only a small sample of gas available. In the analysis of the gas in the electronic device mentioned above, the quantity of gas available was about $\frac{1}{10}$ cubic centimeter at atmospheric pressure.

(5) In cases where a continuous indication of changing composition during a process is desired such as the gas atmosphere in an annealing furnace.

III. INSTRUMENT

Having pointed out some useful applications of the mass spectrometer as an analytical tool, the instrument must now be discussed. The mass spectrometer tube itself and its operation have been discussed earlier with reference to Fig. 1. One reason for using a deflection of 90° rather than 60° is that the path of the ions from source to collector is considerably shortened, thus reducing a little the probability of collision in the analyzer. With shorter path, the alignment for proper focusing is easier. In addition, it is simpler to have all the glass horizontal or vertical rather than slanted at some intermediate angle. In the present case, probably one of the strongest arguments is that, since the envelope is entirely of glass, the decreased length of the tube makes it somewhat less fragile. Of course, the reason that a deflection of 180° was not used was that a much more massive magnet is required to produce the magnetic field. It is not generally realized that the resolution (the percentage difference in mass resolvable) in instruments of this type (where the slits are wide and in a fixed position) is a function only of the radius of curvature of the ion beam in the magnetic field and the widths of the entrance and exit slits. The angle of deflection in the magnetic field is immaterial. To illustrate this, a mass spectrum of CO_2, showing the carbon and oxygen isotopes, is reproduced in Fig. 4. This looks like a reproduction of the curve published by Nier.[5] The radius of curvature and the slit widths were the same in both cases, but the deflection angle was 60° in his tube and 90° here.

In all instruments of this general class, in which ions are made to pass from source to collector through a curved tubing, the problem of electrostatically shielding the ion beam has

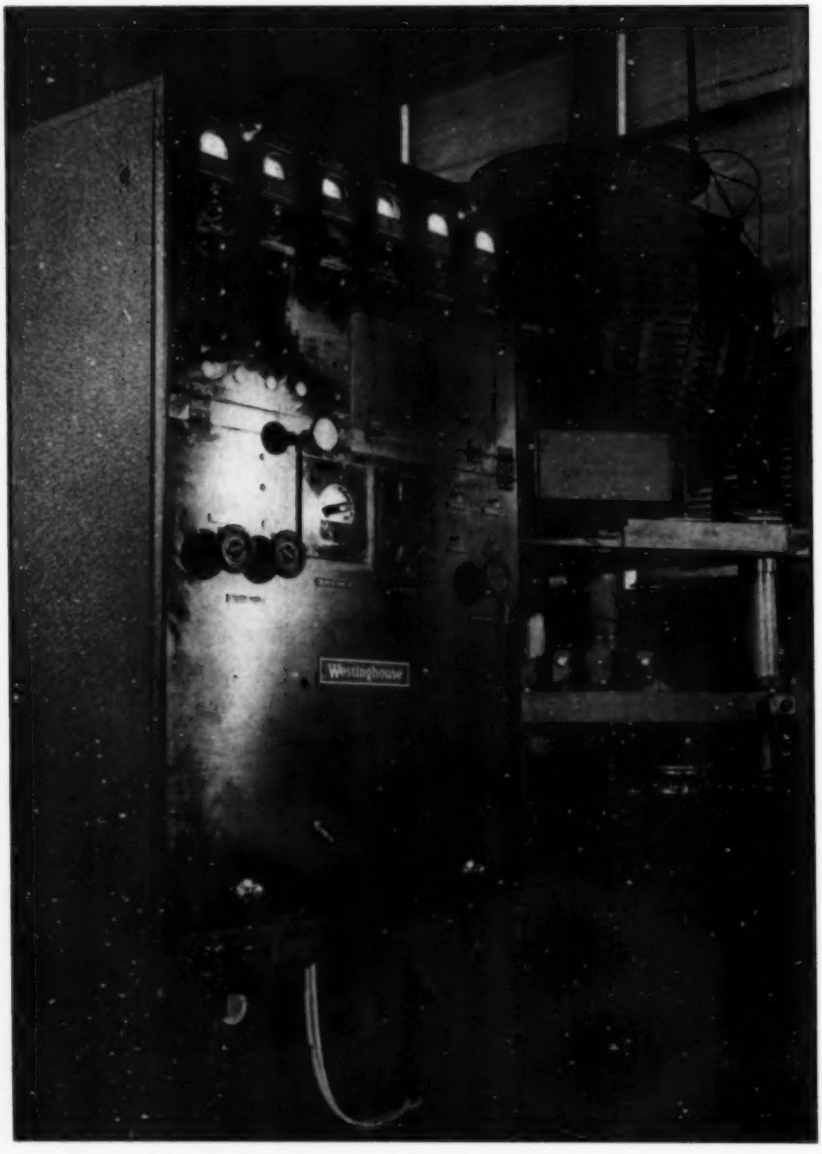

FIG. 6. Front panel of the mass spectrometer. These panels are hinged to permit ready access to the wiring. For adjustment of the stopcocks in the gas-handling system, the small door in the upper panel is opened.

been difficult. One solution is to make the curved portion of the vacuum envelope out of a non-magnetic metal and use metal-glass seals at the ends. Platinizing the inside of a glass tube has been tried, but this coating is difficult to apply satisfactorily. In the present case, the shielding of the inside of the glass was done simply and easily by making a kind of "alligator" out of thin, springy Nichrome V strips; in construction, after the glass tube is removed from its jig, this flexible shield is merely pulled into position, conforming very closely to the inside wall of the glass tube in spite of its curved shape. With this construction it was possible to make a tube using only glass, tungsten, and Nichrome V—an advantage when attempting to get a high vacuum. Figure 7, a side view of the completed instrument with the side panels open, shows the mass spectrometer tube in place.

The magnet is also shown in Fig. 7. The interesting feature of this magnet is that the exciting coils are wound to provide the desired field with an exciting current of 100 ma at 1000 volts. This power is provided with the electronic regulator shown at the top of the figure. The ion accelerating voltage is then tapped off a decade potentiometer in parallel with the magnet, powered from the same source as the magnet. Since the ion accelerating voltage will increase with the magnet current (and hence the magnetic field) some additional regulation is obtained. Additional regulators supply the electron accelerating voltage, the electrometer tube amplifier for the ion current, and the current heating the filament supplying the electrons. (This last regulator was suggested to the author by Nier.) Thus all batteries have been eliminated with the exception of three or four dry batteries having a very small current drain.

The entire assembly is enclosed by steel panels having a black crackle finish, except for the control panels which are micarta. All the panels are hinged or snapped into place so that access

to all parts of the equipment is very easy. All the units inside the frame are quickly removable for shipping, leaving nothing but the hollow frame. For instance, by cracking two small glass joints, the entire pumping and gas-handling system may be immediately removed as shown in Fig. 5. In order that the equipment can be moved to any place in the building where a gas analysis is desired, it is mounted on a rubber-tired truck with leaf springs. This is a standard type of truck which is used for moving pottery. For many applications, this feature is probably not necessary once the equipment is set up; but, in shipping one instrument about the country several times, this portability has been found very helpful. A view of the complete equipment from the control panel side is shown in Fig. 6. The small door in the upper panel is for the purpose of reaching the stopcocks on the gas-handling system. The only outside connections required when the apparatus is in place are 110 volts a.c. and water connections for cooling the pumps.

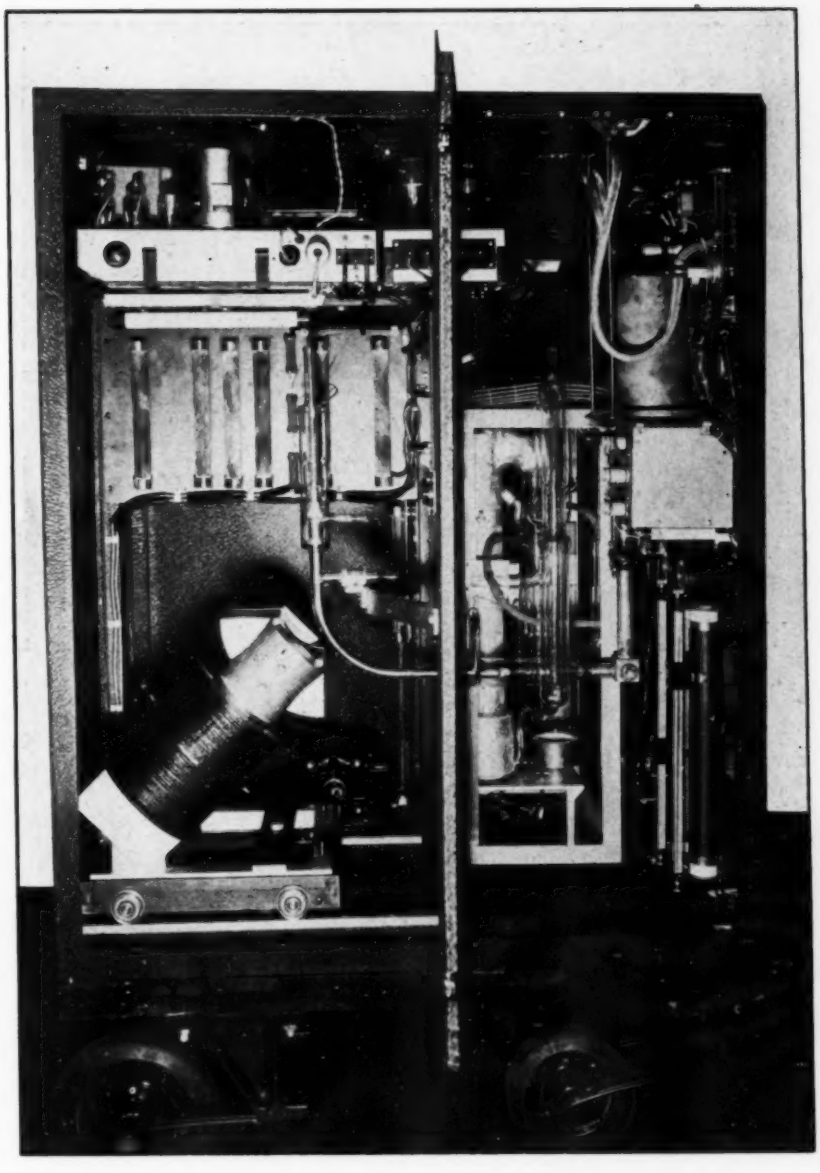

FIG. 7. Side view of mass spectrometer with side panels removed to show the essential parts of the instrument. The mass spectrometer tube is in position but not connected.

BIBLIOGRAPHY

(1) E. B. Jordan and L. B. Young, J. App. Phys. **13**, 526 (1942).
(2) D. Rittenberg, J. App. Phys. **13**, 561 (1942).
(3) A. J. Dempster, Phys. Rev. **11**, 316 (1918).
(4) H. D. Smyth, Rev. Mod. Phys. **3**, 347 (1931).
(5) A. O. Nier, Rev. Sci. Inst. **11**, 212 (1940).
(6) K. T. Bainbridge and E. B. Jordan, Phys. Rev. **50**, 282 (1936).
(7) M. F. Barber, Proc. Leeds Phil. Soc. **2**, 427 (1933); W. E. Stephens and A. L. Hughes, Phys. Rev. **45**, 123 (1934); W. E. Stephens, Phys. Rev. **45**, 513 (1934).
(8) Tate, Smith, and Vaughan, Phys. Rev. **48**, 525 (1935).
(9) K. T. Compton and C. C. Van Voorhis, Phys. Rev. **27**, 724 (1926); J. T. Tate and P. T. Smith, Phys. Rev. **39**, 270 (1932).
(10) Stevenson and Hipple, J. Am. Chem. Soc. (To be published.)
(11) H. H. Hoover, Jr. and H. Washburn, Proc. Calif. Natural Gas. Assn. 16th Annual Fall Meeting (1941).

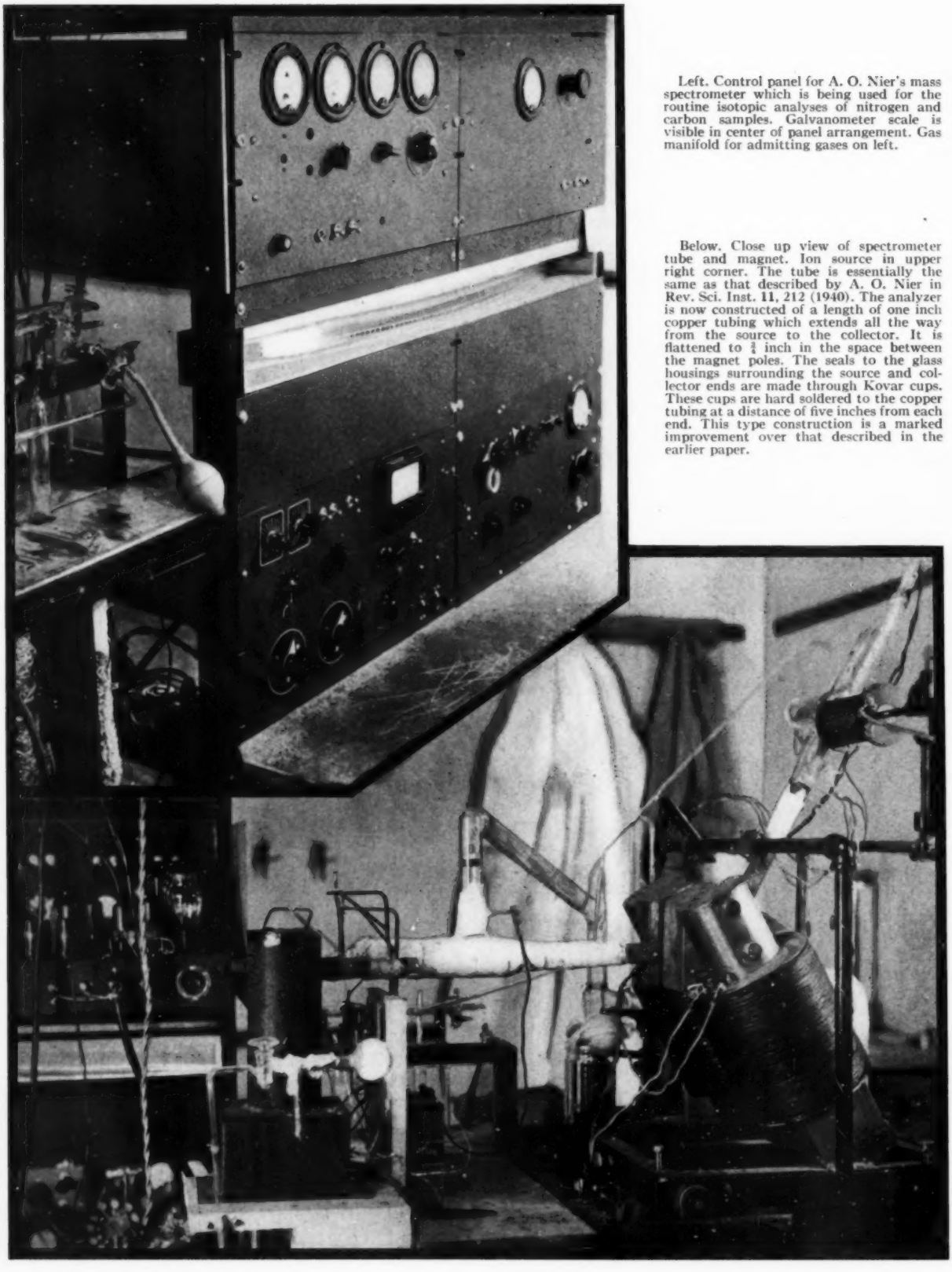

Left. Control panel for A. O. Nier's mass spectrometer which is being used for the routine isotopic analyses of nitrogen and carbon samples. Galvanometer scale is visible in center of panel arrangement. Gas manifold for admitting gases on left.

Below. Close up view of spectrometer tube and magnet. Ion source in upper right corner. The tube is essentially the same as that described by A. O. Nier in Rev. Sci. Inst. 11, 212 (1940). The analyzer is now constructed of a length of one inch copper tubing which extends all the way from the source to the collector. It is flattened to $\frac{3}{4}$ inch in the space between the magnet poles. The seals to the glass housings surrounding the source and collector ends are made through Kovar cups. These cups are hard soldered to the copper tubing at a distance of five inches from each end. This type construction is a marked improvement over that described in the earlier paper.

Some Applications of Mass Spectrometric Analysis to Chemistry*

BY D. RITTENBERG

Department of Biochemistry, College of Physicians and Surgeons, Columbia University, New York, New York

THE properties of the elements of the periodic table were thought originally to be functions of their mass, but are now known to be functions of the atomic number. Two or more isotopes of an element can exist with differing masses but identical atomic number; these have closely similar chemical and physical properties. Most elements have more than one stable isotope.

The differences between the properties of the isotopes of an element are so small that in the usual chemical procedures practically no changes of the isotope abundance are produced. Furthermore, the usual chemical measurements do not differentiate between a compound having a normal isotope distribution among its elements and one in which one or more of its elements have an abnormal isotope distribution. Even so sensitive a chemical selector as the living cell does not respond appreciably to changes in isotopic abundance.

The systematic investigation of the isotopic composition of the elements which was begun by Aston has now embraced every element of the periodic table. So long as the isotopic composition of an element could not be altered, the mass spectrometer was purely a descriptive instrument. The concentration of the heavy isotopes of hydrogen, carbon, nitrogen, oxygen, and sulfur gave rise to a new type of experimentation, for it became possible to label chemical compounds in which organic and biological chemists are interested. This paper will restrict itself to a discussion of these elements. In Table I is shown their natural abundance.

The analytical determination of the concentration of stable isotopes in a particular sample of an element can most easily be carried out with a mass spectrometer. In the case of hydrogen and oxygen, various other analytical methods have been developed which depend on the fact that the density of highly purified water samples can be determined with extremely high precision. It is difficult, however, to purify small samples of water (~0.1 g) for precise determinations without dilution with normal water.

The mass spectrometric determination has the great advantage that the results obtained are not affected by the purity of the sample nor by the concentration of isotopes of other elements. In any method which ultimately determines isotope concentration by measurement of the density of water, the limiting factor is not the determination of the density of water but its purification. It is, of course, recognized that the density of water is affected by the isotope concentration of both hydrogen and oxygen.

NATURAL ABUNDANCE OF THE HEAVY ISOTOPES

Investigations on the isotope abundances of the elements C, H, O, and N from the most diverse sources have shown little variation. The most extensive work on the natural isotope distribution of any element has been carried out with hydrogen. The results of these investigations indicate that the concentration of deuterium in hydrogen of natural origin is relatively constant, the variations being of the order of thousandths of a percent. The careful work of Dole[1] on the deuterium content of benzene, and cholesterol showed a normal isotope distribution in these complex biologically formed compounds. Similarly, only small variations in the concentrations of O^{18} have been observed. Manion, Urey, and Bleakney[2] found that the O^{18} concentration in the oxygen of stony meteorites was the same within their limits of error ($2\frac{1}{2}$ percent) with that of terrestrial rocks, and Smythe found nearly the same ratio in the oxygen of lead dioxide.[3] Extensive investigations of Dole and his collaborators indicate that the O^{18} content of carbonate ores is about 4 percent higher than that

* Publication assisted by the Ernest Kempton Adams Fund of Columbia University.

of Lake Michigan water and that of iron ores is about the same as that of water.[4] Dole had found that the O^{18} content of air is about 0.006 percent higher than that of Lake Michigan water.[5]

Most of the above determinations were made by measurement of the density of water. The accuracy possible by this procedure is greater than that which can be obtained by direct analysis with a mass spectrometer. Density determinations can be made with an error of about 2 parts in ten million, which corresponds to a variation of about 0.0002 atom percent in the concentration of the heavy isotope. Determinations of the ratio of O^{18} to O^{16} with a mass spectrometer can be carried out with an accuracy of 1 percent which, in the region of normal abundance, corresponds to 0.002 atom percent O^{18}.

The natural abundance of N^{15} is 0.37 atom percent. Scarcely any work has been reported on the variation of isotope abundance in nitrogen of different sources. This laboratory has carried out analyses of the nitrogen in some amino acids[6] isolated from the proteins of mammals and compared them to atmospheric nitrogen. Most of the amino acids contained from 0.000 to 0.006 atom percent N^{15} in excess over that of nitrogen from air. One of them, arginine, contained 0.008 atom percent N^{15} excess. It is of some interest that this particular amino acid is involved in a cyclic process by which NH_3 and CO_2 are converted to urea in the mammal. The arginine in this reaction is destroyed and resynthesized as a result of the following reactions:

$$2H_2O+\text{arginine} \xrightarrow{\text{arginase}} \text{urea}+\text{ornithine}$$
$$\text{Ornithine}+CO_2+NH_3 \rightarrow \text{citrulline}+H_2O$$
$$\text{Citrullin}+NH_3 \rightarrow \text{arginine}+H_2O.$$

During this process the fractionation of the N^{15} may occur. In the course of an investigation of the metabolism of antibodies[7] it was found that the natural abundance of the nitrogen of antibodies was 0.006 atom percent higher than that of atmospheric nitrogen. A more careful investigation of this entire subject is necessary before the picture will become clear.

As with nitrogen, relatively little work has been reported on the natural abundance of C^{13} in carbon of various sources. Nier and Gulbransen[8] and Murphey and Nier[9] have found some variations in the C^{12}/C^{13} ratio, depending on the source of the carbon. The carbon of limestone, independent of its geologic age, contains more C^{13} than present-day CO_2 whereas the carbon of plant cells contains a little less C^{13} than CO_2 of the air. The spread from the highest to the lowest values is 5 percent.

None of the variations reported in the isotope abundance is greater than could be explained by a one- or two-plate fractionation involving a reaction such as the following:[10]

$$C^{13}O_2+HC^{12}O_3^- \rightleftharpoons C^{12}O_2+HC^{13}O_3^-.$$

TABLE I. Stable isotopes.

Element	Abundance percent
H	H^1 ... 99.98 H^2 ... 0.02
C	C^{12}... 98.9 C^{13}... 1.1
N	N^{14}... 99.62 N^{15}... 0.38
O	O^{16}... 99.8 O^{17}... 0.03 O^{18}... 0.20
S	S^{32} ... 96 S^{33} ... 1 S^{34} ... 3

No investigation dealing with the variations of the isotope abundances in sulfur appears to have been made.

This paper does not intend to review completely the entire subject of the application of mass spectrographic analysis to chemical research but will be limited to a few investigations which illustrate the scope of the technique. The examples chosen are drawn from widely separated fields, analytical chemistry, reaction kinetics, reaction mechanism, and biological chemistry.

The introduction of the isotope technique has made available a method by means of which a molecule or a portion of a molecule may be labeled and followed through a series of chemical reactions. At present there are two types of isotopes available for such work, the radioactive

and the stable. The choice in any particular experiment depends on the nature of the work to be done. The radioactive isotopes have the advantages that they are more widely available, the analytical procedure is simple, and, as the initial activity is in principle within the control of the experimenter, the dilution to which the starting material can be subjected before the analytical method loses track of the label is greater than that in the case of the stable isotopes.

On the other hand, the stable isotopes have the advantage that time is no factor in the experiment. It is obvious that experiments which may be carried out with N^{13} are limited by its short half-lifetime (10 minutes). Unless a radioactive isotope of nitrogen is prepared with a half-lifetime of at least 50 days, most biological work will be carried out with the stable isotope N^{15}. Similar considerations apply to C^{11} with a half-time of 21 minutes. Extremely important work has been carried out with the aid of C^{11}, but all these experiments were of such nature that they could be completed in a few hours. In the future, it may be expected that C^{13} or C^{14} will displace C^{11} as a label. In the case of oxygen, only short-life radioactive isotopes are available, but for hydrogen and sulfur, radioactive isotopes of relatively long half-life are available.

While the mass spectrometer is not as sensitive as the Geiger counter, it also can detect a labeled compound, even after it has been mixed with large amounts of its normal analogue. A sample of urea prepared so that its nitrogen contains 50 atom percent N^{15} may be diluted with more than ten thousand times its weight of normal urea before the spectrometer loses track of the label. Dilutions as great as this rarely occur during most researches. The factor by which a labeled compound containing, for example, 50 atom percent of a heavy isotope may be diluted, is dependent on the natural abundance of the heavy isotope. The smaller the natural abundance, the greater the sensitivity of the label. Thus a compound labeled with 50 atom percent S^{34} can be diluted by a factor of only one thousand before the investigator loses track of it, whereas a compound labeled with 50 percent D may be diluted by a factor of more than 5000 and still be detected.

THE ISOTOPE DILUTION METHOD

Most chemical methods of analysis involve procedures which completely separate the particular substance for which we are analyzing, either by the formation of a specific precipitate or by means of a specific chemical reaction. While these methods of analysis have been carefully developed for inorganic ions, the analysis of organic compounds is, in general, not so well developed. More specifically, the analysis of individual members of a series of homologous compounds in a mixture still can be carried out only crudely.

The "isotope dilution method" is a new type of analytical procedure peculiarly adapted to the analysis of complex mixtures such as are frequently met with in the study of natural products. It has been applied to the quantitative determination of amino acid in proteins.[11]

The proteins are quantitatively the major organic constituents of protoplasm, and the determination of their structures is one of the important problems of chemistry. Because of their complexity, elementary analysis of proteins throws but little light on their structure. Acid hydrolysis of proteins gives rise to mixtures of about 24 α-amino acids, originally linked together by peptide bonds. Before the structure of the protein can be determined, the quantitative distribution of the amino acids must be known.

If, as is the case for many of them, no characteristic color reaction or specific reagent is known for a particular amino acid, its determination must depend on its isolation in the pure state and in quantitative yield from the protein hydrolysate. Experience has shown that in practice these two requirements are mutually contradictory. One can isolate from such complex mixtures either all of a compound in an impure state or some of the pure compound, but not both.

For the isotope dilution method, only a small sample of the substance to be determined need be isolated in a pure condition, the yield being unimportant. This method is based on the fact that the usual laboratory procedures will not fractionate isotopic isomers, that is, compounds having an abnormal isotope distribution cannot be separated from ordinary compounds by the customary techniques for isolation.

TABLE II. Determination of amino acids in fibrin.

Protein hydrolyzed	Amino acid added		N^{15} excess	N^{15} excess in compound isolated at successive stages of recrystallization	Amino acid in protein, found
	Compound	Weight			
g		g	atom percent	atom percent	percent
4.002	Glycine	0.1315	2.00	0.781 0.784 0.782 0.782	5.12
4.995	*dl*-Glutamic acid	0.1266	2.10	0.182 0.186 0.185	13.2
5.382	*dl*-Glutamic acid	0.1152	2.10	0.162 0.161 0.157	13.0
5.034	*dl*-Glutamic acid	0.1222	2.10	0.185 0.176	12.9
7.675	*dl*-Glutamic acid	0.4005	2.10	0.356 0.355	12.8
	dl-Aspartic acid	0.4000	2.00	0.374 0.383	11.2

This method can most easily be illustrated by describing its application to a determination of the amino acid glycine (CH_2NH_2COOH) in a protein hydrolysate. To the hydrolysate is added a small amount of a synthetic glycine which has been prepared from heavy ammonia. The added isotopic glycine with the glycine already present forms an inseparable mixture. The isotopic concentration of the N^{15} in the glycine mixture will be lower than that of the added glycine and obviously will depend on the relative amount of normal glycine and isotopic glycine mixed. The relation between the amounts of glycine and the isotopic concentrations is given in Eq. (1).

$$y=(C_0/C-1)x, \tag{1}$$

where C_0 = concentration N^{15} in added amino acid in excess over the normal
C = concentration N^{15} in isolated amino acid in excess over the normal
x = wt. amino acid added
y = wt. amino acid originally present in the mixture.

As can be seen from the formula, the amount of the substance isolated does not enter into the calculations. All that it is necessary to know are the two isotope analyses and the amount of glycine added. For this reason, large losses are permissible during the purification procedure. This, of course, considerably simplifies the isolation of a pure specimen of the amino acid.

The results of a determination of glycine in the protein fibrin are shown in Table II.

The application of this method to other amino acids is complicated by the fact that all amino acids with the exception of glycine are optically active. If glutamic acid be determined by addition of isotopic *dl*-glutamic acid to the hydrolysate, only its $l(+)$ component will form an inseparable mixture with the normal $l(+)$-glutamic acid in the protein hydrolysate, while $d(-)$-glutamic acid will be fractionated (as *dl*-) from the $l(+)$ form. The optically active isomers have, in general, solubilities different from those of the racemic compounds. In these cases it is necessary to employ one of three procedures: (A) The protein hydrolysate is completely racemized, racemic amino acid is added, and racemic amino acid is isolated; (B) the synthetic amino acid is first resolved and only the natural isomer added; (C) racemic amino acid is added and a sample of the natural isomer isolated. We have in our laboratory employed all three procedures for the determination of amino acids. The latter method has been used in the case of glutamic acid as it is here possible to separate a sample of pure *l* isomer from a partially racemized mixture. It will be necessary to determine for each individual amino acid which of the three procedures may best be employed.

By methods similar to that used for glutamic acid, Dr. G. L. Foster of this laboratory has been able to separate the *l* isomer from a partial racemate of phenylalamine, arginine, proline, aspartic acid, leucine, and tyrosine. In each case he has found a salt which in a suitable solvent gives rise to a separable mixture of active and racemic mixture. Where such procedures are not available, it should be possible to obtain the optically active amino acid by resolution with a suitable alkaloid. As for this purpose the yield is unimportant, such resolution should be relatively simple.

In Table II are shown the data for some determinations of glutamic acid in the protein fibrin. It may be seen that the four determinations have an average deviation of less than 1 percent from the mean. These values are 30 percent higher than the best values obtained by the isolation procedure. In the last determination, aspartic and glutamic acid were determined in the same sample. While at first sight it would appear that this is not conducive to accurate

results, the contrary is actually true. The more amino acids are determined in the same sample, the more accurate will the determination become. This is true for the following reason. Let us assume that the glutamic acid isolated contains as an impurity 5 percent of aspartic acid. If the aspartic acid is normal, then the isotope content of the glutamic acid will be lowered by about 5 percent. The value for the amount of glutamic acid in the protein is then lowered by about 8 percent. If, however, conditions are so arranged that the isotope content of the aspartic acid is about equal (± 10 percent) to that of the glutamic acid, then the isotope content of the glutamic acid will at most be in error by $\frac{1}{2}$ percent, leading to an error in the determination of about 0.8 percent. It is, therefore, obvious that the more amino acids are determined, the less the error due to cross contamination. By a slight modification of the method it is also possible to determine the amounts of both the *d* and *l* isomer of an amino acid in a protein hydrolysate.[12]

The isotope dilution method seems to have a wide field of application, and one can expect to find it generally employed in analytical chemistry.

CHEMICAL APPLICATIONS OF THE STABLE ISOTOPES

As soon as it became possible to label chemical compounds, an entirely new type of investigation became experimentally feasible; e.g., the determination of rates in systems in a stationary state. The concentration of a substance in such a system is, in general, a function of the ratio of rate constants and not of their absolute values. With the use of labeled compounds, it is possible to measure the individual rate constants. While these quantities could in some cases be indirectly determined in simple physicochemical systems, this was in general not the case with the complex systems met with in biochemistry. As a result the rates of many extremely important reactions in the intact biochemical system were unknown. Shortly after the discovery of the heavy isotope of hydrogen Hevesy, Hofer, and Krogh[13] determined the rate of transport of water in each direction across the skin of a frog. They immersed one foot of a frog in heavy water and measured the rate at which deuterium appeared in the body fluids of the frog. While the resultant net flow of water across the membrane was, of course, zero, the rates in each direction were quite high.

TABLE III. Balance of nitrogen isotope after feeding isotopic leucine.

		Fraction of N^{15} administered (percent)
Excreta	Feces	2.1
	Urine	27.6
Animal body	Non-protein *N*	7.8
	Protein *N*	57.5
Total isotope recovered		95.0

The existence of such processes whose small resultant rate is brought about by the near equality of two rapid opposing reactions has been shown by the isotope technique to be very common in living systems. Little information was previously available, as there was no method of distinguishing a molecule which had just been introduced or synthesized in a cell from one which had been present in the cell before the beginning of the experiment.

Intermediary metabolism deals with the chemical reactions by which a living organism utilizes its food and with the reactions for the final excretion of the end products of the metabolism.

A living organism consists grossly of about 65 percent water, 15 percent protein, 6 percent fat, 10 percent bone; the remaining 4 percent includes all the other organic compounds necessary for the life processes. This organism is capable of oxidizing the food materials with molecular oxygen at 37°C and utilizing this energy for its numerous processes. The living body takes in a mixture of proteins, carbohydrates, and fats, and excretes relatively simple ones, CO_2, urea, H_2O, and traces of others.

The proteins, which constitute an important part of the organism, are at present considered to be formed by the condensation of several hundred amino acids. There have been isolated from proteins 24 amino acids which differ in the structure of the side chain. It is generally believed that the manner in which the various amino acids are distributed in the molecule is specific for each protein. Ingested proteins are not absorbed as such by the organism but are first hydrolyzed to

their constituent amino acids and these are absorbed and utilized.

The role which food plays in the economy of adult animals was quite obscure until the last century. Prior to this period, quite fantastic theories were propounded. With the rise of thermodynamics it became apparent that the food was the source of the energy the animal required for the performance of muscular work and for the maintenance of body temperature. While we are certainly correct in considering the living organism to be a chemical engine, we must recognize that it is an extremely unusual type of engine, since the fuel and the structural components of the machine have essentially the same composition. Food is necessary not only for fuel but, at least in the growing animal, for the production of tissue—that is, of the machine itself.

This similarity of food and cellular components has made the study of intermediary metabolism rather difficult, and relatively little work has been done on the most interesting subject, the normal adult animal. The moment the dietary constituents enter the animal body, they mix with similar compounds already present and the investigator loses track of them. Most studies with adult animals have therefore been performed under abnormal conditions which permit the accumulation of intermediates or end products of the metabolism.

A great deal of information has been accumulated by means of the balance experiment, that is, one so conducted that it is possible to correlate the increase or decrease in amount of one compound by varying the intake of another. In this way, for example, it was demonstrated that the fatty acids could be synthesized from carbohydrates. As the composition of a mature animal is constant within rather narrow limits, such experiments are carried out with young animals of known composition on a diet in which the substance studied, for example, fat, is absent. If, after a known period of feeding, the total fat of the animal has increased, we are justified in stating that fat has been synthesized from other dietary material. While the balance experiment tells us that certain conversions occur, it gives us no information as to the rate of this process; we only measure the difference between the rates at which the substance is being synthesized and destroyed. Negative results from a balance experiment do not prove absence of the particular chemical conversions in question.

The living cell has no difficulty in synthesizing proteins and degrading them. The extent of the interaction of the dietary nitrogen with the tissue nitrogen was long unknown. As the quantity of nitrogen excreted was closely parallel to that in the diet, it was believed that only a small amount of the daily protein intake was used for replacing protein lost by "wear and tear" of the organism and that the remainder was oxidized. By feeding an amino acid labeled with N^{15}, it became possible to measure the interaction of the diet and the total organism in normal adult animals.

TABLE IV. N^{15} concentration in protein nitrogen of blood and organs from four rats given isotopic *l*(−)—leucine.

Organ	N^{15} concentration
	atom percent N^{15} excess
Blood plasma	0.108
Erythrocytes	0.019
Liver	0.061
Intestinal wall	0.097
Kidney	0.089
Heart	0.058
Spleen	0.072
Testes	0.050
Skin	0.012
Muscle	0.020
Carcass	0.030

A sample of leucine was prepared in which the isotope abundance of nitrogen was increased from the normal 0.37 to 6.9 atom percent. This compound was chemically and physiologically indistinguishable from the normal leucine, but could be quantitatively estimated even when mixed with large amounts of leucine present in the organism. After it had been fed to an animal, the rates at which this leucine incorporated into the protein and at which the nitrogen of its amino group was transferred to other compounds could be measured by isotope determinations.

In a typical experiment, full grown adult rats were kept for three days on an adequate diet to which had been added 215 mg of labeled *l*-leucine per rat per day. At the end of this experimental period the animals were killed and the N^{15} distribution determined. In Table III is given the isotope balance of the experiment.[14]

While the total amount of excreted nitrogen was equal to that in the diet, less than one-third of the marked leucine nitrogen was recovered in the excreta. More than half of the nitrogen of the leucine fed was present in the proteins. As a free amino acid had been fed and proteins had been analyzed, it is apparent that what we observed here is due not to a simple mixing process, but to extensive chemical reactions. The process must have been sufficiently rapid for half of the dietary leucine nitrogen to have been incorporated into the protein. The rate of transport of leucine nitrogen into the proteins is faster than its conversion to urea. It may again be stated that this type of information could not have been obtained with other techniques.

By examination of proteins of different organs, one finds that they do not take up equal concentrations of the labeled nitrogen. In Table IV are shown the values obtained in the *l*-leucine experiment. The blood proteins have taken up the labeled nitrogen most rapidly, and those of the skin most slowly. Intestinal wall, kidney, spleen, and liver follow the blood proteins in activity. Similar results are obtained after feeding tyrosine and glycine. The N^{15} content of the proteins is not due solely to the incorporation of the fed amino acid itself since, as will be shown later, the labeled nitrogen can be found in almost all of the amino acids of the protein.

In Table V are given the N^{15} concentrations in several amino acids isolated from the proteins. In each protein the highest N^{15} concentration was found in the leucine. This seems quite reasonable as this was the amino acid fed. From these figures it can be calculated that 8 percent of all the leucine nitrogen of the liver protein was that of the labeled leucine added to the diet. As the diet contains an equal amount of normal leucine, about 16 percent of the liver leucine nitrogen had been directly taken up from the dietary leucine in 3 days, i.e., about 5 percent per day. The labeled nitrogen is found not only in the leucine but also in most of the other amino acids. Thus the labeled nitrogen is present in tyrosine, glycine, the amide groups, etc. This is not a one-way reaction, for when tyrosine or glycine are fed, their labeled nitrogen can be found in the leucine. This transfer of amino groups proceeds even though the total amount of each particular amino acid is constant. It is a general reaction true not only for leucine but also for many of the other constituents of the proteins.

TABLE V. N^{15} concentration (atom percent excess) in protein constituents from rats fed isotopic *l*(−)—leucine.

	Liver	Intestinal wall	Total carcass
Total protein	0.061	0.097	0.030
Amide nitrogen	0.051	0.081	
Glycine	0.048	0.041	
Tyrosine	0.033	0.061	0.013
Aspartic acid	0.076	0.150	0.046
Glutamic acid	0.121	0.194	0.058
Arginine	0.058	0.028	0.016
Lysine	0.004	0.005	
Leucine	0.518	0.480	0.124

One would be inclined to call this a reversible reaction, were it not for the fact that the organism as a whole is not an equilibrium system. It can best be described as a system in a steady state. The composition is kept constant not because there are no reactions, or because the system has come to equilibrium, but because the rate of production of the cellular constituents is equal to their rate of degradation. The composition of the cell is thus governed by the rates of chemical reactions.

Since the glutamic acid of the proteins in the leucine experiment contained labeled nitrogen, this amino acid must have been synthesized. Synthesis took place in spite of the fact that the organism was being supplied with relatively large amounts of glutamic acid in its diet. The synthesis of a substance while the organism is liberally supplied with it is a general phenomenon, observed in the metabolism of fatty acids as well as in that of the amino acids. It is readily understandable by the concept of the steady state. All the enzymatic processes in the organism, whether synthetic or degradative, are in active operation. The systems involved in the synthesis of glutamic acid proceed even though large amounts of glutamic acid are supplied to the organism. The degradative systems also are continuously active though the amount of substrate they decompose is probably dependent on the concentration of the substrate. According to this hypothesis, all the molecules, with but few exceptions, are steadily being degraded and resynthesized.

The use of O^{18} for labeling oxygen is practically

the only method available as there exist no radioactive isotopes of oxygen with a half-lifetime long enough to permit chemical investigations. While oxygen may directly be measured on a mass spectrometer, in practice this is rarely done. Either the O_2 is converted to CO_2 or the water containing O^{18} is equilibrated with CO_2[15] and the CO_2 analyzed. The O^{18} concentration can be calculated from the ratio of the heights of the peaks corresponding respectively to mass 46 and mass 44.

The experiment reported by Ruben and his collaborators[16] on the source of oxygen liberated during the photosynthetic reaction illustrates the use of this isotope. The green plants are able to carry out, with the energy derived from light, the following fundamental reaction:

$$6CO_2+6H_2O\rightarrow 6O_2+C_6H_{12}O_6.$$

The equation as written does not indicate the source of the oxygen liberated, for a chemical equation merely gives the simplest expression for the resultant change of the number of compounds involved in the reaction. The equation indicates only that one water molecule disappears for each CO_2 molecule reduced. The actual mechanism of the reaction might involve many more water molecules. It is thus possible that the source of the liberated oxygen is either the CO_2 or the H_2O or a combination of both.

These authors suspended the unicellular plant, *chlorella*, in a water containing 0.85 atom percent O^{18}. Normal $NaHCO_3$ was added as a source of carbon dioxide. On illumination, oxygen was liberated of which the O^{18} concentration was equal to that of the water. From time to time samples of CO_2 were isolated and analyzed. As a result of an O^{18} exchange reaction, the concentration of O^{18} in the $NaHCO_3$ slowly increased during the experimental period. Even at the end, the O^{18} concentration in the $NaHCO_3$ was less than that of the liberated oxygen. Conversely, when the heavy oxygen was present in the HCO_3^- ion and normal water was employed, the oxygen liberated contained the normal O^{18} content. These results were interpreted by the authors to demonstrate that all the oxygen liberated in photosynthesis is derived from the water. Further work will no doubt throw more light on this interesting reaction. The authors found no evidence for the presence of enzymes in either *chlorella* or yeast which could catalyze the exchange reaction between water and oxygen.

Another reaction in which the heavy isotope of oxygen has been employed is in the study of the rate of hydration of CO_2 and dehydration of H_2CO_3. In solutions in which the pH is less than 8 the predominant reactions are

$$CO_2+H_2O\rightarrow H_2CO_3,$$
$$H_2CO_3\rightarrow HCO_3^-+H^+,$$

in which the first is rate determining. Above pH 10, the principal reaction is

$$CO_2+OH^-\rightarrow HCO_3^-.$$

The result of these reversible reactions will be the exchange of the oxygen atoms of the CO_2 and the H_2O. Mills and Urey have investigated these reactions and have calculated the rate constants of the various reactions involved.[17] The results are in fair agreement with those obtained by other methods. The rate of this reaction was also determined by labeling the CO_2 with C^{13}.

The outstanding result of work with isotopic carbon has been the discovery of the direct utilization of CO_2 by mammalian tissue. This work has been very actively investigated with both stable carbon C^{13} and radioactive carbon C^{11}. In 1936 Wood and Werkman[18] pointed out that propionic acid bacteria in their fermentation of glycerol fixed carbon dioxide. In 1940 Krebs and Eggleston[19] by a set of ingenious experiments, concluded that CO_2 could react with pyruvic acid as shown below.

$$CO_2+CH_3COCOOH\rightarrow COOH\cdot CH_2COCOOH.$$

Direct proof of such a reaction is, of course, extremely difficult, as every living cell continually produces such relatively large amounts of CO_2 that during the course of the experiment it produces more CO_2 than it fixes by the above reaction. At this time it was generally believed that CO_2 was a waste product of the cell. During the year of 1940 three different groups of investigators definitely proved that cells utilized CO_2 in their chemical reactions. Two of them, Evans and Slotkin[20] and Ruben and Kamen[21] used a radioactive carbon isotope, while Wood, Werkman,

Hemingway, and Nier used C^{13}.[22] The latter workers showed that in the fermentation of galactose, pyruvic acid, and citric acid by *B. Coli*, CO_2 is fixed and its carbon may be found in succinic acid. They suggest the following reaction mechanism:

CO_2+pyruvic acid→oxaloacetic acid
→succinic acid.

Evans and Slotkin[20] demonstrated the fixation of CO_2 by minced pigeon liver, isolating keto glutaric acid with carbon originating from CO_2. Fixation of CO_2 by the intact animal has been demonstrated by Solomon *et al* with the aid of C^{11}.[23]

These results have necessitated a revision of our concept of the mechanism of carbohydrate oxidation.

The oxidation of propionic acid by alkaline permanganate has been investigated by labeling the carboxyl group with carbon containing 4 atom percent excess C^{13}.[24] The CO_2 produced in the oxidation contained 1.43 and the oxalic acid 1.19 atom percent. Obviously only 37 percent of the liberated CO_2 comes from the carboxyl, the remainder from the methyl groups. This simple experiment illustrates the possibilities of the isotope technique in the study of reaction mechanism. The field has as yet been little explored, but great progress may be expected when mass spectrometers, in simplified form suitable for routine use, become readily available.

BIBLIOGRAPHY

(1) M. Dole, J. Am. Chem. Soc. **58**, 580 (1936); M. Dole and R. B. Gibney, J. Am. Chem. Soc. **58**, 2552 (1936).

(2) S. H. Manian, H. C. Urey, and W. Bleakney, J. Am. Chem. Soc. **56**, 2601 (1934).

(3) W. R. Smythe, Phys. Rev. **45**, 299 (1934).

(4) M. Dole and R. L. Slobod, J. Am. Chem. Soc. **62**, 471 (1940).

(5) M. Dole, J. Chem. Phys. **4**, 268 (1936); J. A. Swartout and M. Dole, J. Am. Chem. Soc. **61**, 2025 (1939).

(6) R. Schoenheimer and D. Rittenberg, J. Biol. Chem. **127**, 285 (1939).

(7) M. Heidelberger, H. S. Treffers, S. Ratner, and D. Rittenberg, J. Biol. Chem. (in press).

(8) A. O. Nier and E. A. Gulbransen, J. Am. Chem. Soc. **61**, 697 (1939).

(9) B. F. Murphey and A. O. Nier, Phys. Rev. **59**, 771 (1941).

(10) H. C. Urey and L. J. Greiff, J. Am. Chem. Soc. **57**, 321 (1935).

(11) D. Rittenberg and G. L. Foster, J. Biol. Chem. **133**, 737 (1940).

(12) S. Graff, D. Rittenberg, and G. L. Foster, J. Biol. Chem. **133**, 745 (1940).

(13) G. Hevesy, E. Hofer, and A. Krogh, Skand. Arch. Physiol. **72**, 199 (1935).

(14) R. Schoenheimer, S. Ratner, and D. Rittenberg, J. Biol. Chem. **130**, 703 (1939).

(15) M. Cohn and H. C. Urey, J. Am. Chem. Soc. **60**, 679 (1938).

(16) S. Ruben, M. F. Randall, M. D. Kamen, and J. L. Hyde, J. Am. Chem. Soc. **63**, 877 (1941).

(17) G. A. Mills and H. C. Urey, J. Am. Chem. Soc. **62**, 1019 (1940).

(18) H. G. Wood and C. H. Werkman, Biochem. J. **30**, 48 (1936).

(19) H. A. Krebs and L. V. Eggleston, Biochem. J. **34**, 1383 (1940).

(20) E. A. Evans, Jr., and L. Slotkin, J. Biol. Chem. **136**, 301 (1940).

(21) S. Ruben and M. D. Kamen, Proc. Nat. Acad. Sci. **26**, 418 (1940).

(22) H. G. Wood, C. H. Werkman, A. Hemingway, and A. O. Nier, J. Biol. Chem. **139**, 365 (1940).

(23) A. K. Solomon, B. Vennesland, F. W. Klemperer, J. M. Buchanan, and A. B. Hastings, J. Biol. Chem. **140**, 171 (1941).

(24) H. G. Wood, C. H. Werkman, A. Hemingway, A. O. Nier, and C. G. Stuckwisch, J. Am. Chem. Soc. **63**, 2140 (1941).

Here and There

Recent Appointments

Dr. Homer L. Dodge, Dean of the Graduate School of the University of Oklahoma, has been granted leave of absence to assume the position of Director of the Office of Scientific Personnel, National Research Council, Washington, D. C. Dr. Joseph C. Morris, former Director, returned on September 1 to his post at Tulane University to supervise a special electronics training program established at his initiative. Under Dean Dodge's direction the Office of Scientific Personnel will continue its function of assisting the Army, the Navy, and other war agencies to recruit competent scientific staffs. The Office is operated by the National Research Council at the request of, and under contract with, the Office of Scientific Research and Development.

Dr. W. N. Lowry, Professor of Physics at Bucknell University, has been appointed Chairman of the department to succeed Professor Frank M. Simpson who retired on July 1.

Dr. Joseph Haines Moore has been appointed Director of the Lick Observatory, University of California. He became a member of the observatory in 1903 and has been Assistant Director since 1936. He succeeds Dr. William H. Wright who retired July 1. Dr. Wright retains the rank of Astronomer and will continue work at the observatory.

Dr. Felix Adler and Dr. Richard P. Feynman have been appointed Visiting Assistant Professors of Physics at the University of Wisconsin for 1942–43.

The appointment to the physics staff of the Armour Research Foundation of Raymond E. Zenner, formerly a member of the engineering staff of the A. B. Dick Company, has been announced by Mr. Harold Vagtborg, Director.

★

Physicists Required for Civilian War Service

Many of the problems connected with our war program must be solved by scientists. Today the Civil Service Commission is seeking hundreds of physicists to work with specific war problems in the general field of physics.

Physicists are being recruited for the Federal government under a new examination announcement. To qualify, applicants must have a college degree with major study in physics or closely allied subjects. They must also have had a minimum of 2 years of professional experience in the field of physics, or appropriate graduate study in this field, or a combination of the two. The amount and character of the experience required beyond this minimum will vary with the grade and salary of the position for which the applicant is considered. Under this new announcement, teaching of physics will be considered professional experience for any of the grades of positions.

Persons who received eligible ratings under the physicists examination announced in March of this year need not apply unless they now possess the qualifications for eligibility for a higher grade position. The new examination announcement and application forms may be obtained at any first- or second-class post office or from the Commission in Washington, D. C. Applications will be accepted until the needs of the service have been met.

★

Bulletin of Mathematical Biophysics

The September, 1942 issue of the *Bulletin of Mathematical Biophysics*, edited by N. Rashevsky and published by the University of Chicago Press, will contain the following articles:

A Mathematical Theory of Protoplasmic Protrusions. I. HENRY E. STANTON

A Theory of Electrical Polarity in Cells. II. ROBERT R. WILLIAMSON

Green's Functions in Biological Potential Problems. ALVIN M. WEINBERG

Further Contributions to the Mathematical Biophysics of Visual Aesthetics. N. RASHEVSKY

Some Observations on the Simple Neuron Circuit. WALTER PITTS

Delayed Adsorption and Diffusion in Colloidal Media. HERMAN BRANSON

An Expression for the Rate of Return of an Egg after Artificial Deformation. H. D. LANDAHL

An Explanation of Spastic Walk due to Encephalitis Lethargica. FREDERICK R. HIRSCH, JR.

★

Necrology

E. H. Anthes, Manager of the New York branch of the Bausch & Lomb Optical Company since 1933, died on August 3 following a short illness. He had been associated with the company for 33 years.

Maurice L. Carr, Director of Research of the Pittsburgh Testing Laboratory, died on July 13 at the age of 65.

David William Cornelius, Professor of Physics at the University of Chattanooga, Tennessee, died on June 2 at the age of 57.

Andrew Russell Forsyth, Emeritus Professor of Mathematics at the Imperial College of Science and Technology, South Kensington, England, died on June 2 at the age of 83.

Captain William John Peters, formerly Chief Magnetic Observer of the Department of Terrestrial Magnetism of Carnegie Institution of Washington, died on July 10 at the age of 79.

Henry Gerber Reist, who retired as Chief of the Alternating Current Engineering Department of the General Electric Company in 1930, died on July 5 at the age of 80.

Norman Coleman Riggs, Professor Emeritus of Mechanics at the Carnegie Institute of Technology, Pittsburgh, where he had been a member of the faculty for over 30 years, died on July 18 at the age of 71 years.

Dr. Willard L. Roberts, of the department of research lamp development of the General Electric Company, Nela Park, Cleveland, died on July 24 at the age of 52.

★

Through an error the name of Francis Dominic Murnaghan, Professor of Applied Mathematics at Johns Hopkins University, was omitted from the list appearing in the July issue of this Journal of those elected to the National Academy of Sciences.

Contributed Original Research

A Diffraction Adapter for the Electron Microscope

J. Hillier, R. F. Baker, and V. K. Zworykin
Research Laboratories, RCA Manufacturing Company, Camden, New Jersey
(Received June 26, 1942)

An adapter has been developed which allows a conventional electron microscope to be used interchangeably as an electron diffraction camera or an electron microscope. The adapter comprises a unit which takes the place of the projection lens unit of the microscope, and includes a newly designed microscope projection lens, a specimen holder, and a focusing lens. To transform the instrument from a microscope to a diffraction camera (or vice versa) it is necessary only to transfer the specimen from the regular object chamber to the adapter. Diffraction patterns may be obtained by either reflection or transmission. As a result of the excellent reproducibility of voltages and currents from the regulated power supplies used in the electron microscope, the diffraction camera holds its calibration to within 0.1 percent over long periods. Using a calibration determined by measurements of gold patterns, lattice spacings of a number of common materials were determined and found to agree with x-ray values to within 0.5 percent.

THE desirability of augmenting the information obtained by means of an electron microscope with that obtained by means of an electron diffraction camera has been apparent throughout the development of the former instrument. In addition, the fact that many of the experimental conditions are the same in both types of instrument has made the possibility of combining them in one piece of equipment appear very attractive.

As part of a continuing program to extend the usefulness of the electron microscope as a scientific tool, an adapter has been developed which allows a conventional electron microscope to be used interchangeably either as a diffraction camera or as a microscope. The construction and use of this adapter will be described in this paper.

A practical diffraction adapter should satisfy several conditions. First, it should involve a minimum of change in the original instrument and, if possible, it should permit the instrument to be operated either as an electron microscope or as an electron diffraction camera, with the time and manipulation required for conversion kept at a minimum. Secondly, the addition of the adapter should in no way compromise the operation of the equipment as an electron microscope. Finally, there are a number of details which are desirable in a practical design, such as facilities for using the same specimen mount in either form of the instrument and for producing both transmission and reflection-type diffraction patterns. The apparatus to be described appears to meet all of these requirements.

The electron microscope is converted into the dual-purpose instrument by means of a unit which replaces the standard projection lens. A schematic cross section of the adapted instrument is shown in Fig. 1. The external dimensions of the adapter unit—*d*, *s*, and *t*—are made identical with the dimensions of the standard projection lens so that they may be interchanged without altering the microscope column. The upper half of this adapter *d* constitutes the microscope projection lens. It consists of an iron-encased coil fitted with a cylindrical receptacle, which contains the standard projection lens pole pieces. The coil has been designed so that the field strength corresponding to any value of the exciting current is the same as in the standard projection lens. This means that the current regulating circuit used to supply the projection lens current does not have to be modified and that the magnifications obtained with the adapted electron microscope are approximately the same as those obtained with the standard instrument.

Immediately below the projection lens *d* is situated the diffraction camera specimen holder *s*

with its associated adjustments and airlock system. A cross-sectional plan view of this part of the adapter is shown in Fig. 2. The airlock system used is similar to that described in connection with the electron microscope.[1] In this respect the diagram is self-explanatory. It is sufficient to note that the airlock system allows the withdrawal and insertion of specimens without altering the vacuum in the main column of the microscope. The specimen support is provided with three adjustments: (a) A semi-permanent adjustment of the position of the specimen relative to the electron beam, accomplished by the proper manipulation of the specimen mounting rod (*4*) in the block (*5*). This adjustment is very coarse because of the relatively large width of the electron beam; (b) a rotational adjustment of the specimen, which enables the angle of incidence of the electron beam striking the specimen to be adjusted; (c) an adjustment which permits the specimen to be rotated about an axis perpendicular to its own surface. This is useful for the taking of reflection patterns, and is accomplished by means of the nut (*6*) which travels along the threaded rod (*8*) and pulls a flexible belt stretched in a groove in the edge of the rotatable specimen table. The vacuum seal is maintained in the adjustments (b) and (c) by means of a "packing nut" type of gasket seal. When properly lubricated, these seals appear to be satisfactory and greatly simplify the design.

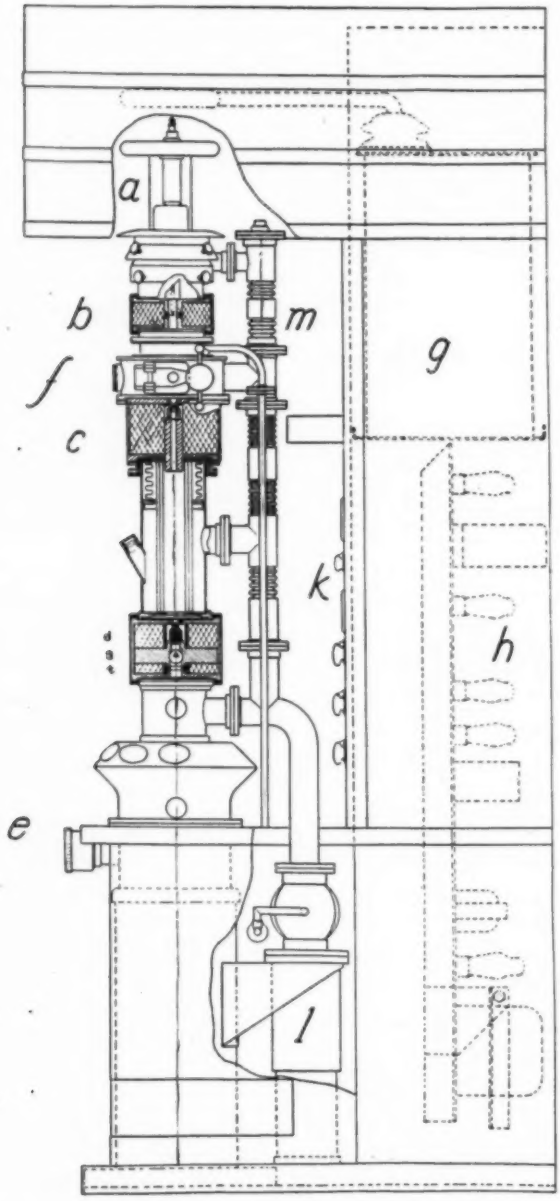

FIG. 1. Schematic cross section view of electron microscope fitted with diffraction adapter.

For transmission patterns, the specimen is mounted on a 200-mesh screen $\frac{1}{8}$ inch in diameter, which is identical with the screen used as specimen mount when making electron micrographs. This screen rests inside a cap which fits over the end of the specimen holder shaft. For reflection patterns, the specimen is mounted on the end of the specimen-holder shaft in such a way that the electron beam is incident at a grazing angle (as shown in Fig. 2). Large diaphragms are placed below the specimen for both types of pattern in order to prevent the occurrence of reflections from the walls of the focusing lens.

The lower half of the adapter, *t* in Fig. 1, constitutes the focusing lens. This consists of a short iron-encased coil, the axis of symmetry of which coincides with the axis of the projection coil. This coil has been designed so that it can be operated from the projection-lens-coil supply. The only modification involved is the addition of external, control, and compensating resistors. These are mounted in an auxiliary panel. A switch is provided by means of which either the projection lens or focusing lens may be connected to the supply, according to whether the instrument is to be used as a microscope or as a diffraction camera.

[1] J. Hillier and A. W. Vance, Proc. I. R. E. **29**, 167 (1941).

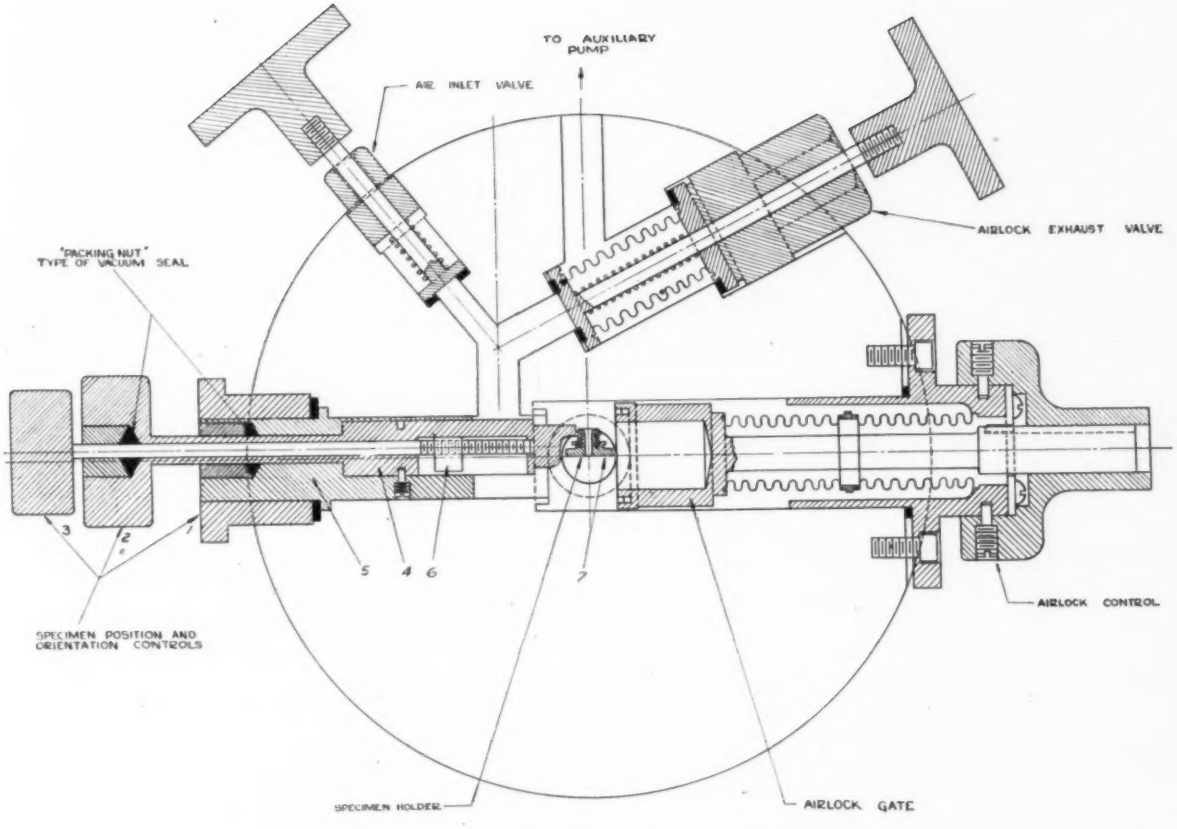

FIG. 2. Plan view of electron microscope diffraction adapter.

Figure 3 is a "ray" diagram of the microscope as fitted with the diffraction adapter. The solid lines represent real electron trajectories, the dashed lines virtual electron trajectories. The condenser lens of the microscope produces an image of the electron source (or its cross-over) at a point just above the objective lens. The objective lens forms a reduced image which acts as an electron source for the diffraction camera. The projection lens current is, of course, made zero when the adapter unit is functioning. An aperture of 0.012-inch diameter placed immediately above the specimen functions as a limiting aperture for the focusing lens rather than as a collimating aperture. In practice, the lens currents are adjusted for maximum definition of the diffraction pattern. For any given voltage there exists a focusing lens current which will give the sharpest definition; once this current has been determined, it can be set at that value until the voltage is changed. The condenser lens can be used for changing the over-all intensity of the pattern just as in taking electron micrographs.

CALIBRATION

The ultimate usefulness of diffraction patterns as a means of analysis depends to a great extent on the precision with which lattice spacings of the specimen can be determined. Since accurately determined standards are available, the technical problem of obtaining precise results reduces to the problem of obtaining an accurate and reproducible calibration. A diffraction pattern is reproducible obviously only to the extent that the experimental conditions—electrical and mechanical—are reproducible. The electrical supplies for the electron microscope are ideal in this respect, since the output voltages and currents are dependent almost entirely on the voltages of standard batteries[2] operating under no-load conditions. As a result, it is not necessary to calibrate

[2] A. W. Vance, RCA Rev. **5**, 293 (1941).

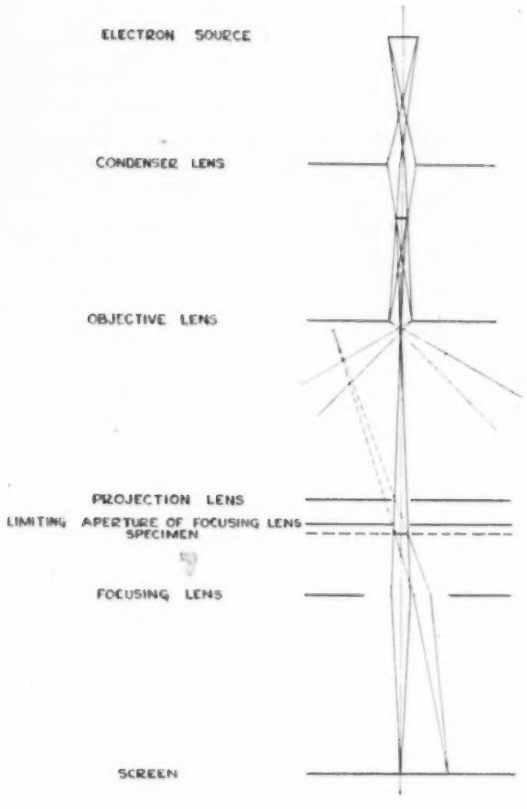

FIG. 3. Ray diagram of electron microscope with diffraction adapter.

TABLE I.

$D(\text{mm}) \pm(\Sigma d^2)^{\frac{1}{2}}/N$	$D(\text{mm}) \pm(\Sigma d^2)^{\frac{1}{2}}/N$
1. 10.0430±0.0026	26.0236±0.0054
2. 10.0547±0.0029	26.0021±0.0056
3. 10.0919±0.0027	25.9964±0.0052
4. 10.063 ±0.012	26.007 ±0.007

the instrument each time accurate measurements are required (for instance, by photographing a standard pattern on each plate). Instead a calibration can be made which will remain valid over a long period of time. Such a calibration can be easily made by photographing a pattern for which the lattice spacings are accurately known, measuring the ring diameters, and plotting these against the lattice spacings. A log-log plot of ring diameter D *versus* lattice spacing d_{hkl} will, in general, be found to be a straight line since these variables must obey the Bragg law

$$D \cdot d_{hkl} = 2k\lambda L, \tag{1}$$

where L is the distance between the specimen and the photographic plate, λ is the de Broglie wavelength of the electron, and k is an instrumental constant. A log-log plot of Eq. (1) is shown as a straight line in Fig. 4, while the experimental points are shown enclosed in circles. There is a

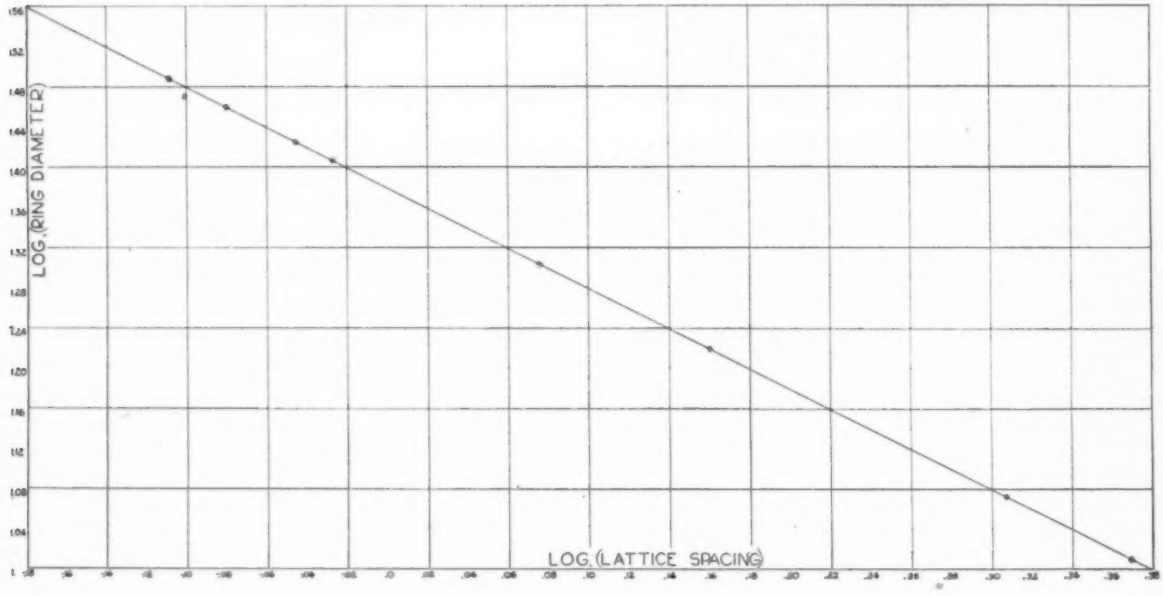

FIG. 4. Calibration of diffraction camera at 78 kilovolts.

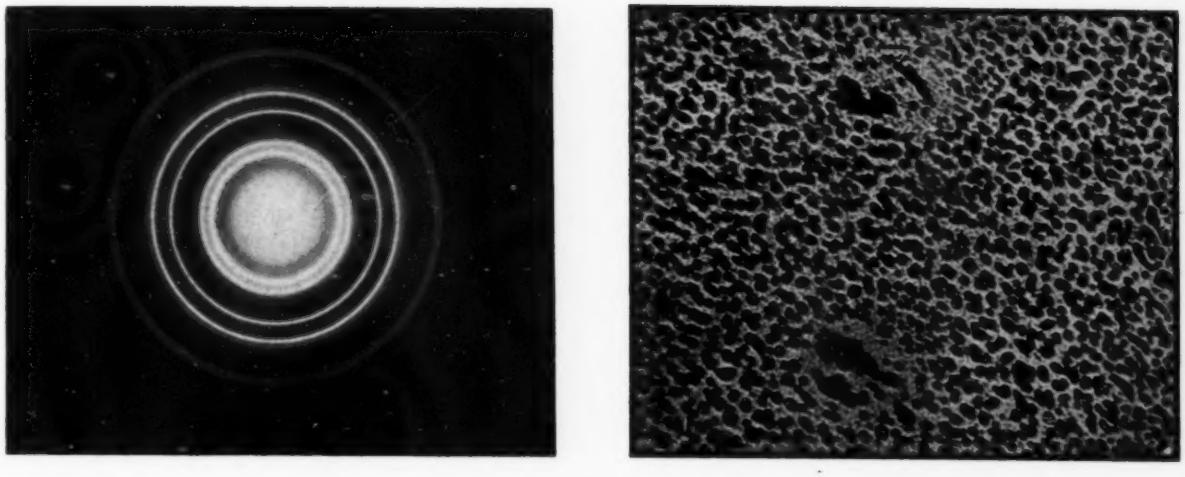

FIG. 5. Evaporated silver film.

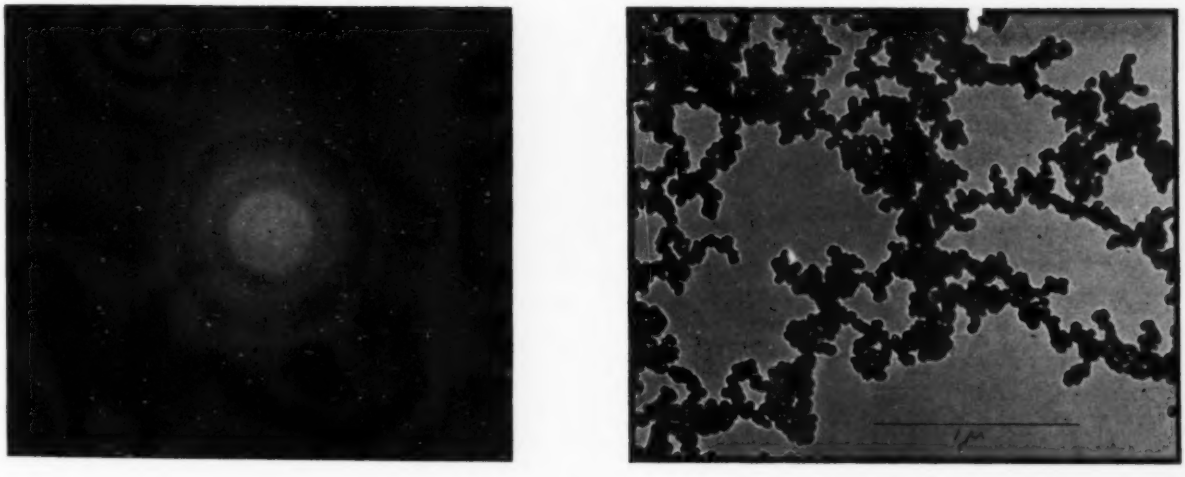

FIG. 6. Carbon black.

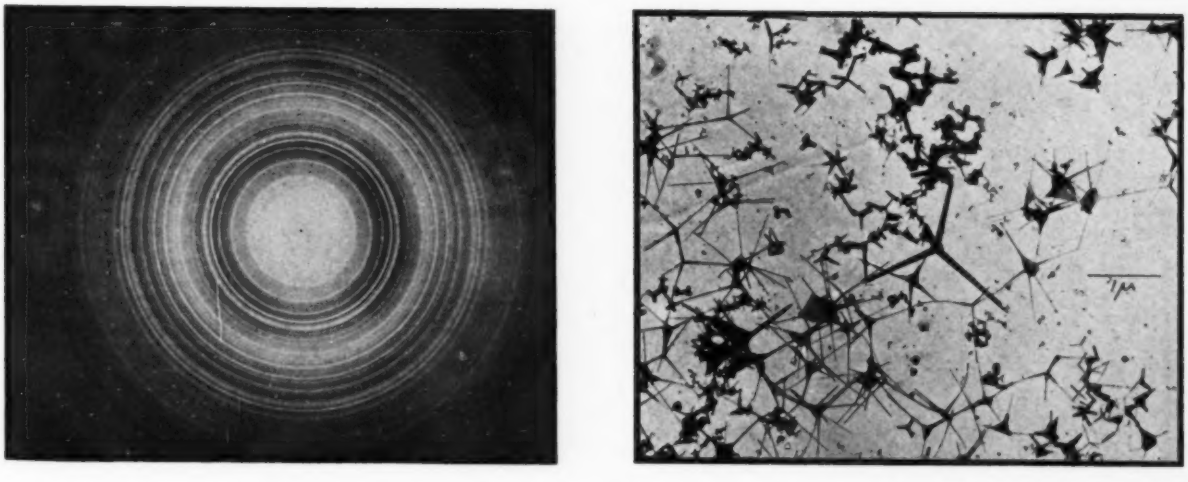

FIG. 7. Zinc oxide smoke.

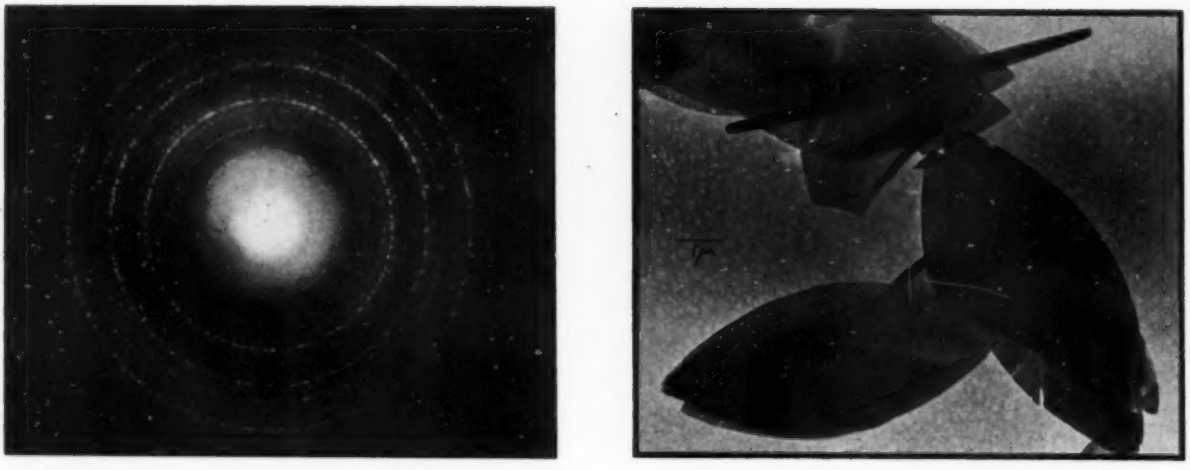

FIG. 8. Monohydrated aluminum oxide.

slight divergence (0.25 percent) from the straight line at large ring diameters. This distortion is introduced as a result of the use of the focusing lens, but in no way affects the accuracy of the empirical calibration described above.

The reproducibility is shown by Table I which exhibits data taken on three gold specimens over a period of about a week. Two rings in each pattern were measured and each ring was measured ten times with a Gaertner comparator. The mean values and the root-mean-square deviations of each set of measurements are listed in Table I. The numbers 1, 2, and 3 refer to the diffraction patterns obtained from the three specimens. The mean of the three diameters is given opposite the number 4. The root-mean-square deviation of this final mean is a measure of the accuracy with which the diffraction camera reproduces a pattern.

As a further test of the instrument a mixture of potassium dichromate and lead oxide was prepared and the diffraction pattern photographed. Seven rings were measured and the corresponding lattice spacings computed on the basis of the calibration given in Fig. 4. Table II shows the agreement obtained with known lattice spacings (powder x-ray method).[3]

[3] Hanawalt, Rinn, and Frevel, Ind. Eng. Chem. **10**, 457 (1938).

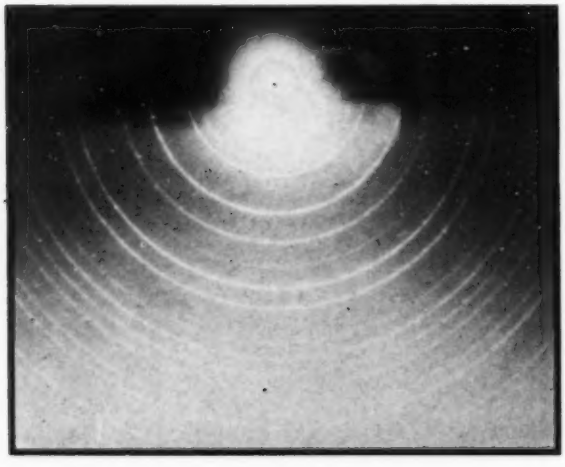

FIG. 9. Reflection pattern from magnesium oxide smoke.

FIG. 10. Reflection pattern from etched single silicon crystal.

TABLE II.

d (x-ray)	d (meas.)	Origin
3.68	3.68	Potass. Dich.
3.29	3.30	Potass. Dich.
3.06	3.07	Lead Oxide
2.85	2.84	Potass. Dich.
2.62	2.62	Potass. Dich.
1.66	1.66	Potass. Dich.
1.52	1.53	Lead Oxide

RESULTS

A number of typical diffraction patterns with accompanying electron micrographs are shown in Figs. 5 to 10. The micrographs and diffraction patterns were photographed within a few minutes of each other without alteration of the specimen in any way except to transfer it from the diffraction holder to the regular microscope holder.

The Reflection of Electromagnetic Waves from a Parabolic Friction-Free Ionized Layer

OLOF E. H. RYDBECK
Chalmers Institute of Technology, Gothenburg, Sweden
(Received May 13, 1942)

THE electron density distribution of the undisturbed F_2 layer of the ionosphere very often is essentially parabolic[1,2] at least at sufficient distances from the equator. It is therefore of general interest to study briefly the reflection of electromagnetic waves from such a layer.

We assume that plane waves are transmitted in a direction normal to the ionized layer, the electron density of which is a function of the vertical (normal) distance only. The wave equation thus has the following form, *viz.*,

$$\frac{d^2\Pi}{dz^2}+\frac{\omega^2}{c^2}\cdot\epsilon\cdot\Pi=0, \tag{1}$$

so that the electric field-strength (transversal) will be given by

$$E=\Pi\cdot e^{-i\omega t}. \quad (i=\sqrt{-1}) \tag{1a}$$

If the electron density distribution is parabolic with half-thickness Δh_m, then

$$N=N_{\max}\left(1-\left(\frac{z}{\Delta h_m}\right)^2\right), \tag{2}$$

where $N_{\max}$ is the maximum electron density and z, the vertical distance, is counted from its level. Remembering that the dielectric "constant" is*

$$\epsilon=1-\frac{4\pi\cdot N\cdot e^2}{m\cdot\omega^2}=1-\frac{f_{cm}^2}{f^2}\left\{1-\left(\frac{z}{\Delta h_m}\right)^2\right\}, \quad (\omega=2\pi f) \tag{3}$$

with f_{cm} denoting the so-called critical or penetration frequency of the layer, it is easily established that

[1] O. Rydbeck, "The propagation of electromagnetic waves in an ionized medium and the calculation of the true heights of the ionized layers of the atmosphere," Phil. Mag. [7] **30**, 282 (Oct. 1940).
[2] O. Rydbeck, "A theoretical survey of the possibilities of determining the distribution of the free electrons in the upper atmosphere," Trans. Chalmers University, No. 3, Gothenburg, Sweden (1942).
* m = mass of electron, e = charge of electron.

the wave equation can be written

$$\frac{d^2\Pi}{dV^2}+\left[i\cdot\rho-\frac{V^2}{4}\right]\cdot\Pi=0, \tag{4}$$

where $$\rho=\pi\cdot\frac{\Delta h_m}{\lambda_{c_m}}\cdot\frac{f_{c_m}{}^2-f^2}{f_{c_m}{}^2} \quad \text{and} \quad V=(4\pi\cdot\Delta h_m/\lambda_{c_m})^{\frac{1}{2}}\cdot(z/\Delta h_m)\cdot e^{i\pi/4}=u\cdot e^{i\pi/4}. \tag{4a}$$

$\Delta h_m/\lambda_{c_m}$ always is large, 2 to 5×10^3 is a typical day-time value for the F_2-layer; ρ is also large except near the penetration frequency. Equation (4) is satisfied by Weber's parabolic cylinder functions. One of them is†

$$\Pi=\underset{i\rho-\frac{1}{2}}{D}(u\cdot e^{i\pi/4}). \tag{5}$$

From Whittaker's integral representation one easily obtains the following asymptotic expansion, *viz.*,

$$\underset{i\rho-\frac{1}{2}}{D}(u\cdot e^{i\pi/4})\backsimeq\exp\left[-i(u^2/4-\rho\cdot\ln u+\pi/8)\right]\cdot\frac{e^{-\pi\cdot\rho/4}}{(u)^{\frac{1}{2}}}\cdot\left[1\overbrace{-\frac{i(\rho+i\frac{1}{2})(\rho+i\frac{3}{2})}{2u^2}+\cdots}^{\text{Phase Angle }-\phi}\right]. \tag{5a}$$

As u always is large the only restriction is that ρ must be sufficiently small. A safe limit is marked by

$$\rho^2/2u^2<1, \quad \text{or} \quad |\Delta f|=|f_{c_m}-f|<(2\cdot c/\pi\cdot\Delta h_m)^{\frac{1}{2}}\cdot(f_{c_m})^{\frac{1}{2}}.$$

If, for example, $f_{c_m}=10^7$ c.p.s. and $\Delta h_m=100$ km then $|\Delta f|$ becomes less than about 1.4×10^5 c.p.s. The present expansion can therefore only be used in the neighborhood of the penetration frequency f_{c_m}. As this is the region where the main deviation from geometrical optics occurs the expansion is sufficient for our present purpose.

Multiplying by the time factor we see that

$$e^{-i\omega t}\cdot\underset{i\rho-\frac{1}{2}}{D}(u\cdot e^{i\pi/4})$$

yields an up-going wave. Another solution is

$$\underset{-i\rho-\frac{1}{2}}{D}(u\cdot e^{-i\pi/4})\backsimeq\exp\left[+i(u^2/4-\rho\cdot\ln u+\pi/8)\right]\cdot\frac{e^{-\pi\cdot\rho/4}}{(u)^{\frac{1}{2}}}\cdot\left[1\overbrace{+\frac{i(\rho-i\cdot\frac{1}{2})(\rho-i\cdot\frac{3}{2})}{2u^2}-\cdots}^{\text{Phase Angle }+\phi}\right], \tag{6}$$

which multiplied by the same time-factor yields a down-coming wave. Next we have to find a suitable circuit relation of the differential equation connecting the incident, the reflected, and the refracted waves. Fortunately enough, there exists a fairly simple one, *viz.*,

$$\underbrace{\underset{i\rho-\frac{1}{2}}{D}(u\cdot e^{i\pi/4})}_{\text{incident wave}}=\underbrace{\frac{(i\rho+\frac{1}{2})!}{(2\pi)^{\frac{1}{2}}}\cdot e^{\pi\rho/2+i\pi/4}\cdot\underset{-i\rho-\frac{1}{2}}{D}(u\cdot e^{-i\pi/4})}_{\text{reflected wave}}+\underbrace{\frac{(i\rho+\frac{1}{2})!}{(2\pi)^{\frac{1}{2}}}\cdot e^{-\pi\rho/2-i\pi/4}\cdot\underset{-i\rho-\frac{1}{2}}{D}(u\cdot e^{i(3/4)\pi})}_{\text{refracted wave}}. \tag{7}$$

Mathematically speaking the above expression is the analytical continuation of the function of the refracted ray, represented by an asymptotic series, for instance, beyond the region for which this special representation is valid. The law of refraction gives us, therefore, a physical visualization of the concept of analytical continuation.

From a practical point of view we are primarily interested in the phase difference between the

† The symbol is that used by Whittaker. See Whittaker and Watson, *A Course of Modern Analysis*, p. 347.

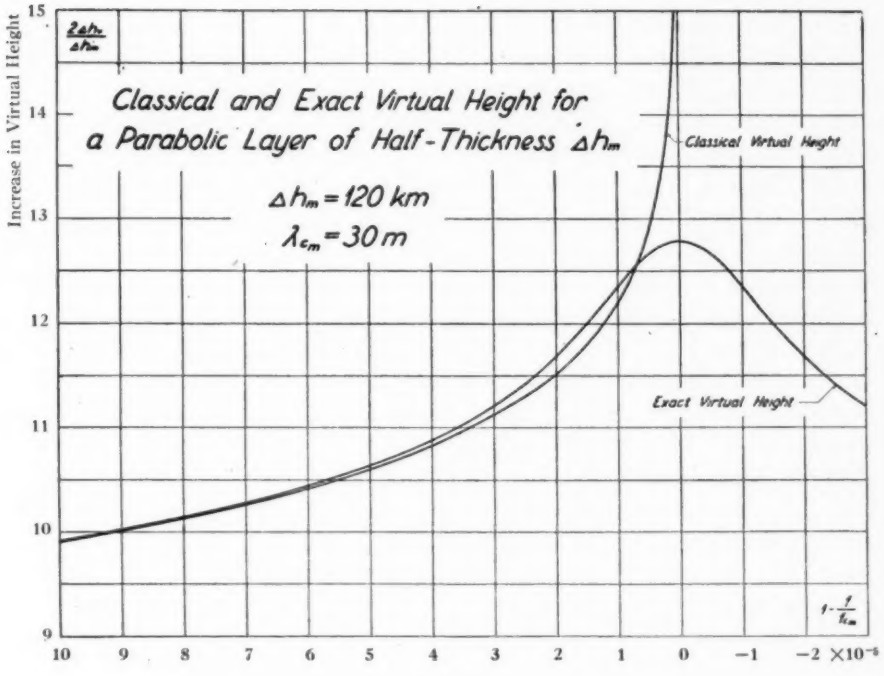

FIG. 1.

up-going and down-coming waves at the bottom of the layer ($z=\Delta h_m$). This is

$$\Delta S=\frac{u^2}{2}-\rho \ln (4u^2)+\text{Phase}\left[\frac{(i2\rho)!}{(i\rho)!}\right]+2\cdot\phi+\frac{\pi}{2}.$$

The time of travel of the returned ray times the velocity of light in vacuum generally is called the virtual path length. This is equal to two times the virtual height (vertical incidence). The virtual height therefore becomes

$$\Delta h_v=(c/2)(d(\Delta S)/d\omega)=c/4\pi[-\ln (4u^2)+2\rho/u^2+Re(\psi(i2\rho)-\psi(i\rho))]d\rho/df,$$

where $\psi(a)$ is the logarithmic derivative of $a!$. This finally yields

$$\Delta h_v=\frac{\Delta h_m}{2}\cdot\frac{f}{f_{c_m}}\left[\gamma+\ln\left(16\cdot\pi\cdot\frac{\Delta h_m}{\lambda_{c_m}}\right)-\rho\left(\frac{2}{u^2}-Re\sum_{n=1}^{\infty}\frac{2\rho-i3n}{n(n+i\rho)(n+2i\rho)}\right)\right], \tag{8}$$

with γ denoting Euler's constant 0.5772. At the penetration frequency the *exact* virtual height becomes

$$\Delta h_v=\Delta h_m/2[\gamma+\ln (16\pi\cdot\Delta h_m/\lambda_{c_m})]. \tag{8a}$$

This is not infinite as should follow from the classical virtual height expression of the geometrical optics, *viz.*,

$$\Delta h_v=(\Delta h_m/2)\cdot f/f_{c_m}\cdot\ln (f_{c_m}+f/f_{c_m}-f). \tag{8b}$$

It is fairly easy to show from Eq. (8) that

$$\lim_{(\Delta h_m/\lambda_{c_m}\to\infty)}\frac{(\Delta h_v)_{\text{exact}}}{(\Delta h_v)_{\text{classical}}}=1.$$

This shows mathematically the transition to diffraction-free optics when the geometrical dimensions

become infinitely great. Figure 1 shows a plot of the classical and true virtual heights near the penetration frequency for a parabolic layer of 120-km half-thickness and a critical wave-length of 30 m. For such a thick layer the discrepancy between the classical and exact virtual heights is appreciable only within a very narrow frequency range. For the layer in question this region is only about 1000 c.p.s. wide. For a thinner layer this region becomes proportionately wider. For a very thin layer, with a half-thickness of only four wave-lengths, i.e., 120 m, the discrepancy region becomes considerable, *viz.*, 10^6 c.p.s. For such a thin layer the reflection coefficient will also differ considerably from the classical one.

A few words should be said about the introduction of the electronic collisional frequency ν. It is formally introduced in the wave function if f_{cm} is given the phase angle $-\alpha$, where $\alpha=\frac{1}{2}$ arc tan (ν/ω). The introduction of the collisional frequency actually complicates the numerical calculation very much. A treatment of this case therefore is outside the scope of the present communication. It should suffice here to state that the influence of the collisional friction is negligible as long as $(\nu/\omega)^2 \ll 1$.*

Figure 2 shows a low loss sensitive recording of ionospheric reflections at Cambridge, Massachusetts, from a practically parabolic layer. The layer half-thickness is about 70 km and the critical wave-length is 47.2 m. The exact virtual height at the critical frequency becomes 5.88 Δh_m. The highest virtual height recorded is 4.60 Δh_m. The absorption therefore does not permit us to register the discrepancy between the classical and the exact theory (for such a thick layer). This could perhaps be done if a very powerful sender were used.

As the medium is non-dissipative, one immediately obtains from the circuit relations that the reflection coefficient R is determined by the relation

$$\frac{R^2}{1-R^2}=e^{2\pi\rho}=\exp\left[\left(4\pi^2\cdot\frac{\Delta h_m}{\lambda_{cm}}\cdot\frac{f_{cm}^2-f^2}{2\cdot f_{cm}^2}\right)\right]. \tag{9}$$

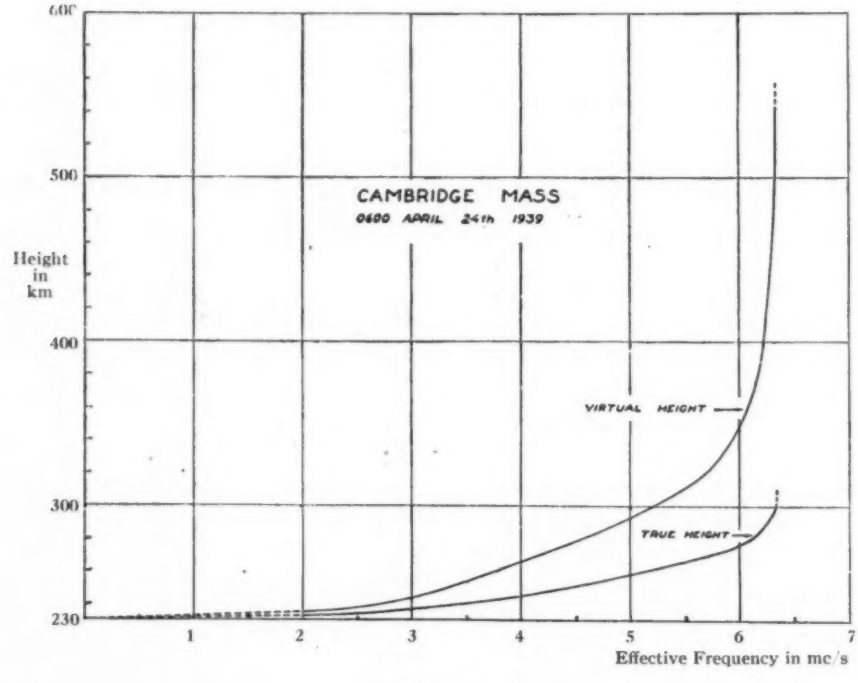

FIG. 2.

* A complete treatment of the dissipative case will appear shortly in the Transactions of Chalmers University, Gothenburg.

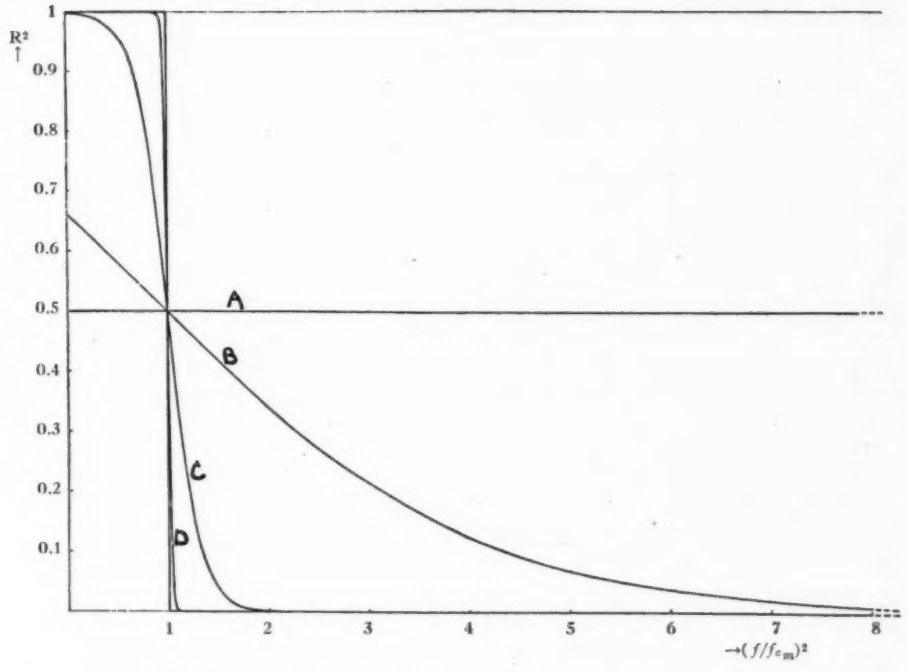

FIG. 3. The reflection coefficient for a friction free parabolic layer as a function of the wave frequency. $\lambda_{c_m} = 30$ m, Δh_m = layer half-thickness. Curve A: $\Delta h_m = 0$; curve B: $\Delta h_m = 1$ m; curve C: $\Delta h_m = 10$ m; curve D: $\Delta h_m = 100$ m.

This holds throughout the frequency range. Figure 3 shows several plots of the reflection coefficient squared as a function of $(f/f_{c_m})^2$. The critical wave-length is 30 m as before. The deviation from classical optics is practically noticeable first for a half-thickness of about four to three wave-lengths. As the layer becomes even thinner appreciable reflections appear at frequencies well above the critical frequency. It is obvious that the critical frequency conception is misleading for a very thin layer.

Finally it should be stated that results similar to Eq. (8) have been obtained by Rawer[3] in an excellent paper on the reflection of electromagnetic waves from dissipative Epstein-layers.

An extended study of the parabolic solutions for other values of frequency necessitates the expansion of the functions in asymptotic series which can be used when not only u but also ρ is large. Interesting as such a study may be it is outside the scope of the present communication. This is especially true because the discrepancy between the classical and the exact theories is entirely negligible for lower frequencies as is clearly demonstrated by Figs. 1 and 3. An account of these expansions will, however, appear shortly in the Transactions of Chalmers University, Gothenburg, Sweden, to which those especially interested are referred.

[3] K. Rawer, "Elektrische Wellen in einem geschichten Medium," Ann. d. Physik **35**, 402 (1939).

Variation of the Axial Aberrations of Electron Lenses with Lens Strength

E. G. RAMBERG
Research Laboratories, RCA Manufacturing Company, Inc., Camden, New Jersey
(Received June 23, 1942)

The variation of refractive power and spherical aberration with electrode voltages and field strengths is studied for two characteristic unipotential lenses, an immersion lens, and a magnetic lens. Conclusions are drawn herefrom regarding the variation, with lens strength and applied voltage, of the resolving power obtainable with the lens as an electron-microscope objective. Scattered measurements by other authors agree satisfactorily with the results. The "relativistic aberration" of the electrostatic unipotential lenses, i.e., the effect on the image of fluctuations in the over-all applied voltage, is calculated and shown to be of significance in the electrostatic electron microscope. Furthermore, the axial chromatic aberrations are computed for the four systems and the question of upper limits of the last two aberrations is discussed.

I. INTRODUCTION

NEARLY all publications which have, in the past, concerned themselves with the determination of the aberrations of specific lens systems have dealt either with weak electron lenses[1–3] or short electron lenses,[4] or have limited themselves to reporting measurements on isolated cases.[5–8] Exceptions to this rule are covered by the measurements of Ruska[9] on a series of magnetic electron microscope objectives, those of Becker and Wallraff[10] on the fields formed by solenoids and by iron-enclosed coils with variable air-gap width, and, finally, the calculations by Rebsch[11] for a series of fields with the common property of having the maximum of the magnetic field strength or of the ratio of the electric field strength to the electric potential coincide with the focal point of the electron lens. While all of these authors determined the aberrations of a number of different (primarily magnetic) fields, they confined themselves to systems of essentially constant refractive power. The present work was undertaken to establish a bridge between the familiar results of weak lens theory and the properties of lenses such as are used in actual practice by investigating mathematically the variation with the electrode voltages or the maximum magnetic field strength of the refractive power and the aperture defect and other axial aberrations for a number of typical lenses. In this connection the mathematical approach has three advantages over the experimental method, such as has been recently described by Spangenberg and Field:[8]

1. It makes it possible to isolate the effect of variations in lens strength from that of imperfections of construction and, in the case of magnetic lenses, from that of changes in the field distribution resulting from saturation phenomena.

2. It permits the determination, undisturbed by higher order terms, of the third-order aberration coefficient, which alone is of importance in the case of electron-microscope objectives in view of their very low effective aperture; an accurate evaluation of the distortion patterns in Spangenberg and Field's method may require ranges of angle for which the contribution of the higher order aberrations is appreciable.

[1] O. Scherzer, "Weak electrostatic equipotential lens with least spherical aberration," Zeits. f. Physik **101**, 23–26 (1936).
[2] R. Rebsch and W. Schneider, "Aperture defect of weak electron lenses," Zeits. f. Physik **107**, 138–143 (1937).
[3] G. N. Plass, "Electrostatic lenses with a minimum of spherical aberration," J. App. Phys. **13**, 49–55 (1942).
[4] W. Glaser, "Short magnetic lens of least aperture defect," Zeits. f. Physik **109**, 700–721 (1938).
[5] D. W. Epstein, "Electron-optical system of two cylinders as applied to cathode ray tubes," Proc. I.R.E. **24**, 1095–1139 (1936).
[6] G. A. Morton and E. G. Ramberg, "Electron optics of an image tube," Physics **7**, 451–459 (1936).
[7] M. v. Ardenne, "Magnitude of the aperture defect of the electron microscope," Zeits. f. tech. Physik **20**, 289–290 (1939).
[8] K. Spangenberg and L. M. Field, "Some simplified methods of determining the optical characteristics of electron lenses," Proc. I.R.E. **30**, 138–144 (1942).
[9] E. Ruska, "Magnetic objective for the electron microscope," Zeits. f. Physik **89**, 90–228 (1943).
[10] H. Becker and A. Wallraff, "Spherical aberration of magnetic lenses," Arch. f. Elektrotechnik **32**, 664–675 (1938).
[11] R. Rebsch, "Theoretical resolving power of the electron microscope," Ann. d. Physik **31**, 551–560 (1938).

3. The mathematical method can be applied over a larger range without loss in accuracy.

It should be emphasized, at the same time, that in many, perhaps most, practical cases the experimental method is to be preferred; this is particularly the case for strong magnetic lenses, for which field measurements are likely to be quite inaccurate and field calculations precluded by the peculiar properties of most ferromagnetic materials.

II. THE WEAK LENS APPROXIMATION

A convenient point of departure for electron-optical calculations is the paraxial ray equation in the form introduced by Scherzer:[12]

$$R''=-TR; \quad T=3\Phi'^2/16\Phi^2+eH^2/8m\Phi. \quad (1)$$

Here Φ is the electric potential and H the magnetic field along the axis of the lens system; the origin of the potential is chosen so that $e\Phi$ represents the kinetic energy of the electron considered, $-e$ and m being the charge and mass of the electron, respectively. $R=r\Phi^{\frac{1}{4}}$, where r is the separation of the electron from the optic axis. Primes indicate differentiation with respect to z, the coordinate measuring distances along the optic axis.

For a very weak or short electron lens, R may be considered as a constant within the lens field.[13] For a ray incident parallel to the axis from the image space (potential Φ_i), the focal length in object space (potential Φ_0) of the weak (or short) lens becomes

$$\frac{1}{f_0}=-\frac{r_0'}{r_i}=-\left(\frac{\Phi_i}{\Phi_0}\right)^{\frac{1}{4}}\frac{R_0'}{R_i}=-\left(\frac{\Phi_i}{\Phi_0}\right)^{\frac{1}{4}}\int_{z_0}^{z_i}T dz, \quad (2)$$

r_0' and R_0' being the slopes of r and R, respectively, at the focal point in object space. If, now,

$$\Phi=\Phi_A(1+a\varphi(z)); \quad H=H_{\max}\cdot H(z)/H_{\max}, \quad (3)$$

and A and $H_{\max}$ are made very small without altering $\varphi(z)$ and $H(z)/H_{\max}$—e.g., by approaching the lens electrode potentials to Φ_A and by reducing the currents in the field coils—

$$\frac{1}{f_0}=-\left(\frac{\Phi_i}{\Phi_0}\right)^{\frac{1}{4}}\left\{\frac{3A^2}{16}\int_{z_0}^{z_i}\varphi'^2dz+\frac{eH^2_{\max}}{8m\Phi_A}\int_{z_0}^{z_i}\frac{H^2}{H^2_{\max}}dz\right\}. \quad (4)$$

The (third-order) aperture defect or spherical aberration may be written

$$\Delta r=\zeta r_a^3=M\cdot C\cdot f_0\theta^3. \quad (5)$$

Here Δr is the separation from the axis in the paraxial or Gaussian image plane of a ray $r(z)$ leaving the center of the object at an inclination θ to the axis; r_a is the separation from the axis of the same ray in an arbitrarily chosen aperture plane. ζ is an aberration constant depending on the location of this plane, while C is a form of the aberration constant which is both dimensionless and independent of the choice of the aperture plane; it does not change if the system is changed in scale, provided the relative dimensions are left unaltered and the electric and magnetic scalar potentials of the lens elements remain the same. M is the magnification of the image. According to Scherzer,[14] if the object is placed substantially at the focal point, i.e., for large magnifications, such as occur in the electron microscope,

$$C=-\frac{1}{16}\left(\frac{R_i}{R_0'}\right)^3\left(\frac{\Phi_i}{\Phi_0}\right)^{\frac{1}{4}}\int_{z_0}^{z_i}\left(\frac{\Phi_0}{\Phi}\right)^{\frac{1}{4}}\times\left[\frac{5}{4}\left(\frac{\Phi''}{\Phi}+\frac{\Phi'}{\Phi}\frac{R'}{R}-\frac{5}{4}\frac{\Phi'^2}{\Phi^2}\right)^2+\left(\frac{\Phi'}{\Phi}\frac{R'}{R}+\frac{5}{8}\frac{\Phi'^2}{\Phi^2}\right)^2+\frac{1}{64}\frac{\Phi'^4}{\Phi^4}+\frac{e}{m\Phi}\left(H'+H\frac{R'}{R}-\frac{3}{2}\frac{H\Phi'}{\Phi}\right)^2+\frac{eH^2}{m\Phi}\frac{R'^2}{R^2}+\frac{e^2H^4}{4m^2\Phi^2}+\frac{eH^2}{32m}\frac{\Phi'^2}{\Phi^2}\right]\frac{R^4}{R_i^4}dz. \quad (6)$$

For a finite image distance the coefficient of the integral must merely be replaced by $-(1/16f_0)(R_i/R_0')^4$. If Eq. (3) is substituted in

[12] O. Scherzer, "Some aberrations of electron lenses," Zeits. f. Physik **101**, 593–603 (1936).

[13] In view of the uniform curvature of the function $R(z)$ toward the axis, this does not lead to error in the case of very weak lenses, while a similar assumption for $r(z)$ does —see Plass, reference 3.

[14] Scherzer, reference 12, Eq. (13).

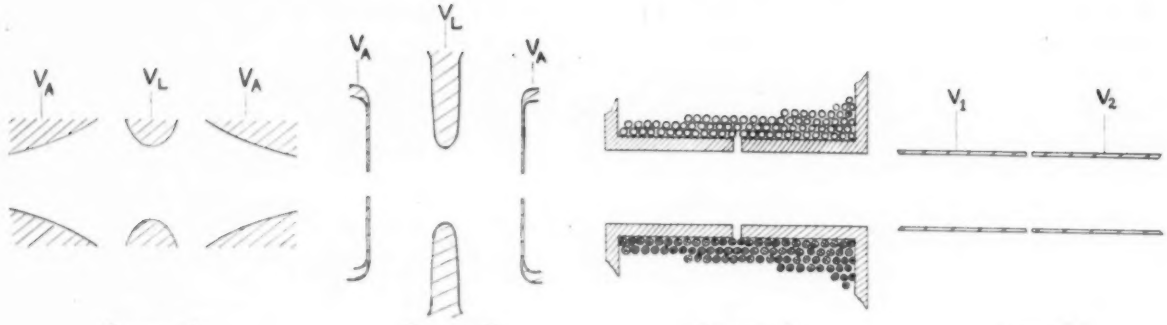

FIG. 1. Electrode and polepiece configuration of the electron lenses studied.

Eq. (6) and terms involving higher powers than the second of A and $H_{\max}/\Phi_A^{\frac{1}{2}}$ are omitted, the weak lens expression for $\zeta/M=C/f_0^2$ becomes

$$\frac{\zeta}{M}=\frac{C}{f_0^2}=-\frac{f_0}{16}\left(\frac{\Phi_i}{\Phi_0}\right)^{\frac{1}{2}}\int_{z_0}^{z_i}\left\{\frac{5}{4}A^2\varphi''^2+\frac{eH^2_{\max}}{m\Phi_A}\left(\frac{H'}{H_{\max}}\right)^2\right\}dz. \quad (7)$$

Since f_0 is of the order $1/A^2$ or $\Phi_A/H^2_{\max}$, ζ/M remains finite, while C becomes infinitely large as the lens is made progressively weaker.

The question of the weak electrostatic unipotential lens of least spherical aberration, with the focal length and the lens thickness as measured by

$$\left(\frac{l}{2}\right)^2=\int_{-\infty}^{\infty}z^2T dz\Big/\int_{-\infty}^{\infty}T dz \quad (8)$$

(the origin of z being chosen so that

$$\int_{-\infty}^{\infty}zT dz=0\Big),$$

held constant, has been fully dealt with by Scherzer.[1] Among all field distributions of equal focal length and thickness, regardless of symmetry, that given by

$$\varphi=\exp(-Bz^2/2), \quad (9)$$

leading to

$$\zeta/M=0.625B,$$

has the least aperture defect.[15] Rebsch and Schneider[2] have extended Scherzer's work to find immersion and magnetic lenses of least aperture defect, making use of the same conditions of constancy of f and l. The optimum lens fields for these two cases are

$$\varphi'=\exp(-Bz^2/2), \quad (10a)$$

$$H/H_{\max}=\exp(-Bz^2/2) \quad (10b)$$

with a spherical aberration 1/9 and 2/15 of that of the optimum electrostatic equipotential lens, respectively. Finally, the optimum rotation-free magnetic lens was found to have a magnetic scalar potential distribution corresponding to Eq. (9) with an aperture defect 6/5 that of the electrostatic equipotential lens. Rebsch and Schneider also showed that combined electric and magnetic weak lenses have a larger spherical aberration than the optimum electrostatic lenses or magnetic lenses by themselves.

Plass determined readily constructed electrodes yielding an axial field distribution defined by Eq. (7) as well as those corresponding to the immersion lens

$$\varphi=\tanh Bz, \quad (11)$$

[15] The distribution $\varphi=\exp[-(z+0.85)^2/2]+\exp[-(z-0.85)^2/2]$ ($\zeta=0.334$) discussed by Plass, reference 3, Eq. (14), leads to a spherical aberration 18 percent larger than Eq. (9) if the constants A and B in the latter are adjusted to yield the same l and f, in accord with Scherzer's prescription ($B=0.452$). On the other hand if, as recommended by Plass, the width of the field is defined as the separation of the points on the axis where φ is equal to 1 percent of the difference of the potential at $z=0$ and $z=\infty$, the more complex field given by Plass becomes, for equal focal length and width, superior, having a spherical aberration only 82 percent of that of Scherzer's optimum lens ($B=0.646$). Which of the two measures of thickness is to be preferred depends on the use to which the lens is to be put. Scherzer's definition is more readily handled analytically and conforms better with the customary concept of the width of a distributed function. The author is indebted to Mr. Plass for some of these corrected figures.

TABLE I.

System	Equation of field	$1/f$ diam.$^{-1}$	$(1/f)(l/2)^2$ diam.	ζ/M diam.$^{-2}$	Relative spher. ab. for equal f and l
A	$\frac{\Phi}{V_A}=1-0.827\left(\frac{V_A-V_L}{V_A}\right)$ $\times\exp(-1.445z^2)$	$0.1935\left[\frac{V_A-V_L}{V_A}\right]^2$	$0.101\left[\frac{V_A-V_L}{V_A}\right]^2$	1.806	1.00
B	——	$0.2233\left[\frac{V_A-V_L}{V_A}\right]^2$	$0.105\left[\frac{V_A-V_L}{V_A}\right]^2$	2.736	1.37
C	$\frac{H}{H_{\max}}=\operatorname{sech}^2(2.630z)$	$0.0772\left(\frac{\text{diam.}}{2.630}\right)^2$ $\times H^2_{\max}/V$	$0.0036\left(\frac{\text{diam.}}{2.630}\right)^2$ $\times H^2_{\max}/V$	2.76	0.137
D	$\frac{2\Phi}{V_2+V_1}=1+\left(\frac{V_2-V_1}{V_2+V_1}\right)$ $\times\tanh(2.630z)$	$0.658\left[\frac{V_2-V_1}{V_2+V_1}\right]^2$	$0.0306\left[\frac{V_2-V_1}{V_2+V_1}\right]^2$	2.31	0.114

which is very closely approximated by the field between two coaxial cylinders with the common diameter $2.6304/B$ at the potentials $\Phi_A(1\pm A)$.[16]

In the present work the four different systems shown in Fig. 1 were studied in detail. Table I indicates their weak lens characteristics, the diameters of the electrodes (or pole pieces) at the center being chosen as unit of length in each case.

In Table I systems A and B represent symmetrical equipotential lenses, V_A being the anode potential or the voltage measuring the velocity of the electrons incident on the lens and V_L measuring the potential of the center electrode. System A is the optimum electrostatic equipotential lens according to Scherzer; the electrode configuration shown in Fig. 1 corresponds to that given by Plass.[3]

System B is a type of equipotential lens with larger electrode separations, suitable for higher voltage work. Its potential distribution was determined with the aid of the electrolytic tank.

System C is the magnetic lens formed by two equidiameter cylinders of infinitely permeable material separated by a narrow gap; $H_{\max}$ measures the maximum magnetic field strength on the axis, located at the gap.

System D is an immersion lens formed, like System C, by two equidiameter cylinders; their respective potentials are V_1 and V_2. The more exact pole-piece and electrode shapes corresponding to Systems C and D were also determined by Plass (reference 3, Fig. 4).

The last two columns in Table I give the absolute and relative magnitudes, respectively, of the weak lens spherical aberration coefficients for large magnification M. The several quantities were calculated by evaluating the integrals in Eqs. (4) and (7) for the specific fields under consideration, T being defined by Eq. (1).

III. VARIATION OF REFRACTIVE POWER AND SPHERICAL ABERRATION WITH FIELD STRENGTH

All the calculations described below were made for the case in which the object is placed substantially at the focal point of the lens, a case realized in practice in the first stage of the electron microscope.

The first step consists of the numerical integration of Eq. (1) or of the equivalent equation

$$d'=d^2+T \qquad (12)$$

where $d=-R'/R$ and $R=R_i\exp[-\int_z^{z_i}d\cdot dz]$, for the initial conditions

$$R_i=R(z_i)=1, \qquad R_i'=0, \qquad d_i=0.$$

Here $z=z_i$ defines a plane in image space in which the lens fields are substantially zero. The point of intersection of the ray with the axis,

[16] S. Bertram, "Determination of the axial potential distribution in axially symmetric electrostatic fields," Proc. I.R.E. **28**, 418–420 (1940).

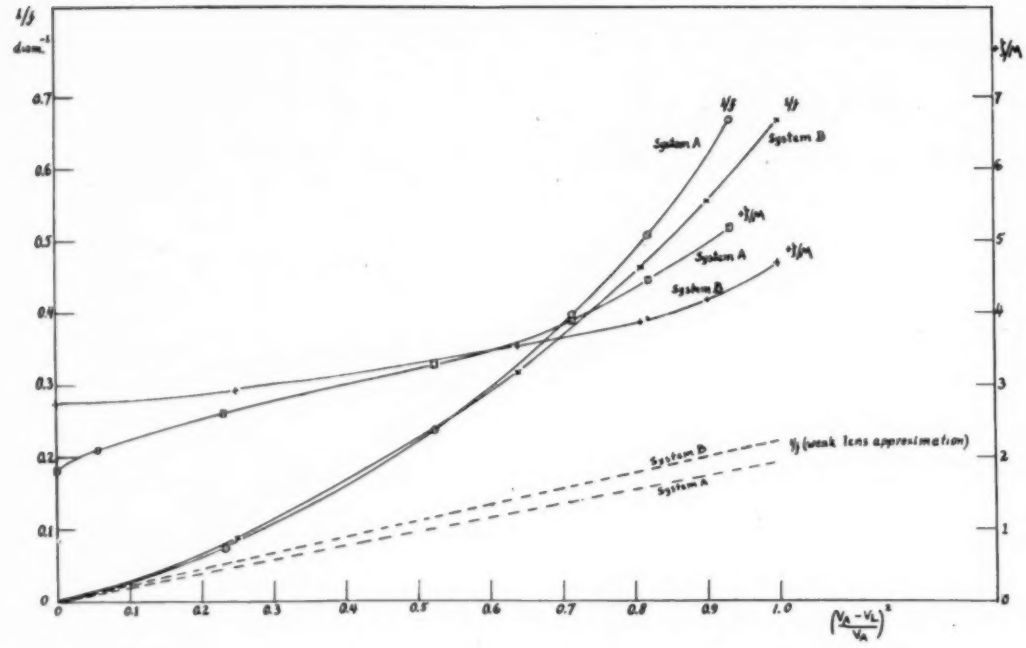

FIG. 2. Variation of refractive power and spherical aberration of unipotential electrostatic lenses with electrode voltages.

$z=z_0$, is the focal point or the object position for the lens, while the focal length is given by the slope of the ray at this point:

$$1/f_0=-(\Phi_i/\Phi_0)^{\frac{1}{2}}R_0'. \tag{13}$$

The position of the object-side principal plane with respect to the center of symmetry of the lens is given by z_0-f_0. A substitution of R, R_i, and R_0 in Eq. (6), finally, yields the spherical aberration coefficient C and, hence, $\zeta/M=C/f^2$.

The results of these calculations have been plotted in Figs. 2–4. The abscissas are in each case parameters proportional to the refractive power of the weak lens approximation. The ordinate scale at the left gives the refractive power $1/f$, while that at the right indicates the spherical aberration constant $\zeta/M=-C/f^2$. In the weak lens approximation the value of the refractive power (for equipotential lenses) is thus given by a straight line through the origin, while ζ/M is represented by a straight line parallel to the axis of the abscissas.

Figure 2 shows the results for the two electrostatic equipotential lenses, systems A and B, with center electrodes made negative with respect to the anode. Both $1/f$ and ζ/M deviate by increasing, positive quantities from the weak lens approximation as the lens strength is increased. The deviation for the refracting power is seen to be much greater than for the spherical aberration coefficient ζ. Furthermore, it is seen that the spherical aberration increases less rapidly for system B than for system A, so that for high lens powers the spherical aberration of the latter is actually the larger. It is probably generally true that the aberration increases more rapidly with voltage in proportion as the field distribution in question is more sharply peaked. This is also illustrated by the field:

$$\text{System } E\text{: } \Phi=1-A'(\exp[-(2.53z+0.85)^2/2]+\exp[-(2.53z-0.85)^2/2]) \tag{14}$$

discussed by Plass.[3] The constant 2.53 has been chosen so that the field in Eq. (14) yields the same "thickness" l (Eq. (8)) in the thin lens approximation as system A. Thus system E, with $A'=0.5735$, corresponding to a refractive power $1/f=0.685$, has a spherical aberration constant $+\zeta/M=3.72$, while for the same focal length system A has $+\zeta/M=5.25$.

For positive center electrodes ($V_L>V_A$) both the refractive power and the spherical aberration coefficients fall below the values given by the weak lens approximation; e.g., system A with

$(V_L - V_A)/V_A = 0.8$ has $-1/f_0 = 0.089$ and $\zeta/M = 1.12$.

Figure 3 indicates the variation of the focal length and the spherical aberration of the magnetic lens, system C, with field strength. The abscissa here is the ratio of the square of the maximum magnetic field along the axis and the "effective accelerating potential" V. For high voltages this effective accelerating potential V differs from the true accelerating potential v and is expressible in terms of the latter as follows:

$$V = v + ev^2/(2mc^2) = v(1 + 0.982 \cdot 10^{-6} v). \quad (15)$$

While with electric lenses a physical object must be effectively outside of the confines of the lens field,[17] as it otherwise will influence the action of the lens, this is not so with the magnetic lens. Here the object may be placed right in the center of the field. Accordingly the curves in Fig. 3 cover a greater range in refractive powers than the curves for the equipotential electrostatic systems in Fig. 2. It is seen that the refractive power curve lies consistently below the weak lens approximation, flattening out, in particular, for the high values of H^2/V, where a progressively larger portion of the lens field does not contribute to the formation of the image. The curve for ζ/M, also, is concave rather than convex toward the axis of the abscissas. A curve for the image rotation θ:

$$\theta = \left(\frac{\text{diam.}}{2.630}\right)\left(\frac{eH^2_{\max}}{8mV}\right)^{\frac{1}{2}} \int_{z_0}^{z_i} \frac{H}{H_{\max}} dz \quad (16)$$

is added for the sake of completeness.

Figure 4, finally, presents the curves for the immersion lens (system D). Here the weak lens approximations for the focal lengths are

$$\frac{1}{f_1} = \left(\frac{\Phi_2}{\Phi_1}\right)^{\frac{1}{2}} 0.658 \left(\frac{V_2 - V_1}{V_2 + V_1}\right)^2;$$
$$\frac{1}{f_2} = \left(\frac{\Phi_1}{\Phi_2}\right)^{\frac{1}{2}} 0.658 \left(\frac{V_2 - V_1}{V_2 + V_1}\right)^2. \quad (17)$$

[17] Even if the object is of such character that it does not prevent the obtaining of a good image, its presence within the field will cause the field distribution to vary with lens strength.

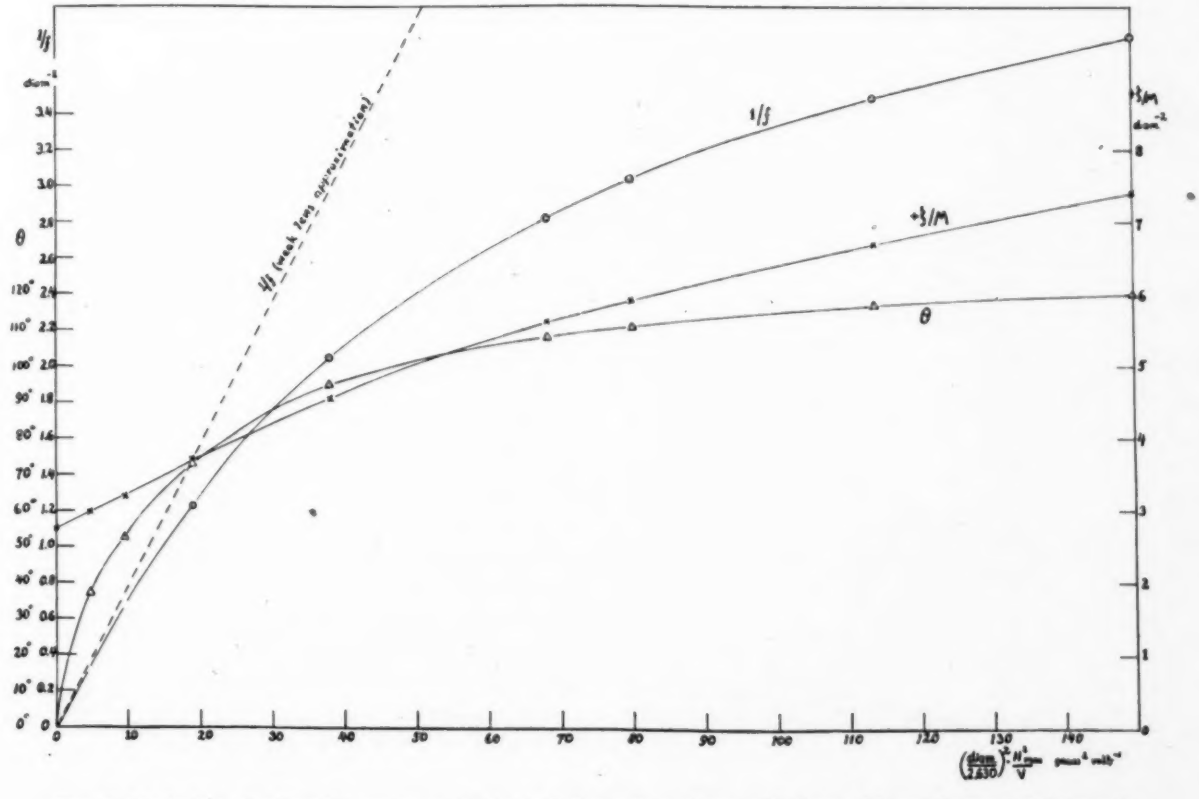

FIG. 3. Variation of refractive power and spherical aberration of magnetic lens with maximum field strength.

The actual refractive powers are again seen to increase much more rapidly with the voltage difference than is suggested by these formulas. The values of ζ_1/M and ζ_2/M—the subscript 1 indicates that the object is placed at the low voltage, the subscript 2, that it is placed on the high voltage side of the lens—are found to increase and decrease, respectively, with voltage. On the other hand the quantities $(+\zeta_1/M)(\Phi_1/\Phi_2)^{\frac{1}{2}}$ and $(+\zeta_2/M)(\Phi_2/\Phi_1)^{\frac{1}{2}}$ are found to be approximately equal and to differ by less than 10 percent from their weak lens value throughout the range of lens-strengths considered.

The constant ζ/M is a measure of the unsharpness due to spherical aberration to be expected with an effective physical aperture of fixed diameter. In the electron microscope, on the other hand, the factor determining the ultimate resolution attainable with a given objective lens is the size of the image of the central point of the object formed with a pencil of fixed aperture angle θ, divided by the magnification M. By Eq. (5) this is given by the quantity Cf_0. More precisely, the least resolvable distance $d_{\min}$ is given by

$$d_{\min}=k\cdot V_0^{-3/8}\cdot(Cf_0)^{\frac{1}{2}},$$

where k is a general constant, independent of the optical system employed, of the order of magnitude of $7\cdot10^{-6}$, if f and d are measured in cm and V, the effective accelerating potential, is measured in volts.[18]

Figure 5 shows the variation with refractive power of Cf_0 and the relative values of $d_{\min}$, the least resolvable separation, (for fixed V_0) for the four systems considered; the units are as before the diameters of the central electrodes or pole-pieces. Since the refractive power is, for large image distances, proportional to the magnification, the curves also indicate the variation in resolution with the magnification of the objective lens as the object is moved closer toward the

[18] See, e.g., Rebsch, reference 11.

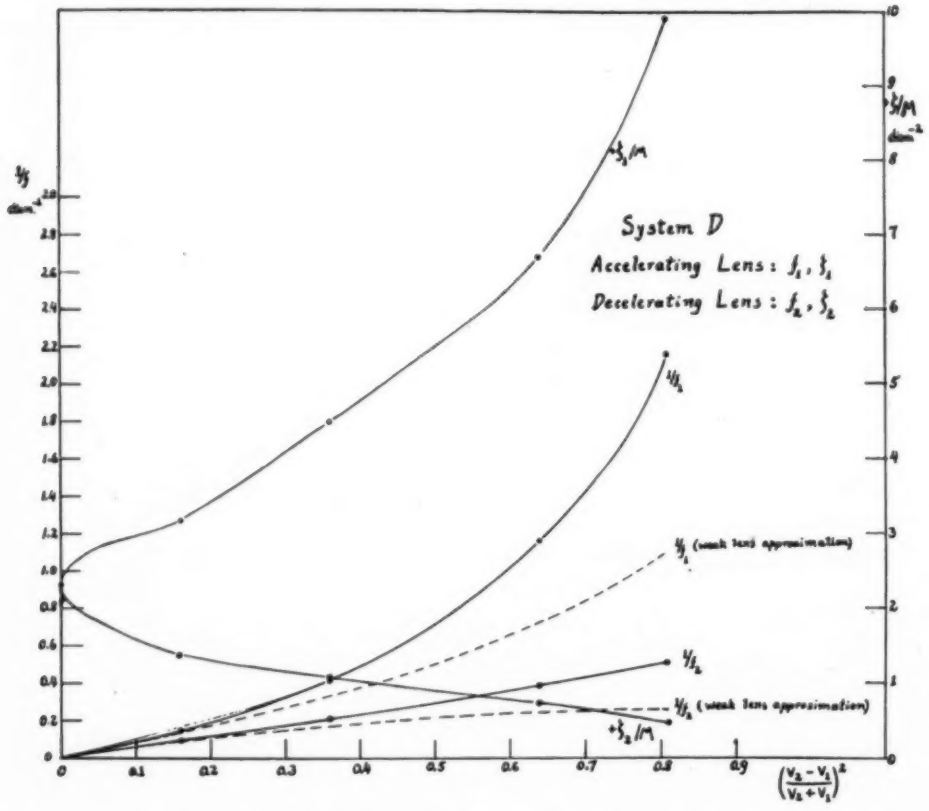

FIG. 4. Variation of refractive power and spherical aberration of immersion lens with applied voltages.

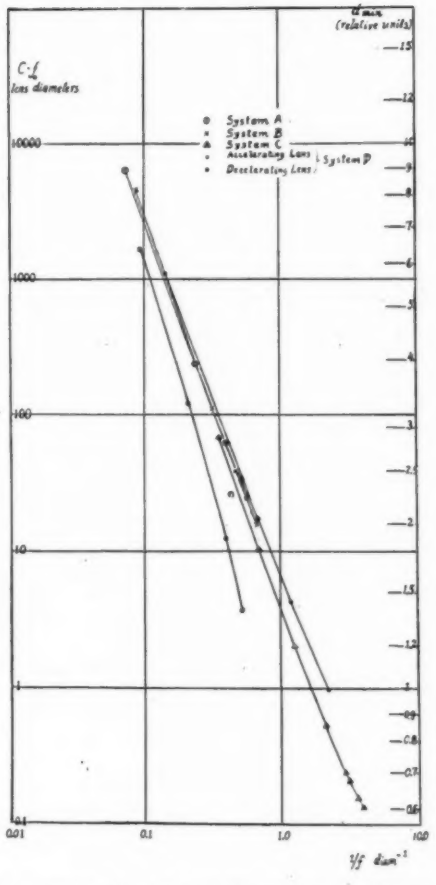

FIG. 5. Variation of spherical aberration coefficient Cf and of resolving power with refractive power.

objective and the lens voltages or coil currents are adjusted to keep the image in focus.

The curves indicate that, at least for the unipotential systems (systems A, B, and C), approximately,

$$d_{\min} \propto f^{\frac{1}{2}} \propto M^{-\frac{1}{2}}.$$

Thus, a decrease in the objective magnification by a factor 2.8 results in a doubling of the least resolvable distance. The resolving power is much more sensitive to changes in the refractive power of a given lens than to scaling the optical system up or down, leaving the electric and magnetic scalar potential unaltered. In order to change the limit of resolution by a factor of two by the latter method, the linear dimensions of the system would have to be increased or decreased by a factor of 16.

Curves closely related to those shown in Fig. 5 are obtained if, in the case of the magnetic lens, the lens field is left unaltered and the accelerating voltage is increased. If it is assumed that (e.g., in view of the saturated condition of the iron, the limited heat dissipation of the coils, or the limited power output of the source of current) the fixed field considered in each case represents the strongest field attainable, the curves in Fig. 6 indicate the reduction in the resolving power with increase in accelerating voltage. The abscissas show the true, rather than the effective, voltage. The corresponding changes in refractive power are shown on the dotted curves; corresponding curves for Cf_0 or $d_{\min}$ and for $1/f$ are identified by similar markers. For the type of lens in question a change in voltage from 50 kilovolts to 200 kilovolts is seen to cause a decrease in resolving power by a factor of from 2 to 2.5, the magnification of the objective being reduced simultaneously by a factor of 3.1 to 3.7.

IV. COMPARISON WITH EARLIER MEASUREMENTS OF SPHERICAL ABERRATION

The calculations for the magnetic lens were found to be in good agreement with measurements of Ruska[9] on strong magnetic objectives. Thus, the poleshoe support without the poleshoes, consisting essentially of equidiameter magnetized cylinders separated by a gap, yielded,

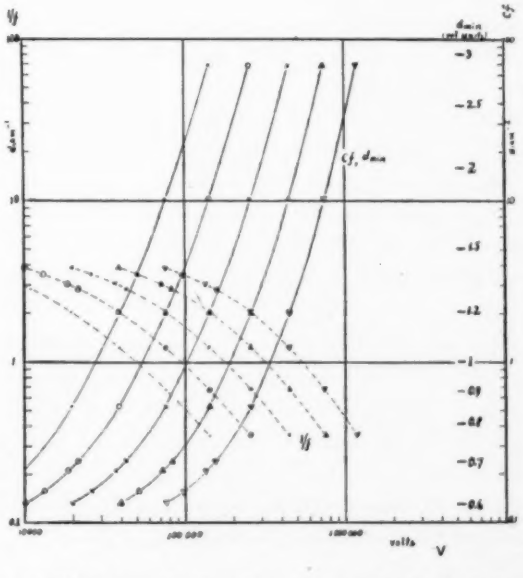

FIG. 6. Variation of refractive power and spherical aberration of magnetic lens with applied voltage.

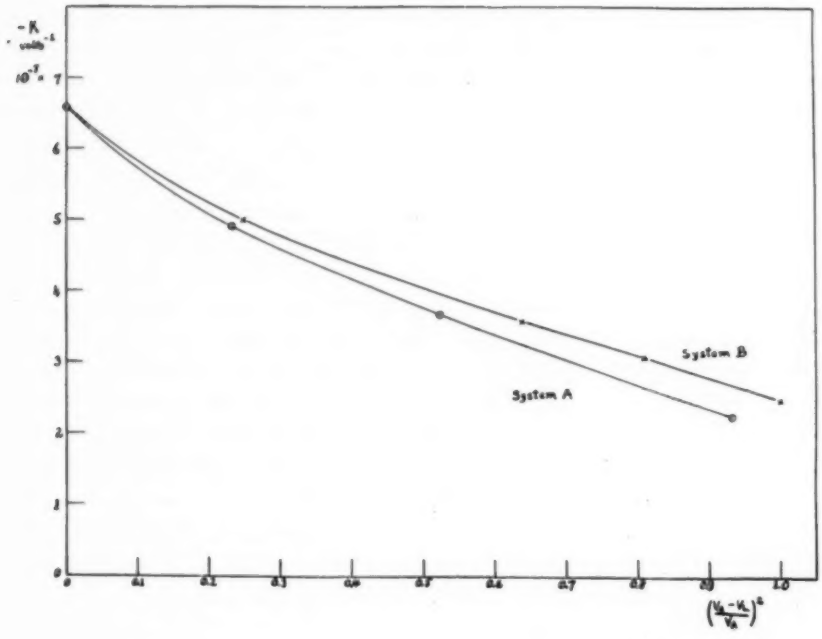

FIG. 7. Variation of "relativistic aberration" of unipotential electrostatic lenses with electrode voltage ratios.

with $1/f \backsimeq 2$ diam.$^{-1}$, $\zeta/M = 5.0$ diam.$^{-2}$ (calc. 4.5 diam.$^{-2}$), while pole pieces in conventional position gave, for gaps equal to 0.86 and 0.29 diam. and $1/f \backsimeq 0.7$ diam.$^{-1}$, $\zeta/M = 3.0$ and 3.9 diam.$^{-2}$, respectively (calc. 3.2 diam.$^{-2}$). With the vertices of the pole pieces turned outward, a condition deviating greatly from that assumed in the calculation. Ruska found, with a gap width of 0.86 diam. (distance between pole-piece vertices: 2.24 diam.) and $1/f \backsimeq 0.7$ diam.$^{-1}$, the much lower value $\zeta/M = 1.1$ diam.$^{-2}$.

Becker and Wallraff[10] find for an iron free coil with $1/f \backsimeq 0.9$ diam.$^{-1}$, $\zeta/M = 2.6$ diam.$^{-2}$. Their results for iron enclosed coils cannot be readily compared with the present calculations.

Measurements of the spherical aberration of strong magnetic objectives by v. Ardenne[7] yielded values for ζ/M varying between 1 and 6 diam.$^{-2}$, $1/f$ lying between 0.25 and 0.33 diam.$^{-1}$.

For an equidiameter cylinder immersion lens (system *D*) E. Gundert[19] measured, for $1/f = 1.38$ diam.$^{-1}$, $\zeta/M = 6.6$ diam.$^{-2}$ (calc. 7.4 diam.$^{-2}$) with an uncertainty of about 20 percent. Insufficient data are given to permit the comparison of his results for longer focal length lenses with the present calculations.

[19] E. Gundert, "Aperture defect of electrostatic cylinder lenses," Zeits. f. Physik **112**, 689–690 (1939).

V. EFFECT OF VARIATIONS IN THE ACCELERATING VOLTAGE ON ELECTROSTATIC LENSES

All the preceding formulas and calculations for electrostatic lenses—and indeed almost all other work on the subject—have tacitly assumed that the electron velocities considered were small compared with the velocity of light. In this case, and only in this case, is it true that the refracting power of an electrostatic lens is unaltered if the potentials on all of its elements are changed by the same factor.[20]

If no limitation is placed on the magnitude of the potentials involved, the pertinent variation principle,[21]

$$\delta \int \left(\varphi + \frac{e}{2mc^2} \varphi^2 \right) ds = 0, \qquad (18)$$

where φ here denotes the total electric potential and where the integration is to be carried out over the path of the electron, the end points of the path being kept fixed during the indicated variation, leads to the following differential

[20] This claim is also often made for the electrostatic electron microscope, for which it is not valid. See, e.g., H. Mahl, "The electrostatic electron microscope of great resolution," Zeits. f. tech. Physik **20**, 316–317 (1939).

[21] E. Brüche and O. Scherzer, *Geometrische Elektronenoptik* (J. Springer, Berlin, 1934), p. 38, Eq. (37).

equation for paraxial rays in a meridional plane:

$$r''+\frac{r'}{2}\frac{\Phi'}{\Phi}\left(\frac{1+2a\Phi}{1+a\Phi}\right)+\frac{r}{4}\frac{\Phi''}{\Phi}\left(\frac{1+2a\Phi}{1+a\Phi}\right)=0 \quad (19)$$

where $a=e/(2mc^2)=0.982\cdot10^{-6}$ volt^{-1}. In terms of the dependent variable $R=r\Phi^{+\frac{1}{4}}$ this differential equation becomes

$$R''+\frac{3}{16}\left(\frac{\Phi'}{\Phi}\right)^2 R = -\frac{a\Phi}{1+a\Phi}R\left(\frac{1}{2}\frac{R'}{R}\frac{\Phi'}{\Phi}+\frac{\Phi''}{4\Phi}-\frac{\Phi'^2}{8\Phi^2}\right) \quad (20)$$
$$=S(z).$$

If R_α and R_γ are two independent solutions of the reduced equation, i.e., Eq. (20) with S set equal to zero, with the initial conditions

$$R_\alpha(z_0)=0, \quad R_\alpha'(z_0)=R_0', \quad R_\gamma(z_0)=1,$$

the solution of Eq. (20) for a ray leaving the object plane $z=z_0$ with the initial values $R(z_0)=0$, $R'(z_0)=R_0'$ becomes[22]

$$R=R_\alpha\left[1+\frac{1}{R_0'}\int_{z_0}^{z}R_\gamma(z')S(z')dz'\right] -\frac{R_\gamma}{R_0'}\int_{z_0}^{z}R_\alpha(z')S(z')dz'. \quad (21)$$

For $z=z_i$, i.e., at the image plane for $a\Phi\to0$,

$$\Delta R_i=R_i=-\frac{M}{R_0'}\left(\frac{\Phi_0}{\Phi_i}\right)^{-\frac{1}{4}}\int_{z_0}^{z_i}R_\alpha(z')S(z')dz'. \quad (22)$$

This solution is exact. The corresponding quantity

$$\Delta r_i=-\frac{M}{r_0'}\Phi_0^{-\frac{1}{4}}\int_{z_0}^{z_i}R_\alpha(z')S(z')dz' \quad (23)$$

may be defined as the axial relativistic aberration. It represents the spreading, due to the variation of the mass of the electron with its velocity, of the central image point as the voltage is increased from zero to the maximum value employed. If everywhere $a\Phi\ll1$, as is normally the case,

$$\Delta r_i=+a\Phi_A M\frac{R_a}{\Phi_0^{\frac{1}{4}}}\frac{R_a}{R_0'}\int_{z_0}^{z_i}\frac{R^2}{R_a^2} \times\left(\frac{1}{2}\frac{R'}{R}\frac{\Phi'}{\Phi_A}+\frac{\Phi''}{4\Phi_A}-\frac{1}{8}\frac{\Phi'}{\Phi}\frac{\Phi'}{\Phi_A}\right)dz \quad (24)$$
$$=-a\Phi_A\frac{M}{8}\frac{R_a}{\Phi_0^{\frac{1}{4}}}\frac{R_a}{R_0'}\int_{z_0}^{z_i}\frac{R^2}{R_a^2}\frac{\Phi'^2}{\Phi\Phi_A}dz,$$

where Φ_A is the anode voltage and R_a is the value of R_α at some arbitrary "aperture plane" in image space. The subscript α has been omitted for convenience. As M and $r_i'\cdot R_0'$ are of the same sign, the shift in the image plane $\Delta z_i=-\Delta r_i/r_i'$ is always positive, i.e., the lens decreases in refractive power with increasing voltage.

For very large image distance:

$$\left(\frac{\Phi_0}{\Phi_i}\right)^{\frac{1}{4}}\frac{\Delta r_i}{M}=-\frac{a\Phi_A}{8}f_0^2\cdot\theta\int_{z_0}^{z_i}\frac{R^2}{R_a^2}\frac{\Phi'^2}{\Phi\Phi_A}dz=K\Phi_A f_0\theta, \quad (25)$$

where

$$K=-1.228\cdot10^{-7}\cdot f_0\cdot\int_{z_0}^{z_i}\frac{R^2}{R_a^2}\frac{\Phi'^2}{\Phi\Phi_A}dz \text{ volts}^{-1}, \quad (26)$$

θ being the aperture angle of the electron ray leaving the object and R_a the value of R in image space for a ray leaving the object-side focal point with an inclination θ to the axis. For weak unipotential lenses (Eq. (3))

$$K=-0.653\cdot10^{-6} \text{ volt}^{-1}.$$

The "relativistic aberration" is thus invariably of the same sign and is proportional to the range of accelerating voltages employed. For weak lenses of any given focal length it is the same for equal heights of incidence of the rays on the lens. As an example of its magnitude, consider the equipotential lens of system B with $V_L=0$ and a focal length of 1 cm operated at voltages between 40,000 and 60,000 volts. If the system is assumed to be focused for 50,000 volts and the aperture angle is 10^{-3} radian, the circle of confusion due to the relativistic aberration will have a diameter

$$2\Delta r_i=2\cdot M\cdot2.46\cdot10^{-7}\cdot10^4\cdot1\cdot10^{-3} =4.92\cdot10^{-6}\cdot M \text{ cm}$$
$$=492\cdot MA,$$

[22] E. P. Adams, *Smithsonian Mathematical Formulae and Tables of Elliptic Functions* (Washington, D. C., 1922), Formula 8410.

since K is calculated to be equal to $2.46\cdot10^{-7}$ volt^{-1}. For the electron microscope this is a very significant amount and indicates the necessity for some voltage stabilization also for the electrostatic instrument.

Figure 7 shows the variation of the relativistic aberration constant K with lens strength for systems A and B. It is seen that the constant decreases fairly rapidly as the lens strength is increased. The fact that Eq. (26) can be written

$$K=-0.653\cdot10^{-6}\int_{z_0}^{z_i}\frac{\Phi}{\Phi_A}\frac{R^2}{R_a^2}\frac{\Phi'^2}{\Phi^2}dz\Big/\int_{z_0}^{z_i}\cdot\frac{R}{R_a}\frac{\Phi'^2}{\Phi^2}dz$$

shows that, since $R\leq R_a$, $|K|\leq0.653\cdot10^{-6}$ volt^{-1} if the center electrode is negative with respect to the anode ($\Phi\leq\Phi_A$). In the converse case that the center electrode is positive with respect to the anode, it is to be expected that normally $|K|\geq0.653\cdot10^{-6}$ volt^{-1}, since the effect of the factor $\Phi/\Phi_A(\geq1)$ will outweigh that of the added factor $R/R_a(\leq1)$.

VI. CHROMATIC ABERRATION

The axial chromatic aberration of the four systems studied can, in principle, be derived directly from the curves indicating the distance z_F of the focal point from the center of the lens, shown in Fig. 8. The longitudinal chromatic aberration is the change in the image distance resulting from a change $e\Delta V$ of the kinetic energy eV_0 of the electrons incident on the lens. For large values of the magnification M it is equal to

$$\Delta z_i=M^2\Delta z_F\left(\frac{\Phi_i}{\Phi_0}\right)^{\frac{1}{2}}=M^2\frac{dz_F}{dV_0}\Delta V\left(\frac{\Phi_i}{\Phi_0}\right)^{\frac{1}{2}}. \quad (27)$$

The lateral chromatic aberration under the same circumstances is

$$\Delta r_i=\Delta z_i\cdot\theta_i=M\cdot\Delta V\cdot(dz_F/dV_0)\cdot\theta. \quad (28)$$

If the parameters y and V, with the significance: $y=(V_A-V_L)/V_A$, $V=V_A$, for systems A and B,

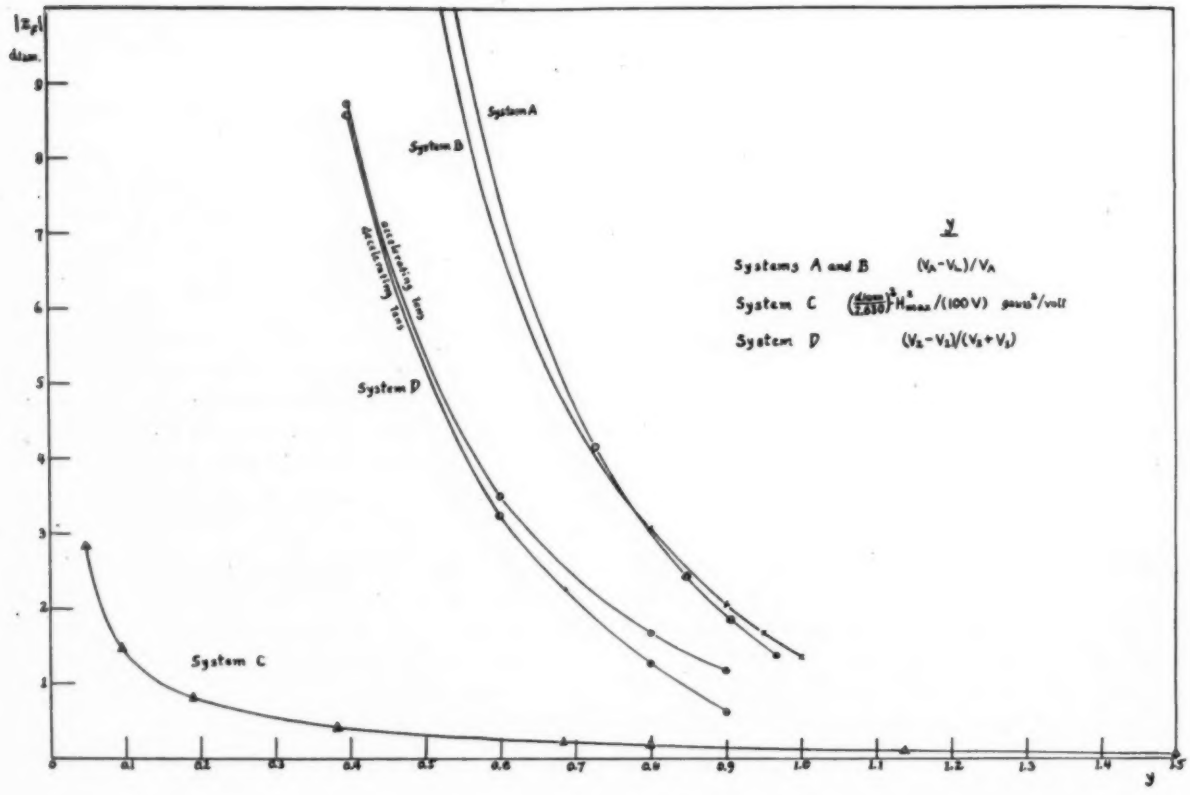

FIG. 8. Variation of position of focal point with lens strength.

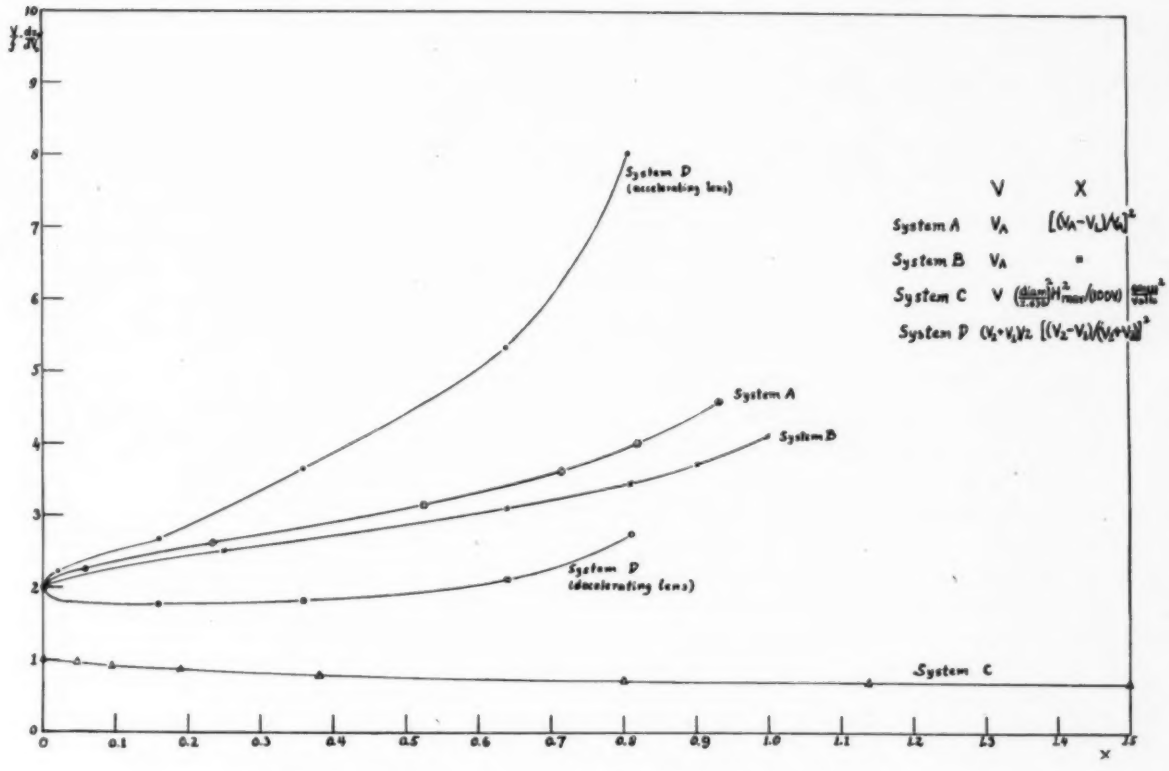

FIG. 9. Variation of chromatic aberration with lens strength.

$$y=(V_2-V_1)/(V_2+V_1),$$
$$V=(V_2+V_1)/2, \quad \text{for system } D,$$

and

$$y=H_{\max}{}^2/V\cdot(\text{diam.}/2.630)^2,$$
$$V=V, \quad \text{for system } C$$

are introduced, it is possible to write generally

$$dz_F/dV_0=-(dz_F/dy)\cdot(y/V).$$

This quantity may be determined directly from the slopes of the curves in Fig. 8.

For weak lenses, since here $z_F \backsimeq f$,

$$dz_F/dV_0=2f/V \quad \text{for electrostatic lenses}$$

and

$$dz_F/dV_0=f/V \quad \text{for magnetic lenses.}$$

For strong lenses the quantity $(V/f)\cdot(dz_F/dV_0)$ can be determined with greater accuracy than by graphical differentiation by evaluating the expression for the chromatic aberration given, e.g., by W. Glaser:[23]

$$\frac{V}{f}\cdot\frac{dz_F}{dV_0}=\frac{R_i}{R_0'}\left(\frac{\Phi_i}{\Phi_0}\right)^{\frac{1}{4}} \times\int_{z_0}^{z_i}\left(\frac{3}{8}\frac{\Phi'^2}{\Phi^2}+\frac{eH^2}{8m\Phi}\right)\frac{V}{\Phi}\frac{R^2}{R_i^2}dz. \quad (29)$$

Figure 9 shows the variation with lens strength of the chromatic-aberration coefficient of the four systems considered. The quantity $(V/f)\cdot(dz_F/dV_0)$ is seen to decrease uniformly with increasing lens strength for the magnetic lens, to increase uniformly for the electric equipotential lenses with negative center electrode. Glaser[23] has shown that, quite generally, the chromatic-aberration coefficient of a strong magnetic lens is less or equal to that of a weak or thin magnetic lens, i.e., that for magnetic lenses

$$dz_F/dV\leq f/V. \quad (30)$$

In like manner it may be shown that for an electrostatic unipotential lens with *positive* center electrode

$$dz_F/dV_0\leq 2f/V. \quad (31)$$

[23] W. Glaser, "Chromatic aberration of electron lenses," Zeits. f. Physik **116**, 56–67 (1940).

This is not the case, however, for a lens with a negative center electrode, as is evident from the curves for systems A and B.[24]

VII. CONCLUSIONS

The above mathematical study of the axial aberrations with lens strength of four typical electron lenses leads to the following conclusions:

Using the physical diameter of the central lens electrodes or pole pieces as unit of length, the spherical aberration for fixed height of incidence of the imaging rays is a constant for weak electron lenses. For strong lenses it increases with lens strength both for unipotential electrostatic lenses and, less rapidly, for magnetic lenses. For the immersion lens the same quantity, multiplied by the square root of the ratio of the object-side and image-side potentials, remains practically constant. The relative values of the spherical aberrations of different systems change as the lens strength is increased, that of the less sharply peaked fields increasing less rapidly.

For the equipotential lenses, both electric and magnetic, the spherical aberration for fixed angle of incidence decreases with increasing refractive power $1/f$ approximately as $f^{8/3}$. Hence, the least resolvable distance varies, assuming that these lenses are employed as electron microscope objectives, as f^1 if the physical dimensions of the lenses are kept fixed and only the coil currents or electrode voltages are varied. Thus, increasing the field strength of the lenses in this manner is far more effective for improving resolution than a reduction of the objectives in scale. The magnetic lens is found to be superior to the electrostatic lenses from the point of view of spherical aberration.

A comparison of the calculated spherical aberrations with isolated measurements by other authors indicates satisfactory agreement.

Due to the change of the electron mass with velocity, electrostatic lenses with fixed ratios of the electrode voltages increase in focal length with increasing over-all applied voltage. This "relativistic aberration" is sufficiently large to demand, in the case of the electrostatic electron microscope, keeping the fluctuation amplitude of the operating voltage well below a thousand volts. The relativistic aberration for fixed height of incidence decreases with increasing lens strength for lenses with negative center electrode, but may be expected to increase for lenses with positive center electrode.

The chromatic aberration (for fixed height of incidence) of weak equipotential electrostatic lenses is twice as large as that of weak magnetic lenses. Furthermore, for the electrostatic lenses with negative center electrode the chromatic aberration increases with lens strength, while that of magnetic lenses decreases. Thus, for lenses such as are employed as electron microscope objectives the chromatic aberration of the electrostatic lenses is approximately 5–6 times as large as that of the magnetic lenses.

The author wishes to express his thanks to Dr. V. K. Zworykin, Associate Director of the RCA Research Laboratories, and to Dr. James Hillier for their encouragement and advice.

[24] Glaser's deduction that Eq. (31) is valid for all electrostatic unipotential lenses is erroneous; a general upper limit for such lenses:

$$\frac{dz_F}{dV_0} \leqq \frac{2f}{V_0^{\frac{1}{2}} V_{\min}^{\frac{1}{2}}},$$

where $V_{\min}$ is the lowest potential within the lens, can, however, be established.

Calendar of Meetings

September

29–Oct. 1 Technical Association of Pulp and Paper Industry, Boston, Massachusetts

October

5– 9 National Safety Council, Chicago, Illinois
12–14 American Society of Mechanical Engineers, Rochester, New York
12–16 American Welding Society, Detroit, Michigan
12–16 American Society for Metals, Detroit, Michigan
19–24 American Society for Metals, Chicago, Illinois
19–24 American Society for Metals, Cleveland, Ohio
30–31 Optical Society of America, New York, New York
30–31 Society of Rheology
30–31 American Mathematical Society, New York, New York

November

7 American Physical Society, New York State Section, Albany, New York
16–18 American Institute of Chemical Engineers, Cincinnati, Ohio
27–28 American Physical Society, Chicago, Illinois
27–28 American Mathematical Society, Notre Dame, Indiana
30–Dec. 4 American Society of Mechanical Engineers, New York, New York

December

27–Jan. 1 American Society of Naturalists, New York, New York
28–31 American Physical Society, New York, New York
28–Jan. 2 American Association for the Advancement of Science, New York, New York
28–Jan. 2 American Standards Association, New York, New York